This dissertation has been
microfilmed exactly as received

67-16,483

DORMAN, Charles Franklin, 1933-
THE MAGNETIC SUSCEPTIBILITY OF Cu^{2+} IN ZnO.

The University of Oklahoma, Ph.D., 1967
Physics, solid state

University Microfilms, Inc., Ann Arbor, Michigan

Downloaded from SHAREOK. Persistent Handle URL: https://hdl.handle.net/11244/2269

THE UNIVERSITY OF OKLAHOMA

GRADUATE COLLEGE

THE MAGNETIC SUSCEPTIBILITY OF Cu^{2+} IN ZnO

A DISSERTATION

SUBMITTED TO THE GRADUATE FACULTY

in partial fulfillment of the requirements for the

degree of

DOCTOR OF PHILOSOPHY

BY

CHARLES FRANKLIN DORMAN

Norman, Oklahoma

1967

THE MAGNETIC SUSCEPTIBILITY OF Cu^{2+} IN ZnO

APPROVED BY

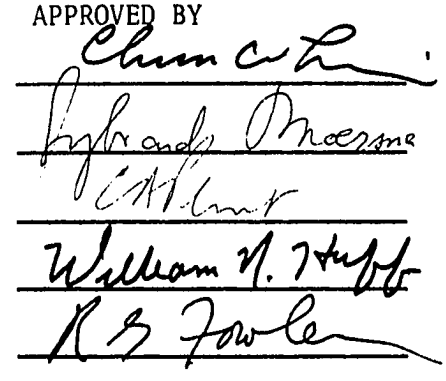

DISSERTATION COMMITTEE

ACKNOWLEDGEMENTS

The author wishes to express his appreciation to Professor Chun C. Lin for suggesting the research problem and his patient guidance.

Thanks are due to Professor W. H. Brumage, Mr. C. R. Yarger and Mr. J. P. Mahoney for supplying the susceptibility measurements.

TABLE OF CONTENTS

PAGE

LIST OF TABLES v

LIST OF ILLUSTRATIONS. vii

Chapter

I. INTRODUCTION 1

II. PRELIMINARY CONSIDERATIONS 8

Cubic Field
Trigonal Perturbation
Spin-Orbit Considerations
External Magnetic Field

III. SECOND ORDER PERTURBATION THEORY 25

General Considerations
Field Independent Terms
External Magnetic Field

IV. Cu^{2+} IN THE TETRAHEDRAL SITES OF CdS, ZnS, and ZnO 56

V. MAGNETIC SUSCEPTIBILITY OF Cu^{2+} IN ZnO 73

VI. DELOCALIZATION OF THE Cu^{2+} 3d ORBITAL. 85

Orthoganalization to Bloch Functions
Crystal Structure of ZnO
Evaluation of the Two Center Overlap Integrals
Normalization of the Delocalized Function
Orbital Reduction Parameter
Spin-Orbit Parameter

CONCLUSIONS. 119

APPENDICES 122

LIST OF REFERENCES 140

LIST OF TABLES

Table		Page
1.	One Electron Cubic Wave Functions	10
2.	Matrix Elements of V_t in the Cubic Representation . . .	14
3.	Cubic Field Functions Forming Basis for the Irreducible Representations of the $\overline{C}_{3v}$ Double Group	17
4.	Matrix Elements of $\lambda \vec{\ell}\cdot\vec{s}$ in the Uncoupled Representation	20
5.	Matrix Elements of $(\ell_z+g_s s_z)$ in the Uncoupled Representation	23
6.	Matrix Elements of $(\ell_x+g_s s_x)$ in the Uncoupled Representation	24
7.	Matrix Elements of the Hamiltonian Exclusive of the Magnetic Field Terms in the Uncoupled Representation .	30
8.	The Transformed Hamiltonian for the $\Gamma_6(^2T_2)$ Subblock . .	37
9.	Magnetic Elements of $H^m = \mu_o(\ell_x+g_s s_x)\mathcal{H}$ in the Representation Diagonalizing the Field Independent Terms	44
10.	Magnetic Elements Contributing to the Linear and Quadratic Zeeman Effect for the Magnetic Field Directed Perpendicular to the Hexagonal c-Axis	46
11.	Matrix Elements of $H^m = \mu_o(\ell_z+g_s s_z)\mathcal{H}$ in the Representation Diagonalizing the Field Independent Terms	54
12.	Experimental G-Factors of Cu^{2+}:ZnO	66

Tables Page

13. Sensitivity of the Mixing Coefficients and the Orbital Reduction Parameter to Second Order Corrections 70

14. Magnetic Susceptibility (Per Gram Sample) of Cu^{2+} Dopped ZnO Crystal 74

15. The Real Wave Functions for the 2p and 3d Orbitals . . . 96

16. The Two Center Overlap Integrals Expressed in Terms of the Slater Koster Parameters 97

LIST OF ILLUSTRATIONS

Figure		Page
1.	Energy Level Diagram of Cu^{2+} in a Tetrahedral Field (Strong Axial Field)	18
2.	Energy Level Diagram of Cu^{2+} in a Tetrahedral Field (Weak Axial Field)	57
3.	Optical Emission Spectra of Cu^{2+}:ZnS and Cu^{2+}:CdS . . .	60
4.	Optical Obsorption Spectrum of Cu^{2+}:ZnO	65
5.	Magnetic Susceptibility (Per Gram Sample) of Cu^{2+}:ZnO .	76
6.	Calculated Magnetic Susceptibility of Cu^{2+}:ZnO (Optical Parameters)	80
7.	Calculated Magnetic Susceptibility of Cu^{2+}:ZnO (Dietz's Parameters)	81
8.	The Calculated Magnetic Susceptibility (Per Gram Sample) For a Larger $\Gamma_6(^2T_2)$ Ground State Energy Separation	83
9.	The Calculated Magnetic Susceptibility (Per Gram Sample) For a Smaller Value for the Interlevel Spin-Orbit Parameter	84
10.	Unit Cell of Wurtzite on the Conventional Hexagonal Axis.	90
11.	Base Plane Projection of the Wurtzite Structure	92

THE MAGNETIC SUSCEPTIBILITY OF Cu^{2+} IN ZnO

CHAPTER I

INTRODUCTION

Considerable study, both experimental and theoretical, has been devoted to the analysis of impurity states in host crystals. Generally the characteristics exhibited by the impurity states are thought to arise from one of two models. The localized picture, i.e., crystal field theory,[1,5] treats the impurity state as arising from the impurity free ion states. The free ion states are then perturbed by localized electrostatic fields due to the nearest neighbor ligands and exhibit Stark splittings. As there usually exists covalency[5] between the impurity ion and its nearest neighbor ligands, the free ion values for the spectroscopic parameters are reduced, e.g., the spin-orbit and Slater-Condon parameters. The delocalized picture or effective mass theory[6] treats the impurity states as arising from either the unperturbed conduction or valence band states, depending upon whether the impurity ion is a donor or acceptor respectively. Since the introduction of the impurity ion into the crystal lattice destroys the periodicity of the crystalline potential, the effect of the impurity ion is

to introduce a perturbation to the crystalline potential centered at the impurity site. Due to the nonperiodicity of the perturbing potential, the crystal momentum $\vec{k}$ is no longer a good quantum number and hence the perturbation introduces interactions between the band states forming wave functions localized around the impurity site. This then results in the formation of discrete levels.

The impurity problem to be treated here is that of a transition metal ion in a diamagnetic host crystal, i.e., Cu^{2+} in ZnO, ZnS and CdS. On entering the host lattice, the electronic configuration of the transition metal becomes [Ar] $(3d)^n$ where the Argon subshell is designated by [Ar]. The $(4s)^2$ valence electron of the transition metal have been given up to the valence band of the crystal and participates in the crystal bonding. As the 3d electrons which are responsible for the impurity states are tightly bound, crystal field theory has been successful in interpreting the impurity levels attributed to the transition metal ion.[4]

The electronic ground state configuration of Cu^{2+} is [Ar] $(3d)^9$ where the core electrons denoted by the Argon subshell form deep lying core states and will not be considered further. It is well known that the free ion electronic configurations d^n and d^{10-n} have identical multiplet terms[7] and that the energy spacing between the multiplet terms is the same for both the d^n and d^{10-n} configurations. The intervals for the d^{10-n} configuration are inverted relative to those of d^n. Similarly it can be shown that the Stark splitting of the free ion levels due to the crystal field of the surrounding ligands

is the same for the d^n and d^{10-n} configurations, only the sign of the crystal field parameters being reversed.[9] Thus except for the constant shift of all electronic levels, the solution for the $(3d)^9$ configuration may be found from that for the $(3d)^1$ configuration by employing the hole formalism. Here one need only reverse the sign of those parameters which depend upon the sign of the electronic charge. The hole formalism will be used throughout this work.

The one electron quantum mechanical Hamiltonian for the free ion will then be taken as

$$H_{fi} = -\frac{\hbar^2}{2m}\nabla^2 + V(\vec{r}) + \lambda\,\vec{\ell}\cdot\vec{s}$$

where the first and second terms are the kinetic and potential energy of the system respectively and the last term is the spin-orbit interaction energy arising from the relative motion of the electron and the nucleus. The solution of the free ion Hamiltonian for a $(3d)^1$ configuration gives the multiplet terms $^2D_{3/2}$ and $^2D_{5/2}$.

For the host crystals under consideration, the paramagnetic ion enters a lattice site having local tetrahedral symmetry.[25,14] Since the crystal field experienced by the impurity ion due to the nearest neighbor ligands obeys the Laplace equation, the tetrahedral field may be expanded in terms of the generalized Legendre polynomials

$$V_c(\vec{r}) = \sum_{\ell}\sum_{m=-\ell}^{\ell} A_\ell^m\, r^\ell\, Y_\ell^m(\theta,\phi)$$

where r,θ and ϕ are the coordinates of the 3d electron. Simplification of the potential V_c may be carried out on noting the following. For

matrix elements of V_c within the $(3d)^1$ configuration, the triangular rule of spherical harmonics rules out those terms in the expansion for which $\ell > 4$ and for odd ℓ. Since V_c commutes with the operations of the T_d point group, symmetry considerations then dictate the form of V_c. Thus on choosing the axis of quantization to be the hexagonal c-axis, the form of V_c is given by[10]

$$V_c = A_4^o \, r^4 \left(Y_4^o \ (\theta,\phi) + \sqrt{\frac{10}{7}} \ [Y_4^3 \ (\theta,\phi) - Y_4^{-3} \ (\theta,\phi)] \right). \qquad \text{(I-1)}$$

The constant term for which $\ell = 0$ has not been retained in the expansion of V_c as this term serves only to shift the ^2D multiplet.

For wurtzite structures, there usually exists a slight trigonal distortion along the hexagonal c-axis. This results from the fact that the parameter u denoting the cation-ligand spacing along the hexagonal c-axis in the unit cell is somewhat different than its value in the ideal hexagonal structure.[13] Thus a perturbing local field having the point symmetry C_{3v} will be superimposed on the predominant tetrahedral field. For reasons given in the preceeding paragraph, the trigonal perturbation assumes the form[11]

$$V_t = B_2^o \, r^2 \, Y_2^o \ (\theta,\phi) + B_4^o \, r^4 \, Y_4^o \ (\theta,\phi). \qquad \text{(I-2)}$$

As the point group C_{3v} is a subgroup of T_d, there exist terms in V_t which have the same functional form as V_c. Thus these terms may be incorporated in the larger tetrahedral potential term V_c and have not

been included in the expression for V_t.

On inclusion of the magnetic interaction energy

$$H_m = \mu_o (\vec{\ell} + g_s \vec{s}) \cdot \vec{\mathcal{H}} \qquad \text{(I-3)}$$

of an external magnetic field with the orbital and spin magnetic moments of the electron, the Hamiltonian for the impurity ion is then given by

$$H = - \frac{\hbar^2}{2m} \nabla^2 + V(r) + V_c + V_t + \lambda \vec{\ell}\cdot\vec{s} + \mu_o (\vec{\ell} + g_s \vec{s})\cdot \vec{\mathcal{H}} , \qquad \text{(I-4)}$$

where the diamagnetic term $(e^2/8mc^2) \left|\vec{\mathcal{H}} \times \vec{r}\right|^2$ is neglected. As the crystal field interaction energy V_c is much larger than the spin-orbit interaction energy for the 3d electrons of the iron group,[5] the unperturbed Hamiltonian for the impurity ion will be taken as

$$H_o = - \frac{\hbar^2}{2m} \nabla^2 + V(r) + V_c \qquad \text{(I-5)}$$

and on inclusion of the magnetic dipole interaction of the electronic magnetic moment with the external field, the perturbation to the unperturbed Hamiltonian is then given by

$$H_1 = \lambda \vec{\ell}\cdot\vec{s} + V_t + \mu_o(\vec{\ell} + g_s \vec{s})\cdot\vec{\mathcal{H}} \quad . \qquad \text{(I-6)}$$

Here the spin-orbit interaction energy will then be treated as being the same order of magnitude as the trigonal field.

In this work, the temperature dependence of the magnetic susceptibility of the paramagnetic ion Cu^{2+} in the diamagnetic host

lattice ZnO will be investigated. If the medium is sufficiently rarefied so that Boltzmann statistics is applicable, the molar susceptibility is given by

$$\chi = \frac{N}{\mathcal{H}} \frac{\sum_n \mu_n e^{-W_n/kT}}{\sum_n e^{-W_n/kT}} , \qquad \text{(I-7)}$$

where the magnetic moment

$$\mu_n = - \partial W_n / \partial \mathcal{H}$$

is the time average of the magnetic moment for the stationary state W_n. The summation over the quantum index n denotes a summation over all stationary states. If it is assumed that the energy W_n can be expanded in a power series of the magnetic field strength

$$W_n = W_n^o + W_n^{(1)} \mathcal{H} + W_n^{(2)} \mathcal{H}^2 , \qquad \text{(I-8)}$$

the average magnetic moment for the stationary state n becomes

$$\mu_n = -W_n^{(1)} - 2 \mathcal{H} W_n^{(2)} - \ldots . \qquad \text{(I-9)}$$

On substituting the relations (I-8) and (I-9) for W_n and μ_n respectively into equation (I-7) for χ, the Boltzmann factor may then be developed as a power series in $\mathcal{H}$ and the portion of the susceptibility χ which is independent of the field strength reduces to[2]

$$\chi = N \frac{\sum_n [(W^{(1)})^2/kT - 2W_n^{(2)}] e^{-W_n^\circ/kT}}{\sum_n e^{-W_n^\circ/kT}} \qquad \text{(I-10)}$$

As symmetry considerations gives qualitative information about the properties of the solutions of the Hamiltonian and provides simplifications in the calculation of the eigenstates, some group theoretical results will be considered in the work to follow. The character tables of the T_d and C_{3v} point groups and the additional characters of their double groups may be found in Appendix 2. Here it will be seen that the notation used is that of both Bethe's and Mulliken's since both are used extensively.

CHAPTER II

PRELIMINARY CONSIDERATIONS

Cubic Field

The solutions diagonalizing the unperturbed impurity Hamiltonian

$$H_o = -\frac{\hbar^2}{2m}\nabla^2 + V(r) + V_c$$

are the one electron cubic wave functions[12] which have been given in Table 1. Here the hexagonal c-axis is the axis of quantization and the phase of the basis for the $^2T_2(T_d)$ manifold are chosen to conform with that of the pseudoangular momentum functions.[15,16]

The eigenvalues of H_o may be found using the triangular rule of spherical harmonics and the relation

$$\int_o^{2\pi}\int_o^{\pi} Y_\ell^{m*}(\theta,\phi)\, Y_k^{m-m'}(\theta,\phi)\, Y_\ell^{m'}(\theta,\phi)\, \sin\theta\, d\theta\, d\phi = \sqrt{\frac{2k+1}{4\pi}}\, C^k(\ell m, \ell' m'),$$

where the values for $c^k(\ell m, \ell' m')$ may be found in Condon and Shortley.[8] If the term energy $\langle 3d_m|-\frac{\hbar^2}{2m}\nabla^2 + V(r)|3d_m\rangle$ for the (3d) configuration is neglected, the Stark splitting is then

$$\langle e|V_c|e\rangle = -\frac{9}{21}\sqrt{\frac{9}{4\pi}}\, A_4^o\, \langle\overline{r^4}\rangle_{3d};\ \langle t_2^+|V_c|t_2^+\rangle = \frac{6}{21}\sqrt{\frac{9}{4\pi}} A_4^o\, \langle\overline{r^4}\rangle_{3d}$$

where $\overline{\langle r^4 \rangle}_{3d}$ is the expectation value of r^4 calculated using the normalized (3d) radial functions. As the hole formalism is being employed, the sign of the coefficient A_4° is negative and hence the doubly degenerate $^2E(T_d)$ manifold lies above the triply degenerate $^2T_2(T_d)$ manifold. In crystal field theory, the Stark splitting of the $^2E(T_d)$ and $^2T_2(T_d)$ manifolds is designated as 10Dq where

$$10Dq = -\frac{15}{21}\sqrt{\frac{9}{4\pi}}\ A_4^\circ\ \overline{\langle r^4 \rangle}_{3d}$$

thus

$$\langle e|V_c|e\rangle = 6Dq$$

and

$$\langle t_2^+|V_c|t_2^+\rangle = -4Dq$$

Trigonal Perturbation

As the crystals under consideration have a small axial distortion along the hexagonal c-axis, the cubic potential must then be modified by a small trigonal component having the lower symmetry C_{3v}. The effect of the trigonal perturbation on the cubic field levels is ascertained on noting that when the local symmetry of the cation site is lowered from T_d to C_{3v}, the irreducible representation $^2E(T_d)$ remains irreducible in the C_{3v} point group while the $^2T_2(T_d)$ representation is reducible and can be factored into the irreducible representations $^2A_1(C_{3v})$ and $^2E(C_{3v})$ of the C_{3v} point group, (see for

TABLE 1

ONE ELECTRON CUBIC WAVE FUNCTIONS

---

^2E

$$e = \sqrt{\frac{1}{3}}\, d_2 + \sqrt{\frac{2}{3}}\, d_{-1}$$

$$e' = -\sqrt{\frac{1}{3}}\, d_{-2} + \sqrt{\frac{2}{3}}\, d_1$$

$^2T_2$

$$t_2^+ = \sqrt{\frac{2}{3}}\, d_2 - \sqrt{\frac{1}{3}}\, d_{-1}$$

$$t_2^\circ = d_\circ$$

$$t_2^- = -\sqrt{\frac{2}{3}}\, d_{-2} - \sqrt{\frac{1}{3}}\, d_1$$

example Wilson, Decius and Cross[43]). Hence under the influence of the trigonal perturbation, the $^2E(T_d)$ level remains degenerate while the triply degenerate $^2T_2(T_d)$ level splits into an orbital doublet $^2E(C_{3v})$ and an orbital singlet $^2A_1(C_{3v})$. The relative positions of the $^2E(C_{3v})$ and $^2A_1(C_{3v})$ levels derived from the $^2T_2(T_d)$ level will depend upon whether the trigonal distortion represents a compression or distention along the hexagonal c-axis.

The matrix elements of the trigonal perturbation

$$V_t = B_2^\circ r^2 Y_2^\circ(\theta,\phi) + B_4^\circ r^4 Y_4^\circ(\theta,\phi)$$

are evaluated using as basis the cubic wave functions and are given below

$$\langle t_2^+ |V_t| t_2^+\rangle = \langle t_2^- |V_t| t_2^-\rangle = D\sigma + \frac{2}{3} D\tau$$

$$\langle t_2^\circ |V_t| t_2^\circ\rangle = -2D\sigma - 6D\tau$$

$$\langle e|V_t|e\rangle = \langle e'|V_t|e'\rangle = \frac{7}{3} D\tau$$

$$\langle t_2^+ |V_t|e\rangle = \langle t_2^-|V_t|e'\rangle = \sqrt{2}(D\sigma - \frac{5}{3}D\tau),$$

where the trigonal parameters $D\sigma$ and $D\tau$ are defined as follows

$$D\sigma = -\frac{1}{14}\sqrt{\frac{5}{\pi}}\, B_2^\circ \langle\overline{r^2}\rangle_{3d}$$

$$D\tau = -\frac{1}{21}\sqrt{\frac{9}{4\pi}}\, B_4^\circ \langle\overline{r^4}\rangle_{3d}\,.$$

In the presence of a trigonal field, it is customary to define the energy separation of the $^2E(T_d)$ level from the center of gravity of the $^2T_2(T_d)$ levels to be 10Dq even though a small part of this energy splitting is due to the trigonal field, (see Figure I). This, in effect, modifies the expressions (I-1) and (I-2) given previously for the tetrahedral field and trigonal perturbation respectively. The cubic field term giving rise to the energy separation 10Dq must then be redefined to be

$$V_c = r^4(A_4^\circ + \frac{7}{27} B_4^\circ)[Y_4^\circ + \sqrt{\frac{10}{7}}(Y_4^3 - Y_4^{-3})] \qquad \text{(II-1)}$$

and the perturbation representing the trigonal distortion becomes

$$V_t = B_2^\circ r^2 Y_2^\circ - \frac{1}{27} B_4^\circ r^4[20Y_4^\circ + \sqrt{70}(Y_4^3 - Y_4^{-3})] \qquad \text{(II-2)}$$

The above expressions for the cubic and axial fields offers the simplification that matrix elements of V_t within the $^2E(T_d)$ manifold vanish. The matrix elements for the terms V_c and V_t given by equations (II-1) and (II-2) respectively are shown in Table 2. The non-zero matrix elements not shown in Table 2 may be determined from the Hermitian property of the operator V_t. Here the energy splitting 10Dq is then defined by

$$10Dq = (-\frac{5}{7}\sqrt{\frac{9}{4\pi}} A_4^\circ - \frac{35}{9} D\tau) \langle r^4 \rangle_{3d}$$

and the trigonal parameters K and K' are given by the relations

$$K = -D\sigma - \frac{20}{9} D\tau \qquad \text{(II-3)}$$

and

$$K' = D\sigma - \frac{5}{3} D\tau, \qquad \text{(II-4)}$$

where the energy separation of the $^2T_2(T_d)$ manifold split apart by the trigonal field is 3K.

Spin-Orbit Considerations

As discussed previously, one need only consider the one electron spin-orbit interaction energy

$$H_{so} = - \zeta \vec{\ell} \cdot \vec{s}. \qquad \text{(II-5)}$$

Since a $(3d)^9$ configuration is under consideration, the multiplet structure is inverted as the shell is more than half filled yielding a negative value for the spin-orbit parameter (see Condon and Shortley[7]) Here the spin-orbit parameter will be defined as being positive, the negative sign appearing in the spin-orbit interaction energy, equation (II-5), then takes into account the inverted multiplet structure.

The energy level splitting, including the spin-orbit interaction energy, may be investigated qualitatively as follows. The spin-orbit interaction energy transforms like the identity representation under the operations of the full rotation group,[17] the irreducible representations of the full rotation group being labeled by J, the total angular momentum of the system with the inclusion of spin. The components of the basis for the irreducible representations of the full rotation group are then labeled by M_z, the component of the total angular momentum along the z-axis.

TABLE 2

MATRIX ELEMENTS OF V_t IN THE CUBIC REPRESENTATION *

	e	e'	t_2^+	t_2^-	t_2°
e			$\sqrt{2}\,K'$		
e'				$\sqrt{2}\,K'$	
t_2^+			$-K$		
t_2^-				$-K$	
t_2°					$2K$

* The non-zero matrix elements not listed may be found from the Hermitian property of the operator V_t.

On lowering the spatial symmetry of the Hamiltonian with the inclusion of the tetrahedral and axial fields, the symmetry of the Hamiltonian is lowered from that of the full rotation group to C_{3v}. The wave functions with the inclusion of spin will then form basis for the irreducible representations of the $\overline{C}_{3v}$ double group, here the double group must be used as the total angular momentum of the system is half integer.[18] Since the ultimate degeneracies of the energy levels is independent of the initial functions, one may then investigate the reduction of the reducible representation formed from the direct product of the cubic functions forming the basis of the irreducible representations of the C_{3v} group with the spin functions under the operations of the $\overline{C}_{3v}$ double group (for character table see reference 42). Under the symmetry operations of the $\overline{C}_{3v}$ group, the spin functions $\frac{1}{2}$ and $-\frac{1}{2}$ form basis for the two fold degenerate double valued representation Γ_6 while the orbital functions form basis for the single valued representations A_1 and E. The direct product representation of the spin and orbital functions is reducible and on reduction give

$$\Gamma_6 \times A_1 \longrightarrow \Gamma_6$$

$$\Gamma_6 \times E \longrightarrow \Gamma_6 + \Gamma_4 + \Gamma_5$$

Direct Product Representation — Irreducible Representations of the $\overline{C}_{3v}$ Group

Either by inspection of the secular equation or by investigating the transformation properties of the direct product functions, linear combinations of these functions may be constructed exhibiting the symmetry of the $\overline{C_{3v}}$ group. These functions are given in Table 3. The transformation properties of the wave functions given in Table 3 are indicated and following standard convention the first index labels the irreducible representation of the $\overline{C}_{3v}$ double group and the second and third indices label the parent trigonal and tetrahedral levels respectively from which the functions were derived.

Without the inclusion of the spin-orbit interaction energy in the Hamiltonian, the energy level splitting exhibited by the Hamiltonian

$$H = H_{fi} + V_c + V_t$$

using the functions given in Table 3 as basis remains the same as discussed previously except now the levels exhibit twice the degeneracy due to the inclusion of the spin functions. On including the spin-orbit interaction energy in the Hamiltonian, the energy pattern is now split owing to the scrambling of the free ion $^2D_{5/2}$ and $^2D_{3/2}$ states in the cubic wave functions. The final energy splitting of the ^2D free ion state is shown in Figure 1. The spin-orbit levels Γ_4 and Γ_5 are still shown to remain degenerate up through the spin-orbit perturbation even though Γ_4 and Γ_5 are distinct irreducible representations of the $\overline{C}_{3v}$ double group. This remaining degeneracy is due to the fact that the Hamiltonian is invariant under time reversal,[19] an additional symmetry operation which has not been considered here.

TABLE 3

CUBIC FIELD FUNCTIONS FORMING BASIS

FOR THE IRREDUCIBLE REPRESENTATIONS

OF THE $\bar{C}_{3v}$ DOUBLE GROUP

	$^2E\ (T_d)$
$\Gamma_6\ (^2E(^2E))$	$\frac{1}{2}\ e$
	$-\frac{1}{2}\ e'$
$\Gamma_4, \Gamma_5\ (^2E(^2E))$	$\psi_5 = \sqrt{\frac{1}{2}}\ [(\frac{1}{2}\ e') + i(-\frac{1}{2}\ e)]$
	$\psi_6 = \sqrt{\frac{1}{2}}\ [(\frac{1}{2}\ e') - i(-\frac{1}{2}\ e)]$
	$^2T_2\ (T_d)$
$\Gamma_6(^2A_1(^2T_2))$	$\frac{1}{2}\ t_2^\circ$
	$-\frac{1}{2}\ t_2^\circ$
$\Gamma_6(^2E(^2T_2))$	$\frac{1}{2}\ t_2^+$
	$-\frac{1}{2}\ t_2^-$
$\Gamma_4, \Gamma_5(^2E(^2T_2))$	$\psi_3 = \sqrt{\frac{1}{2}}\ [(\frac{1}{2}\ t_2^-) + i(-\frac{1}{2}\ t_2^+)]$
	$\psi_4 = \sqrt{\frac{1}{2}}\ [(\frac{1}{2}\ t_2^-) - i(-\frac{1}{2}\ t_2^+)]$

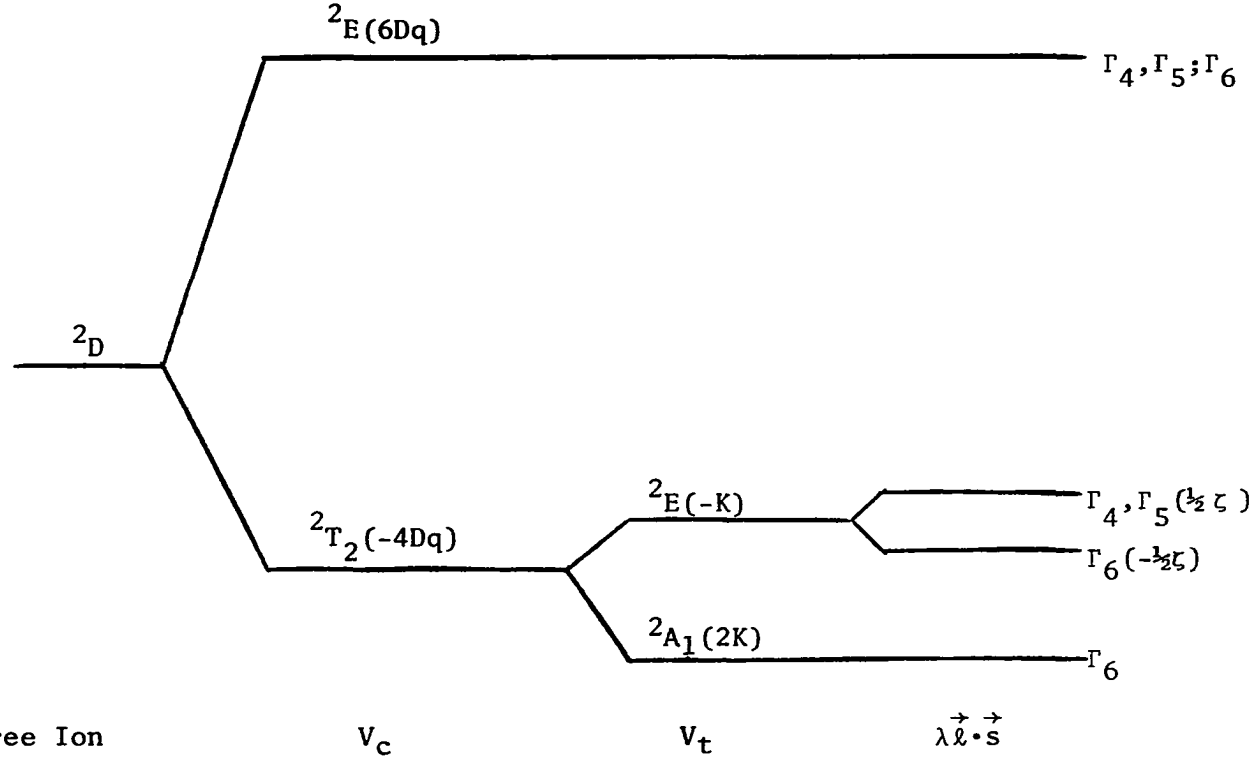

Figure 1. Energy level diagram of Cu^{2+} in a Tetrahedral field (Strong axial field)

Under time reversal the basis of the irreducible representations Γ_4 and Γ_5 are interchanged,[19] thus they must correspond to the same eigenvalue of the Hamiltonian and serve as basis for the doubly degenerate Γ_4, Γ_5 level.

The matrix elements of $H_{so} = -\zeta\, \vec{\ell}\cdot\vec{s}$ may be evaluated in the representation given in Table 3 using the relation

$$H_{so} = -\zeta[\ell_z s_z + \frac{1}{2}(\ell_+ s_- + \ell_- s_+)], \tag{II-6}$$

and[20]

$$(J_+)_{op}\,\psi(J,M) = \hbar\sqrt{(J-M)(J+M+1)}\;\;\psi(J,M+1) \tag{II-7}$$

$$(J_-)_{op}\,\psi(J,M) = \hbar\sqrt{(J-M+1)(J+M)}\;\;\psi(J,M-1)$$

$$(J_z)_{op}\,\psi(J,M) = \hbar\, M\,\psi(J,M),$$

where the operators J_+ and J_- are the step operators constructed from the angular momenta operators and are defined by the general relations

$$J_+ = J_x + i\,J_y$$

$$J_- = J_x - i\,J_y.$$

The matrix elements for H_{so} are shown in Table 4. Here it is seen that the spin-orbit parameter ζ has been defined such that

$$\zeta = 2\left\langle \frac{1}{2}\,t_2^+ \left|H_{so}\right| \frac{1}{2}\,t_2^+ \right\rangle$$

TABLE 4

MATRIX ELEMENTS OF $\lambda \vec{\ell}\cdot\vec{s}$ IN THE

UNCOUPLED REPRESENTATION

Γ_6

	$\frac{1}{2}$ e	$-\frac{1}{2}$ e'	$\frac{1}{2}$ t_2°	$-\frac{1}{2}$ t_2°	$-\frac{1}{2}$ t_2^-	$\frac{1}{2}$ t_2^+
$\frac{1}{2}$ e				$-\zeta'$		$-\zeta'/\sqrt{2}$
$-\frac{1}{2}$ e'			$-\zeta'$		$-\zeta'/\sqrt{2}$	
$\frac{1}{2}$ t_2°					$\zeta/\sqrt{2}$	
$-\frac{1}{2}$ t_2°						$\zeta/\sqrt{2}$
$-\frac{1}{2}$ t_2^-					$-\zeta/2$	
$\frac{1}{2}$ t_2^+						$-\zeta/2$

Γ_4, Γ_5

	ψ_5	ψ_6	ψ_3	ψ_4
ψ_5			$(\sqrt{1/2}-i)\zeta'$	
ψ_6				$(\sqrt{1/2}+i)\zeta'$
ψ_3			$\zeta/2$	
ψ_4				$\zeta/2$

and

$$\zeta' = \sqrt{2} \left\langle \frac{1}{2}\, t_2^+ \left| H_{so} \right| \frac{1}{2}\, e \right\rangle,$$

where $\zeta = \zeta'$ for the pure ionic model. Although in the free ion the radial part of the wave function is independent of the magnetic quantum number m, the cubic wave functions for the $^2T_2$ and ^2E levels constructed from the free ion functions may exhibit somewhat different radial dependence owing to covalency with the surrounding ligands. Thus the spin-orbit parameters ζ and ζ' need not be equal and are reduced from their free ion values.

External Magnetic Field

For the case of an external magnetic field applied parallel to the hexagonal c-axis, the magnetic energy term is given by

$$H_{\parallel}^{m} = \mu_o (\ell_z + g_s\, s_z) \mathcal{H} .$$

The relation (II-7) may be employed to determine the matrix of the operator $(\ell_z + g_s\, s_z)$ in the representation given in Table 3 and the results are shown in Table 5. Here again owing to the mixing of the cation 3d orbitals with the nearest neighbor ligand 2s and 2p orbitals, an orbital reduction parameter has been included in the formalism.

The orbital reduction parameter for the intrablock $^2T_2$ elements is defined as

$$k = \left\langle t_2^+ \left| \ell_z \right| t_2^+ \right\rangle \qquad \text{(II-8)}$$

and for the interblock elements

$$k' = \sqrt{\frac{1}{2}} \langle t_2^+ | \ell_z | e \rangle \qquad \text{(II-9)}$$

It is seen that when there is no covalency between the substitutional cation and the nearest neighbor ligands, the orbital reduction parameters become $k = k' = 1$.

For the external magnetic field directed perpendicular to the hexagonal c-axis, the magnetic energy term resulting from the interaction of the magnetic moment with the external field may be written as

$$H_{\perp}^{m} = \mu_o (\ell_x + g_s s_x) \mathcal{H} .$$

Similarly as above, the matrix elements of the operator $(\ell_x + g_s s_x)$ have been evaluated in the representation given in Table 3 and are shown in Table 6. The orbital reduction parameters found in Table 6 are defined consistent with the definitions (II-8) and (II-9) for k and k' respectively.

TABLE 5

MATRIX ELEMENTS OF $(\ell_z + g_s s_z)$ IN THE UNCOUPLED REPRESENTATION

		Γ_4, Γ_5			
		ψ_5	ψ_6	ψ_3	ψ_4
Γ_4, Γ_5	ψ_5		$\frac{1}{2} g_s$		$-\sqrt{2}\, k'$
	ψ_6			$-\sqrt{2}\, k'$	
	ψ_3				$-k + \frac{1}{2} g_s$
	ψ_4				

		Γ_6				
	$\frac{1}{2} e$	$-\frac{1}{2} e'$	$-\frac{1}{2} t_2^-$	$\frac{1}{2} t_2^+$	$\frac{1}{2} t_2^\circ$	$-\frac{1}{2} t_2^\circ$
$\frac{1}{2} e$	$\frac{1}{2} g_s$			$\sqrt{2}\, k'$		
$-\frac{1}{2} e'$		$-\frac{1}{2} g_s$	$-\sqrt{2}\, k'$			
$-\frac{1}{2} t_2^-$			$-k - \frac{1}{2} g_s$			
$\frac{1}{2} t_2^+$				$k + \frac{1}{2} g_s$		
$\frac{1}{2} t_2^\circ$					$\frac{1}{2} g_s$	
$-\frac{1}{2} t_2^\circ$						$-\frac{1}{2} g_s$

TABLE 6

MATRIX ELEMENTS OF $(l_x + g_s s_x)$ IN THE UNCOUPLED REPRESENTATION

Interblock Elements

	ψ_3	ψ_4	$\frac{1}{2}t_2^\circ$	$-\frac{1}{2}t_2^\circ$	$-\frac{1}{2}t_2^-$	$\frac{1}{2}t_2^+$
ψ_5			$\sqrt{\frac{1}{2}}\,k'$	$-i\sqrt{\frac{1}{2}}\,k'$	$i\sqrt{\frac{1}{2}}\,k'$	$\sqrt{\frac{1}{2}}\,k'$
ψ_6			$\sqrt{\frac{1}{2}}\,k'$	$i\sqrt{\frac{1}{2}}\,k'$	$-i\sqrt{\frac{1}{2}}\,k'$	$\sqrt{\frac{1}{2}}\,k'$
$\frac{1}{2}e$	$-\sqrt{\frac{1}{2}}\,k'$	$-\sqrt{\frac{1}{2}}\,k'$	k'			
$-\frac{1}{2}e'$	$i\sqrt{\frac{1}{2}}\,k'$	$-i\sqrt{\frac{1}{2}}\,k'$		k'		

Intrablock Elements

	ψ_3	ψ_4	$\frac{1}{2}t_2^\circ$	$-\frac{1}{2}t_2^\circ$	$-\frac{1}{2}t_2^-$	$\frac{1}{2}t_2^+$
ψ_3			$-\frac{1}{2}k$	$i\frac{1}{2}k$	$\frac{1}{2}\sqrt{\frac{1}{2}}\,g_s$	$-i\frac{1}{2}\sqrt{\frac{1}{2}}\,g_s$
ψ_4			$-\frac{1}{2}k$	$-i\frac{1}{2}k$	$\frac{1}{2}\sqrt{\frac{1}{2}}\,g_s$	$i\frac{1}{2}\sqrt{\frac{1}{2}}\,g_s$
$\frac{1}{2}t_2^\circ$				$\frac{1}{2}g_s$		$-\sqrt{\frac{1}{2}}\,k$
$-\frac{1}{2}t_2^\circ$					$-\sqrt{\frac{1}{2}}\,k$	
$-\frac{1}{2}t_2^-$						
$\frac{1}{2}t_2^+$						

CHAPTER III

SECOND ORDER PERTURBATION THEORY

General Considerations

Dietz et. al.[14] have worked out the first order theory for an one electron system in their analysis of the optical spectrum of Cu^{2+}:ZnO. Since the spin-orbit parameter for the Cu^{2+} free ion is rather large, ζ = 830 cm^{-1}, and the Dq value for Cu^{2+}:ZnO is approximately 600 cm^{-1},[14,26] one finds that there are large off diagonal elements connecting the cubic field $^2E(T_d)$ and $^2T_2(T_d)$ manifolds. Thus a first order theory may not be adequate to interpret the system.

The problem is then to reduce the 10×10 secular equation to one of manageable size. This can be achieved if a similarity transformation is carried out to reduce the magnitude of the elements connecting the $^2T_2(T_d)$ and $^2E(T_d)$ manifolds. The perturbing effect of the $^2E(T_d)$ manifold on the $^2T_2(T_d)$ ground state manifold is then reduced and the $^2T_2(T_d)$ manifold may then be diagonalized independently of the excited $^2E(T_d)$ manifold.

This transformation may be constructed using the second order degenerate perturbation formulism developed by Van Vleck.[22,23] A

brief discussion of this method is as follows. Assume that the Hamiltonian of the system can be expressed as

$$H = H_o + \lambda H_1 + \lambda^2 H_2 , \qquad \text{(III-1)}$$

where H_o is the Hamiltonian of the unperturbed system and H_1 and H_2 are the perturbing terms. The parameter λ, as is customary, designates the order of magnitude of terms appearing in the expansion of the Hamiltonian and is chosen such that when $\lambda \to 0$ the Hamiltonian of the system reduces to the unperturbed Hamiltonian H_o. Further let the unperturbed Hamiltonian be diagonal in those quantum numbers represented by the high frequency index k which labels the coarse structure of the energy matrix. The low frequency quantum index j is then reserved to label the subblock structure of a given k manifold.

A unitary transformation is then to be constructed which eliminates elements of magnitude λ arising from the perturbing term H_1 connecting the ground state manifold labeled by the symmetry index k with other perturbing levels ($k' \neq k$). The form of the transformation may be taken as[24]

$$T = e^{i\lambda S} = I + i\lambda S - \frac{1}{2} \lambda^2 S^2 + \ldots, \qquad \text{(III-2)}$$

where I represents the unit matrix and S is a Hermitian matrix chosen to satisfy the conditions to be imposed on the transformation. The transformed Hamiltonian matrix G may be written as

$$G = T^{-1} H T = G_o + \lambda G_1 + \lambda^2 G_2 + \ldots \qquad \text{(III-3)}$$

or on multiplying through on the left in the above expression by T, the equation for the determination of G takes the form

$$(I + i\lambda S - \frac{1}{2}\lambda^2 S^2 - \ldots)(G_o + \lambda G_1 + \lambda^2 G_2 + \ldots)$$

$$= (H_o + \lambda H_1 + \lambda^2 H_2)(+ i\lambda S - \frac{1}{2}\lambda^2 S^2 + \ldots) ,$$

where in the above relation, the expansion for T given by equation (III-2) has been introduced. On equating coefficients of like powers of λ, one finds that up to the second order the elements of the transformed Hamiltonian, equation (III-3), are given by

$$\begin{aligned} G_o &= H_o \\ G_1 &= H_1 + i(H_o S - S G_o) \\ G_2 &= H_2 + i(H_1 S - S G_1) - \frac{1}{2}(H_o S^2 - S^2 G_o) \ . \end{aligned} \qquad \text{(III-4)}$$

The transformation matrix S is defined from the following conditions, first that there be no elements of G_1 connecting the ground state manifold with other perturbing levels and the second condition is that the transformation does not effect the intrablock elements $H(kj,kj')$ of the ground state manifold. The first condition is fullfilled if the transformation satisfies the condition that

$$G_1 (kj;k'j') = 0 \qquad (k \neq k')$$

or

$$H_1(kj;k'j') = i[H_o(k'j';k'j') - H_o(kj;kj)]\ S(kj;k'j')$$

from which it is seen that the interblock elements of S are given by

$$S(kj;k'j') = i\ \frac{H_1(kj;k'j')}{E^\circ_k - E^\circ_{k'}} \quad . \tag{III-5}$$

Here the j dependence of the unperturbed energy difference $(E^\circ_{kj}-E^\circ_{k'j'})$ is ignored as it is assumed that the unperturbed intralevel spacing of the ground state manifold is much smaller than the interlevel spacing of the ground state manifold with other perturbing levels. The unperturbed energy difference $(E^\circ_k-E^\circ_{k'})$ is then to be measured from the center of gravity of the two manifolds under consideration. The intrablock elements of S may be chosen to be zero

$$S(kj;kj') = 0$$

and hence the second condition is satisfied.

The elements for the k manifold of the transformed energy matrix G may now be determined on substituting equation (III-5) for S into the expression (III-4) for the transformed energy matrix, thus we have

$$G_o(kj;kj) = H_o(kj;kj) \tag{III-6}$$

$$G_1(kj;kj') = H_1(kj;kj') \tag{III-7}$$

and

$$G_2(kj;kj') = H_2(kj;kj') \qquad \text{(III-8)}$$

$$+ \sum_{k' \neq k} \sum_{j''} \frac{H_1(kj;k'j'')\, H_1(k'j'';kj')}{E_k^\circ - E_{k'}^\circ} \quad .$$

Field Independent Terms

First, only those terms up through the spin-orbit interaction energy and trigonal field will be treated. From the optical spectrum it is found that the cubic field splitting is about an order of magnitude larger than the intralevel splitting of the $^2T_2(T_d)$ manifold which arises from the spin-orbit interaction energy and trigonal field.[14] Thus the unperturbed Hamiltonian will be taken as

$$H_o = H + V_c$$

and the perturbation is then given by

$$H_1 = V_t - \zeta \vec{\ell}\cdot\vec{s}$$

$$H_2 = 0 \quad ,$$

where the elements for H_1 are given in Table 7. The wave functions diagonalizing H_o are found in Table 3 and here it is seen that those quantum numbers associated with the quantum index k are the symmetry indices $^2T_2(T_d)$ and $^2E(T_d)$ denoting the Stark levels into which the

TABLE 7

MATRIX ELEMENTS OF THE HAMILTONIAN EXCLUSIVE OF THE MAGNETIC FIELD TERMS IN THE UNCOUPLED REPRESENTATION

			Γ_6			
	$\frac{1}{2}$ e	$-\frac{1}{2}$ e'	$\frac{1}{2}$ t_2°	$-\frac{1}{2}$ t_2°	$-\frac{1}{2}$ t_2^-	$\frac{1}{2}$ t_2^+
$\frac{1}{2}$ e	6Dq			$-\zeta'$		$\sqrt{\frac{1}{2}}(2K'-\zeta')$
$-\frac{1}{2}$ e'		6Dq	$-\zeta'$		$\sqrt{\frac{1}{2}}(2K'-\zeta')$	
$\frac{1}{2}$ t_2°			$-4Dq+2K$		$\sqrt{\frac{1}{2}}\zeta$	
$-\frac{1}{2}$ t_2°				$-4Dq+2K$		$\sqrt{\frac{1}{2}}\zeta$
$-\frac{1}{2}$ t_2^-					$-4Dq-K-\frac{1}{2}\zeta$	
$\frac{1}{2}$ t_2^+						$-4Dq-K-\zeta/2$

TABLE 7 (continued)

Γ_4, Γ_5

	ψ_5	ψ_6	ψ_3	ψ_4
ψ_5	6Dq	$\sqrt{\frac{1}{2}}(2K'+\zeta')-i\zeta'$		
ψ_6		6Dq	$\sqrt{\frac{1}{2}}(2K'+\zeta')+i\zeta'$	
ψ_3			$-4Dq-K+\frac{1}{2}\zeta$	
ψ_4				$-4Dq-K+\frac{1}{2}\zeta$

free ion $(3d)^9\ ^2D$ configuration splits under the influence of the tetrahedral field. The quantum index j are those symmetry indices labeling the irreducible representations of the $\overline{C}_{3v}$ group. From symmetry arguements alone, the basis chosen give maximum factorization of the Hamiltonian matrix H as can be seen from inspection of Table 7. Since the perturbation H_1 introduces first order elements connecting the $^2E(T_d)$ and $^2T_2(T_d)$ manifolds, a transformation is to be carried out such that the transformed Hamiltonian does not contain first order interlevel elements. The first symmetry species to be treated are those elements associated with the $\Gamma_4,\Gamma_5(^2T_2)$ and $\Gamma_4,\Gamma_5(^2E)$ levels. The second order elements which fold into the $^2T_2(T_d)$ manifold may be found on substituting the first order interlevel elements given in Table 7 into equation (III-8) for G_2. It is then found that

$$G_2(\psi_3;\psi_3) = G_2(\psi_4;\psi_4) = -\frac{1}{20Dq}(2K'+\zeta')^2 - \frac{1}{10Dq}\zeta'^2 . \qquad \text{(III-9)}$$

As there are no first or second order elements connecting the components of the $\Gamma_4,\Gamma_5(^2T_2)$ subblock with other symmetry species of the $^2T_2(T_d)$ manifold, the second order energy for the doubly degenerate $\Gamma_4,\Gamma_5(^2T_2)$ level is given by

$$W(kj;kj) = H_o(kj;kj) + H_1(kj;kj) + G_2(kj;kj) \qquad \text{(III-10)}$$

and on substituting into the above relation (III-10) the elements given in Table 7 for $G_o(\psi_3;\psi_3)$ and $G_1(\psi_3;\psi_3)$, and the expression (III-9) for $G_2(\psi_3;\psi_3)$, the second order energy expression (III-10) becomes

$$W(\Gamma_4,\Gamma_5(^2T_2)) = -4Dq-K + \frac{1}{2}\zeta - \frac{1}{20Dq}(2K' + \zeta')^2 - \frac{1}{10Dq}\zeta'^2 . \qquad \text{(III-11)}$$

From inspection of Table 7, it is seen that those elements of H associated with the Γ_6 symmetry species may be grouped into two identical subblocks. There are first order elements connecting components having the same transformation properties of the two distinct $\Gamma_6(^2T_2)$ representations as well as first order elements connecting the components of the $\Gamma_6(^2E)$ and $\Gamma_6(^2T_2)$ levels. The second order correction to the energy arising from folding the interblock elements into the $^2T_2(T_d)$ manifold may be evaluated as previously shown for the $\Gamma_4,\Gamma_5(T_d)$ subblock and it is found that

$$G_2(-\tfrac{1}{2}t_2^o;\ \tfrac{1}{2}t_2^o) = G_2(-\tfrac{1}{2}t_2^o;\ -\tfrac{1}{2}t_2^o) = -\frac{\zeta'^2}{10Dq} \qquad \text{(III-12)}$$

$$G_2(\tfrac{1}{2}t_2^+;\ \tfrac{1}{2}t_2^+) = G_2(-\tfrac{1}{2}t_2^-;\ -\tfrac{1}{2}t_2^-) = -\frac{1}{20Dq}(2K'-\zeta')^2$$

$$G_2(-\tfrac{1}{2}t_2^o;\ \tfrac{1}{2}t_2^+) = G_2(\tfrac{1}{2}t_2^o,-\tfrac{1}{2}t_2^-) = \sqrt{\tfrac{1}{2}}\,\frac{\zeta'}{10Dq}(2K'-\zeta') .$$

The elements for the $\Gamma_6(^2T_2)$ manifolds of the transformed Hamiltonian G are then determined on substituting into the relation

$$G(kj;kj') = H_o(kj;kj') + H_1(kj;kj') + G_2(kj;kj') \ , \qquad \text{(III-13)}$$

the intralevel elements of $\Gamma_6(^2T_2)$ for H_o and H_1 given in Table 7 and the second order corrections evaluated in equation (III-12).

On isolating the $\Gamma_6(^2T_2)$ manifold, (see Table 8), it is found that there are now first and second order elements connecting the components of the two unperturbed $\Gamma_6(^2T_2)$ levels. Thus to obtain the second order energy expressions, a 2×2 energy matrix must be diagonalized. On diagonalization the eigenvalues are found to be given by

$$W^+(\Gamma_6(^2T_2)) = -4Dq + \frac{1}{2}K - \frac{1}{4}\zeta - \frac{\zeta'^2}{20Dq} \qquad \text{(III-14)}$$

$$- \frac{1}{40Dq}(2K'-\zeta')^2 + \frac{1}{2}\left[\left(3K + \frac{1}{2}\zeta - \frac{\zeta'^2}{10Dq} + \frac{1}{20Dq}(2K'-\zeta')^2\right)^2\right.$$

$$\left. + 2\left(\zeta + \frac{\zeta'}{10Dq}(2K'-\zeta')\right)^2\right]^{\frac{1}{2}}$$

and

$$W^-(\Gamma_6(^2T_2)) = -4Dq + \frac{1}{2}K - \frac{1}{4}\zeta - \frac{\zeta'^2}{20Dq} \qquad \text{(III-15)}$$

$$- \frac{1}{40Dq}(2K'-\zeta')^2 - \frac{1}{2}\left[\left(3K + \frac{1}{2}\zeta - \frac{\zeta'^2}{10Dq} + \frac{1}{20Dq}(2K'-\zeta')^2\right)^2\right.$$

$$\left. + 2\left(\zeta + \frac{\zeta'}{10Dq}(2K'-\zeta')^2\right]^{\frac{1}{2}}\right. \ .$$

The eigenfunctions for the doubly degenerate $W^{+}(\Gamma_6(^2T_2))$ level may be expressed as

$$\psi_1^{+} = \alpha[(-\frac{1}{2}t_2^{\circ}) + \frac{\zeta'}{10Dq}(-\frac{1}{2}e')] + \beta[(-\frac{1}{2}t_2^{-}) - \sqrt{\frac{1}{2}}\,\frac{1}{10Dq}(2K'-\zeta')(-\frac{1}{2}e')]$$

$$\psi_2^{+} = \alpha[(-\frac{1}{2}t_o) + \frac{\zeta'}{10Dq}(\frac{1}{2}e)] + \beta[(\frac{1}{2}t_2^{+}) - \sqrt{\frac{1}{2}}\,\frac{1}{10Dq}(2K'-\zeta')(\frac{1}{2}e)] \qquad \text{(III-16)}$$

and for the $W^{-}(\Gamma_6(^2T_2))$ level

$$\psi_3^{-} = \beta[(\frac{1}{2}t_2^{\circ}) + \frac{\zeta'}{10Dq}(-\frac{1}{2}e')] - \alpha[(-\frac{1}{2}t_2^{-}) - \sqrt{\frac{1}{2}}\,\frac{1}{10Dq}(2K'-\zeta')(\frac{1}{2}e')]$$

$$\psi_4^{-} = \beta[(-\frac{1}{2}t_2^{\circ}) + \frac{\zeta'}{10D}(\frac{1}{2}e)] - \alpha[(\frac{1}{2}t_2^{+}) - \sqrt{\frac{1}{2}}\,\frac{1}{10Dq}(2K'\zeta')(\frac{1}{2}e)] \qquad \text{(III-17)}$$

The mixing coefficients α and β are defined by the condition of normalization

$$\alpha^2 + \beta^2 = 1$$

and by the relation

$$\frac{\alpha\beta}{(\alpha^2-\beta^2)} = \frac{\sqrt{\frac{1}{2}}[\zeta + \frac{\zeta'}{10Dq}(2K'-\zeta')]}{(3K + \frac{1}{2}\zeta - \frac{\zeta'^2}{10Dq} + \frac{1}{20Dq}(2K'-\zeta')^2)}$$

and it is found that

$$\alpha = \sqrt{\frac{1}{2}} \left(1 + \delta/\Delta_1\right)^{\frac{1}{2}} \qquad \text{(III-18)}$$

$$\beta = \sqrt{\frac{1}{2}} \left(1 - \delta/\Delta_1\right)^{\frac{1}{2}} ,$$

where the unperturbed energy splitting of the $\Gamma_6(^2T_2)$ manifold is given by

$$\delta = 3K + \frac{1}{2}\zeta - \frac{\zeta'^2}{10Dq} + \frac{1}{20Dq}\left(2K' - \zeta'\right)^2 \qquad \text{(III-19)}$$

and the perturbed energy splitting is

$$\Delta_1 = W^+\left(\Gamma_6(^2T_2)\right) - W^-\left(\Gamma_6(^2T_2)\right). \qquad \text{(III-20)}$$

Two useful expressions relating the unperturbed energy δ and the interaction energy W_{12}, where

$$W_{12} = \sqrt{\frac{1}{2}}\left[\zeta + \frac{\zeta'}{10Dq}\left(2K' - \zeta'\right)\right] , \qquad \text{(III-21)}$$

to the perturbed energy separation Δ_1 may be obtained from equations (III-18) and on reduction it is found that

$$\delta = (\alpha^2 - \beta^2)\,\Delta_1 \qquad \text{(III-22)}$$

and

$$W_{12} = \alpha\,\beta\,\Delta_1 . \qquad \text{(III-23)}$$

TABLE 8

THE TRANSFORMED HAMILTONIAN FOR

THE $\Gamma_6(^2T_2)$ SUBBLOCK

	$\frac{1}{2}\,t_2^\circ$	$-\frac{1}{2}\,t_2^\circ$	$-\frac{1}{2}\,t_2^-$	$\frac{1}{2}\,t_2^+$
$\frac{1}{2}\,t_2^\circ$	$2K-\frac{\zeta'^2}{10Dq}$		$\sqrt{\frac{1}{2}}\left[\zeta+\frac{\zeta'}{10Dq}(2K'-\zeta')\right]$	
$-\frac{1}{2}\,t_2^\circ$		$2K-\frac{\zeta'^2}{10Dq}$		$\sqrt{\frac{1}{2}}\left[\zeta+\frac{\zeta'}{10Dq}(2K'-\zeta')\right]$
$-\frac{1}{2}\,t_2^-$			$-K-\frac{\zeta}{2}-\frac{1}{20Dq}(2K'-\zeta')^2$	
$\frac{1}{2}\,t_2^+$				$-K-\frac{\zeta}{2}-\frac{1}{20Dq}(2K'-\zeta')^2$

External Magnetic Field

To interpret the paramagnetic resonance spectra and susceptibility measurements, it is necessary to include into the Hamiltonian formalism the energy arising from the external magnetic field. The case to be treated first is that for which the external field is directed perpendicular to the hexagonal c-axis. The Hamiltonian for the magnetic energy assumes the form

$$H^m = \mu_o(\ell_x + g_s s_x)\mathcal{H} ,$$

(see equation (I-3)). The matrix elements of the operator $(\ell_x+g_s s_x)$ have been previously evaluated using as basis the uncoupled representation and are given in Table 6. It is seen from inspection of Table 6 that there are magnetic elements connecting the $^2T_2(T_d)$ ground state with the excited $^2E(T_d)$ state. As these terms give rise to second order corrections to the g-factors and quadratic Zeeman effect, they must be folded into the $^2T_2(T_d)$ manifold.

A transformation matrix T is then to be constructed such that it reduces to the second order not only the perturbation H_1 treated in the previous section but also those magnetic terms resulting from the magnetic energy H^m. This can be achieved if we take for the perturbation the Hamiltonian

$$H_p = H_1 + H^m ,$$

where

$$H_1 = V_t - \zeta \vec{\ell}.\vec{s} \tag{III-24}$$

and

$$H^m = \mu_o(\ell_x + g_s s_x)\mathcal{H} . \tag{III-25}$$

The elements of the transformation matrix S may be determined from equation (III-5) and are given by

$$S(kj;k'j') = - \frac{i}{10Dq} [H_1(kj;k'j') + H^m(kj;k'j')]$$

and the second order correction to the energy (III-8) becomes

$$G_2(kj;kj') = - \frac{1}{10Dq} \sum_{j''} [H_1(kj;k'j'')H_1(k'j'';kj') \tag{III-26}$$

$$H_1(kj;k'j'')H^m(k'j'';kj')+H^m(kj;k'j'')H_1(k'j'';kj')+H^m(kj;k'j'')H^m(k'j'';kj')].$$

$$(k' \neq k)$$

The summation over the high frequency index k' has already been carried out effectively as there are only two manifolds under consideration. The first term in the above expression for G_2, equation (III-26), have been evaluated previously and will not be considered further. The second and third terms are seen to be linear in the magnetic field strength and give rise to second order corrections to the g-factors

and quadratic Zeeman effect. The last term in equation (III-26) is quadratic in the field strength $\mathcal{H}$ and contributes to the quadratic Zeeman effect.

If the expression G_2^m represents those terms in equation (III-26) which contributes to the magnetic energy

$$G_2^m(kj;kj') = -\frac{1}{10Dq}[H_1(kj;k'j'')H^m(k'j'';kj') \qquad \text{(III-27)}$$

$$+ H^m(kj;k'j'')H_1(k'j'';kj')+H^m(kj;k'j'')H^m(k'j'';kj')] \ ,$$

explicit expressions for the magnetic terms folded into the $^2T_2(T_d)$ manifold may be obtained on substitution into the above expression (III-27) the interlevel elements for H^m and H_1 listed in Tables 6 and 7 respectively, thus

$$G_2^m\ (\psi_3;\psi_3) = G_2^m\ (\psi_4;\psi_4) \qquad \text{(III-28)}$$

$$= G_2^m\ (-\tfrac{1}{2}t_2^-;\ -\tfrac{1}{2}t_2^-) = G_2^m(\tfrac{1}{2}t_2^+;\ \tfrac{1}{2}t_2^+) = -\frac{k'^2}{10Dq}\mu_o^2\mathcal{H}^2$$

$$G_2^m\ (\tfrac{1}{2}t_2^\circ;\ \tfrac{1}{2}t_2^\circ) = G_2^m\ (-\tfrac{1}{2}t_2^\circ;\ -\tfrac{1}{2}t_2^\circ) = -\frac{2k'^2}{10Dq}\mu_o^2\mathcal{H}^2$$

$$G_2^{m*}\ (\psi_4;\ -\tfrac{1}{2}t_2^\circ) = G_2^m\ (\psi_3;\ -\tfrac{1}{2}t_2^\circ) = \frac{ik'}{10Dq}[\ \tfrac{1}{2}\ (2K'+\zeta')+i\sqrt{2}\ \zeta']\mu_o\mathcal{H}$$

$$+\frac{ik'^2}{\sqrt{2}10D_q}\mu_o^2\mathcal{H}^2$$

$$G_2^{m*}(\psi_4; \tfrac{1}{2}t_2^{\circ}) = G_2^{m}(\psi_3; \tfrac{1}{2}t_2^{\circ}) = -\frac{k'}{10Dq}\left[\tfrac{1}{2}(2K'+\zeta')+i\sqrt{2}\zeta'\right]\mu_o\mathcal{H} + \frac{k'^2}{\sqrt{2}\,10Dq}\mu_o^2\mathcal{H}^2$$

$$G_2^{m*}(\psi_4; -\tfrac{1}{2}t_2^{-}) = G_2^{m}(\psi_3; -\tfrac{1}{2}t_2^{-}) = \frac{k'\zeta'}{10Dq}\left(\sqrt{\tfrac{1}{2}} - i\right)\mu_o\mathcal{H}$$

$$G_2^{m*}(\psi_4; \tfrac{1}{2}t_2^{+}) = G_2^{m}(\psi_3; \tfrac{1}{2}t_2^{+}) = -i\frac{k'\zeta'}{10Dq}\left(\sqrt{\tfrac{1}{2}} - i\right)\mu_o\mathcal{H}$$

$$G_2^{m}\left(\tfrac{1}{2}t_2^{\circ}; -\tfrac{1}{2}t_2^{\circ}\right) = \frac{2k'\zeta'}{10Dq}\mu_o\mathcal{H}$$

$$G_2^{m}\left(\tfrac{1}{2}t_2^{\circ}; \tfrac{1}{2}t_2^{+}\right) = -\frac{k'}{\sqrt{2}\,10Dq}(2K'-\zeta')\mu_o\mathcal{H} - \frac{k'^2}{10Dq}\mu_o^2\mathcal{H}^2$$

$$G_2^{m}\left(-\tfrac{1}{2}t_2^{\circ}; -\tfrac{1}{2}t_2^{-}\right) = -\frac{k'}{\sqrt{2}\,10Dq}(2K'-\zeta')\mu_o\mathcal{H} + \frac{k'^2}{10Dq}\mu_o^2\mathcal{H}^2 .$$

The magnetic elements $G^m(kj;kj')$, i.e.,

$$G^m(kj;kj') = H^m(kj;kj') + G_2^m(kj;kj'), \qquad \text{(III-29)}$$

for the $^2T_2(T_d)$ manifold of the transformed Hamiltonian G may then be written on compiling the results given in Table 6 for the intrablock elements $H^m(kj;kj')$ and the second order terms $G_2^m(kj;kj')$ evaluated in equations (III-28). After carrying out the following simplification

$$\eta_1 = -\frac{1}{2}\left[k + \frac{k'}{10Dq}\,(2K'+\zeta')\right] \qquad \text{(III-30)}$$

$$\eta_2 = \frac{1}{2}\,g_s + k'\zeta'/10Dq$$

$$\eta_3 = -\sqrt{2}k'\zeta'/10Dq$$

$$\eta_4 = \frac{1}{2}\,g_s + 2\,k'\zeta'/10Dq$$

$$\eta_5 = -\sqrt{\frac{1}{2}}\left[k + \frac{k'}{10Dq}\,(2K'-\zeta')\right],$$

the magnetic elements, equation (III-29), of the transformed Hamiltonian may then be reduced to the form

$$G^m(\psi_3;\,\psi_3) = G^m(\psi_4;\,\psi_4) = G^m\left(-\frac{1}{2}t_2^-;-\frac{1}{2}t_2^-\right) \qquad \text{(III-31)}$$

$$= G^m\left(\frac{1}{2}t_2^+;\,\frac{1}{2}t_2^+\right) = -\frac{k'^2}{10Dq}\,\mu_o^2\,\mathcal{H}^2$$

$$G^m\left(\frac{1}{2}t_2^\circ;\,\frac{1}{2}t_2^\circ\right) = G^m\left(-\frac{1}{2}t_2^\circ;-\frac{1}{2}t_2^\circ\right) = -\frac{2k'^2}{10Dq}\,\mu_o^2\,\mathcal{H}^2$$

$$G^{m*}\left(\psi_4;-\frac{1}{2}t_2^\circ\right) = G^m\left(\psi_3;-\frac{1}{2}t_2^\circ\right) = -i(\eta_1 + i\eta_3)\mu_o\mathcal{H} + \frac{ik'^2}{\sqrt{2}\,10Dq}\,\mu_o^2\,\mathcal{H}^2$$

$$G^{m*}\left(\psi_4;\,\frac{1}{2}t_2^\circ\right) = G^m\left(\psi_3;\,\frac{1}{2}t_2^\circ\right) = (\eta_1 + i\eta_3)\mu_o\mathcal{H} + \frac{k'^2}{\sqrt{2}\,10Dq}\,\mu_o^2\,\mathcal{H}^2$$

$$G^{m*}\left(\psi_4;-\frac{1}{2}t_2^-\right) = G^m\left(\psi_3;-\frac{1}{2}t_2^-\right) = \sqrt{\frac{1}{2}}\,(\eta_2 + i\eta_3)\,\mu_o\,\mathcal{H}$$

$$G^{m*}\ (\psi_4;\ \tfrac{1}{2}t_2^+) = G^m\ (\psi_3;\ \tfrac{1}{2}t_2^+) = -\,i\sqrt{\tfrac{1}{2}}\,(\eta_2 + i\eta_3)\ \mu_o \mathcal{H}$$

$$G^m\ (\tfrac{1}{2}\ t_2^\circ;\ -\tfrac{1}{2}t_2^\circ) = \eta_4\ \mu_o \mathcal{H}$$

$$G^m\ (\tfrac{1}{2}t_2^\circ;\ \tfrac{1}{2}t_2^+) = \eta_5\ \mu_o \mathcal{H} - \frac{k'^2}{10Dq}\ \mu_o^2 \mathcal{H}^2$$

$$G^m\ (-\tfrac{1}{2}t_2^\circ;\ -\tfrac{1}{2}t_2^-) = \eta_5\ \mu_o \mathcal{H} + \frac{k'^2}{10Dq}\ \mu_o^2 \mathcal{H}^2\ .$$

The form of the magnetic elements in the energy representation, i.e., the representation which diagonalizes the Hamiltonian up through the spin-orbit interaction energy and trigonal field, is found on carrying out the transformation indicated by the expressions (III-16) and (III-17) for the basis of the energy representation. With the help of the magnetic elements evaluated in the uncoupled representation, equation (III-31), the specific form of the elements in the energy representation are obtained and have been listed in Table 9. The simplification

$$s = (\alpha\eta_1 + \sqrt{\tfrac{1}{2}}\beta\eta_2) + i\eta_3\ (\alpha + \sqrt{\tfrac{1}{2}}\ \beta) \qquad \text{(III-32)}$$

$$t = (\beta\eta_1 - \sqrt{\tfrac{1}{2}}\alpha\eta_2) + i\ \eta_3\ (\beta - \sqrt{\tfrac{1}{2}}\alpha)$$

has been carried out on expressing the magnetic elements in the energy representation and those off diagonal-elements quadratic in the field strength $\mathcal{H}$ connecting the subblock structure associated with the

TABLE 9

MAGNETIC ELEMENTS OF $H^m = \mu_o(\ell_x + g_s s_x)\mathcal{H}$ IN THE REPRESENTATION DIAGONALIZING THE FIELD INDEPENDENT TERMS

	ψ_3	ψ_4	ψ_1^+	ψ_2^+	ψ_1^-	ψ_2^-
ψ_3	$-\frac{k'^2}{10Dq}\mu_o^2\mathcal{H}^2$		$s\mu_o\mathcal{H}$	$-is\mu_o\mathcal{H}$	$t\mu_o\mathcal{H}$	$-it\mu_o\mathcal{H}$
ψ_4		$-\frac{k'^2}{10Dq}\mu_o^2\mathcal{H}^2$	$s^*\mu_o\mathcal{H}$	$is^*\mu_o\mathcal{H}$	$t^*\mu_o\mathcal{H}$	$it^*\mu_o\mathcal{H}$
ψ_1^+			$-\frac{k'^2}{10Dq}(1+\alpha^2)\mu_o^2\mathcal{H}^2$	$[\alpha^2\eta_4+2\alpha\beta\eta_5]\mathcal{H}$		$[\alpha\beta\eta_4+(\beta^2-\alpha^2)\eta_5]\mathcal{H}$
ψ_2^+				$-\frac{k'^2}{10Dq}(1+\alpha^2)\mu_o^2\mathcal{H}^2$	$[\alpha\beta\eta_4+(\beta^2-\alpha^2)\eta_5]\mathcal{H}$	
ψ_1^-					$-\frac{k'^2}{10Dq}(1+\beta^2)\mu_o^2\mathcal{H}^2$	$[\beta^2\eta_4-2\alpha\beta\eta_5]\mathcal{H}$
ψ_2^-						$-\frac{k'^2}{10Dq}(1+\beta^2)\mu_o^2\mathcal{H}^2$

$W(\Gamma_4,\Gamma_5(^2T_2))$, $W^+(\Gamma_6(^2T_2))$ and $W^-(\Gamma_6(^2T_2))$ energy levels have not been shown as they contribute to the third and fourth order Zeeman terms.

Since there are magnetic elements connecting the subblock structure of the $^2T_2(T_d)$ manifold, (see Table 9), a second order transformation must be carried out to fold these elements into the respective subblocks associated with the $W(\Gamma_4,\Gamma_5(^2T_2))$, $W^+(\Gamma_6(^2T_2))$ and $W^-(\Gamma_6(^2T_2))$ levels as these terms contribute to the quadratic Zeeman effect. The quadratic terms $^1G_2^m$ brought into the respective subblocks may be obtained as shown previously and it is found that

$$^1G_2^m(\psi_3;\psi_3) = {}^1G_2^m(\psi_4;\psi_4) = \left(\frac{2|s|^2}{\Delta_2-\Delta_1} + \frac{2|t|^2}{\Delta_2}\right)\mu_o^2\mathcal{H}^2 \qquad \text{(III-33)}$$

$$^1G_2^m(\psi_1^+;\psi_1^+) = {}^1G_2^m(\psi_2^+;\psi_2^+) = \left(-\frac{2|s|^2}{\Delta_2-\Delta_1} + \frac{1}{\Delta_1}[(\beta^2-\alpha^2)\eta_5+\alpha\beta\eta_4]^2\right)\mu_o^2\mathcal{H}^2$$

$$^1G_2^m(\psi_1^-;\psi_1^-) = {}^1G_2^m(\psi_2^-;\psi_2^-) = \left(-\frac{2|t|^2}{\Delta_2} - \frac{1}{\Delta_1}[(\beta^2-\alpha^2)\eta_5+\alpha\beta\eta_4]^2\right)\mu_o^2\mathcal{H}^2,$$

where the energy denominators are defined by equation (III-20) and

$$\Delta_2 = W(\Gamma_4,\Gamma_5(^2T_2)) - W^-(\Gamma_6(^2T_2)). \qquad \text{(III-34)}$$

On isolating the subblock structure of the $^2T_2$ manifold, the magnetic elements of the transformed Hamiltonian are obtained on combining the second order elements evaluated in equation (III-33) with the intra-level elements given in Table 9. The results are shown in Table 10.

TABLE 10

MAGNETIC ELEMENTS CONTRIBUTING TO THE LINEAR AND QUADRATIC ZEEMAN EFFECT FOR THE MAGNETIC FIELD DIRECTED PERPENDICULAR TO THE HEXAGONAL c-AXIS

$W(\Gamma_4, \Gamma_5(^2T_2))$

ψ_3	ψ_4
$\left(\frac{2\lvert s\rvert^2}{\Delta_2-\Delta_1} + \frac{2\lvert t\rvert^2}{\Delta_2} - \frac{k'^2}{10Dq}\right)\mu_o^2 \mathcal{H}^2$	$\left(\frac{2\lvert s\rvert^2}{\Delta_2-\Delta_1} + \frac{2\lvert t\rvert^2}{\Delta_2} - \frac{k'^2}{10Dq}\right)\mu_o^2 \mathcal{H}^2$

$W^+(\Gamma_6(^2T_2))$

ψ_1^+	ψ_2^+
$\left(-\frac{2\lvert s\rvert^2}{\Delta_2-\Delta_1} - \frac{k'^2}{10Dq}(1+\alpha^2) + \frac{1}{\Delta_1}[(\beta^2-\alpha^2)\eta_5+\alpha\beta\eta_4]^2\right)\mu_o^2 \mathcal{H}^2$	$(\alpha^2\eta_4 + 2\alpha\beta\eta_5)\,\mu_o \mathcal{H}$
	$\left(-\frac{2\lvert s\rvert^2}{\Delta_2-\Delta_1} - \frac{k'^2}{10Dq}(1+\alpha^2) + \frac{1}{\Delta_1}[(\beta^2-\alpha^2)\eta_5+\alpha\beta\eta_4]^2\right)\mu_o^2 \mathcal{H}^2$

TABLE 10 (continued)

$W^{-}(\Gamma_6(^2T_2))$

ψ_1^-	ψ_2^-
$\left(-\frac{2\lvert t\rvert^2}{\Delta_2-\Delta_1} - \frac{k'^2}{10Dq}(1+\beta^2)\right.$	$(\beta^2\eta_4 - 2\alpha\beta\eta_5)\mu_o\mathcal{H}$
$\left. - \frac{1}{\Delta_1}[(\beta^2-\alpha^2)\eta_5+\alpha\beta\eta_4]^2\right)\mu_o^2\mathcal{H}^2$	
	$\left(-\frac{2\lvert t\rvert^2}{\Delta_2-\Delta_1} - \frac{k'^2}{10Dq}(1+\beta^2)\right.$
	$\left. - \frac{1}{\Delta_1}[(\beta^2-\alpha^2)\eta_5+\alpha\beta\eta_4]^2\right)\mu_o^2\mathcal{H}^2$

The energy matrix given in Table 10 may then be diagonalized to determine the g-factors and the coefficients of the quadratic Zeeman terms, (the coefficients of those terms proportional to $\mu_o \mathcal{H}$ and $\mu_o^2 \mathcal{H}^2$ respectively), and it is found that for the $W(\Gamma_4,\Gamma_5(^2T_2))$ level

$$g_\perp (\Gamma_4,\Gamma_5(^2T_2)) = 0 \qquad \text{(III-35)}$$

and

$$W_\perp^{(2)}(\Gamma_4,\Gamma_5(^2T_2)) = \frac{2|s|^2}{\Delta_2-\Delta_1} + \frac{2|t|^2}{\Delta_2} - \frac{k'^2}{10Dq} \quad ; \qquad \text{(III-36)}$$

the $W^+(\Gamma_6(^2T_2))$ level

$$g_\perp (\Gamma_6^+(^2T_2)) = \pm 2\left(\frac{1}{2}\alpha^2 g_s - \sqrt{2}\alpha\beta k + \frac{k'}{10Dq}[2\alpha^2\zeta' - \sqrt{2}\alpha\beta(2K'-\zeta')]\right) \qquad \text{(III-37)}$$

and

$$W_\perp^{(2)} (\Gamma_6^+(^2T_2)) = -\frac{2|s|^2}{\Delta_2-\Delta_1} + \frac{1}{\Delta_1}[\alpha\beta\eta_4+(\beta^2-\alpha^2)\eta_5]^2 - \frac{k'^2}{10Dq}(1+\alpha^2) \qquad \text{(III-38)}$$

and for the $W^-(\Gamma_6(^2T_2))$ level

$$g_\perp(\Gamma_6^-(^2T_2)) = 2\left(\frac{1}{2}\beta^2 g_s + \sqrt{2}\alpha\beta k + \frac{k'}{10Dq}[2\beta^2\zeta' + \sqrt{2}\alpha\beta(2K'-\zeta')]\right) \qquad \text{(III-39)}$$

and

$$W_\perp^{(2)}(\Gamma_6^-(^2T_2)) = -2\frac{|t|^2}{\Delta_2} - \frac{1}{\Delta_1}[\alpha\beta\eta_4+(\beta^2-\alpha^2)\eta_5]^2 - \frac{k'^2}{10Dq}(1+\beta^2), \qquad \text{(III-40)}$$

where the parameters s and t, and η_1, η_2, η_3, η_4, and η_5 appearing in the expressions for the quadratic Zeeman terms may be eliminated by the relations (III-32) and (III-30) respectively. The sign for the

ground state g-factor $g(\Gamma_6^-(^2T_2))$ has been chosen such that when the trigonal field is set equal to zero ($K = K' = 0$) and the orbital reduction parameters are set equal to the no-covalency values ($k = k' = 1$), the ground state g-factor reduces to the spin only value ($g_s = 2$). As the excited state g-factor $g_\perp(\Gamma_6^+(^2T_2))$ vanishes for the above simplification, the relative sign of $g_\perp(\Gamma_6^+(^2T_2))$ is left arbitrary

For the case of the external magnetic field directed parallel to the hexagonal c-axis, the magnetic energy is given by

$$H^m = \mu_o(\ell_z + g_s s_z)\mathcal{H},$$

where the z-axis is parallel to the hexagonal c-axis. The matrix elements of $(\ell_z + g_s s_z)$ using as basis the uncoupled representation are shown in Table 5. Here it is seen that the structure of the magnetic elements is somewhat simpler than that for the case treated previously, i.e., $\mathcal{H} \perp$ c-axis.

The magnetic elements folded into the $^2T_2(T_d)$ manifold are determined on substituting the interlevel elements given in Table 5 and Table 7 for $(\ell_z + g_s s_z)$ and H_1 respectively into equation (III-27) for $G_2^m(kj;kj')$ and it is found that

$$G_2^m(\psi_3;\psi_3) = G_2^m(\psi_4;\psi_4) = -\frac{2k'^2}{10Dq}\mu_o^2\mathcal{H}^2 \qquad \text{(III-41)}$$

$$G_2^m(\psi_3;\psi_4) = \frac{2k'}{10Dq}(2K' + \zeta' + i\sqrt{2}\zeta')\mu_o\mathcal{H}$$

$$G_2^m\left(-\frac{1}{2}t_2^-;-\frac{1}{2}t_2^-\right)=\frac{2k'}{10Dq}\left(2K'-\zeta'\right)\mu_o\mathcal{H}-\frac{2k'^2}{10Dq}\mu_o^2\mathcal{H}^2$$

$$G_2^m\left(\frac{1}{2}t^+;\frac{1}{2}t^+\right)=-\frac{2k'}{10Dq}\left(2K'-\zeta'\right)\mu_o\mathcal{H}-\frac{2k'^2}{10Dq}\mu_o^2\mathcal{H}^2$$

$$G_2^m\left(-\frac{1}{2}t_2^\circ;\frac{1}{2}t_2^+\right)=-G_2^m\left(\frac{1}{2}t_2^\circ;-\frac{1}{2}t_2^-\right)=\sqrt{2}\,\frac{\zeta'k'}{10Dq}\mu_o\mathcal{H}$$

On inclusion of the intralevel elements $H^m(kj;kj')$ given in Table 5, (see equation (III-29)), the magnetic elements appearing in the $^2T_2(T_d)$ manifold of the transformed Hamiltonian are

$$G^m\left(\psi_3;\psi_3\right)=G^m\left(\psi_4;\psi_4\right)=-2\,\frac{k'^2}{10Dq}\mu_o^2\mathcal{H}^2 \qquad \text{(III-42)}$$

$$G^m\left(\psi_3;\psi_4\right)=\left[-k+\frac{1}{2}g_s+\frac{2k'}{10Dq}\left(2K'+\zeta'+i\sqrt{2}\zeta'\right)\right]\mu_o\mathcal{H}$$

$$G^m\left(\frac{1}{2}t_2^\circ;\frac{1}{2}t_2^\circ\right)=-G^m\left(-\frac{1}{2}t_2^\circ;-\frac{1}{2}t_2^\circ\right)=\frac{1}{2}g_s\mu_o\mathcal{H}$$

$$G^m\left(\frac{1}{2}t_2^+;\frac{1}{2}t_2^+\right)=\left[k+\frac{1}{2}g_s-\frac{2k'}{10Dq}\left(2K'-\zeta'\right)\right]\mu_o\mathcal{H}-\frac{2k'^2}{10Dq}\mu_o^2\mathcal{H}^2$$

$$G^m\left(-\frac{1}{2}t_2^-;-\frac{1}{2}t_2^-\right)=-\left[\frac{1}{2}g_s+k-\frac{2k'}{10Dq}\left(2K'-\zeta'\right)\right]\mu_o\mathcal{H}-\frac{2k'^2}{10Dq}\mu_o^2\mathcal{H}^2$$

$$G^m\left(\frac{1}{2}t_2^\circ;-\frac{1}{2}t_2^-\right)=-G^m\left(-\frac{1}{2}t_2^\circ;\frac{1}{2}t_2^+\right)=-\sqrt{2}\,\frac{k'\zeta'}{10Dq}\mu_o\mathcal{H}$$

The form of the magnetic elements in the energy representation may be found using the transformation which diagonalizes the field independent terms, equations (III-16) and (III-17). The magnetic elements in the energy representation are given in Table 11. From inspection of Table 11, it is seen that there are linear terms in G^m connnecting components of the $W^+(\Gamma_6(^2T_2))$ and $W^-(\Gamma_6(^2T_2))$ levels having the same transformation properties. These elements contribute to the quadratic Zeeman effect and may be folded into the respective subblock structures on carrying out a second similarity transformation to isolate the subblock structure of the $^2T_2(T_d)$ manifold and it is found that

$$^1G_2^m(\psi_1^+;\psi_1^+) = {}^1G_2^m(\psi_2^+;\psi_2^+) = \frac{1}{\Delta_1}\left(\alpha\beta\left[g_s+k-\frac{2k'}{10Dq}(2K'-\zeta')\right] + \sqrt{2}(\alpha^2-\beta^2)\frac{k'\zeta'}{10Dq}\right)^2 \mu_o^2 \mathcal{H}^2 \qquad \text{(III-43)}$$

and

$$^1G_2^m(\psi_1^-;\psi_1^-) = {}^1G_2^m(\psi_2^-;\psi_2^-) = -\frac{1}{\Delta_1}\left(\alpha\beta\left[g_s+k-\frac{2k'}{10Dq}(2K'-\zeta')\right] + \sqrt{2}(\alpha^2-\beta^2)\frac{k'\zeta'}{10Dq}\right)^2 \mu_o^2 \mathcal{H}^2 , \qquad \text{(III-44)}$$

where the perturbed energy splitting Δ_1 has been defined in equation (III-20). Since the $\Gamma_4,\Gamma_5(^2T_2)$ manifold does not have connecting elements with the $\Gamma_6(^2T_2)$ manifolds, the g-factors and the coefficient of

the quadratic Zeeman effect for the $\Gamma_4,\Gamma_5(^2T_2)$ level may be determined on diagonalization of the $\Gamma_4,\Gamma_5(^2T_2)$ energy matrix given in Table 11 and it is found that

$$g_{\parallel}\ (\Gamma_4,\Gamma_5(^2T_2)) = \pm\ 2\left(\left[\ \frac{1}{2}\,g_s - k + \frac{2k'}{10Dq}\ (2K'+\zeta')\right]^2 + \left[2\sqrt{2}\ \frac{k'\zeta'}{10Dq}\ \right]^2\right)^{1/2} \qquad \text{(III-45)}$$

and

$$W_{\parallel}^{(2)}\ (\Gamma_4,\Gamma_5(^2T_2)) = -\ 2k'^2/10Dq \qquad \text{(III-46)}$$

The g-factors and coefficients of the quadratic Zeeman effect for the $W^+(\Gamma_6(^2T_2))$ and $W^-(\Gamma_6(^2T_2))$ levels are obtained on combining the transformed elements, equations (III-43) and (III-44), with the diagonal elements given in Table 11, thus we find for the $W^+(\Gamma_6(^2T_2))$ level

$$g_{\parallel}\ (\Gamma_6^+(^2T_2)) = \pm\ 2\left(\left[\ \frac{1}{2}\ (\alpha^2-\beta^2)g_s\ -\beta^2 k\right] + \frac{2k'}{10Dq}\ \left[\beta^2(2K'-\zeta')\ -\sqrt{2}\alpha\beta\zeta'\ \right]\right) \qquad \text{(III-47)}$$

and

$$W_{\parallel}^{(2)}\ (\Gamma_6^+(^2T_2)) = \frac{1}{4}\left(\alpha\beta\left[g_s + k\ -\ \frac{2k'}{10Dq}\ (2K'-\zeta')\right] + \sqrt{2}\ \ (\alpha^2-\beta^2)\ \frac{k'\zeta'}{10Dq}\right)^2 - 2\ \frac{\beta^2 k'^2}{10Dq} \qquad \text{(III-48)}$$

and for the $W^{-}(\Gamma_6(^2T_2))$ level

$$g_{\|}\ (\Gamma_6^{-}(^2T_2)) = 2\left(\left[\frac{1}{2}\ (\alpha^2-\beta^2)g_s + \alpha^2 k\right]\right. \tag{III-49}$$

$$\left. - \frac{2k'}{10Dq}\ \left[\ \alpha^2(2K'-\zeta')+\sqrt{2}\alpha\beta\zeta'\ \right]\right)$$

and

$$W_{\|}^{(2)}\ (\Gamma_6^{-}(^2T_2)) = -\frac{1}{\Delta_1}\left(\alpha\beta\left[g_s+k - \frac{2k'}{10Dq}\ (2K'-\zeta')\right]\right. \tag{III-50}$$

$$\left. + \sqrt{2}\ (\alpha^2-\beta^2)\ \frac{k'\zeta'}{10Dq}\right)^2 - 2\ \frac{\alpha^2 k'^2}{10Dq}\ .$$

The sign of the ground state g-factor $g_{\|}\ (\Gamma_6^{-}(^2T_2))$ has been chosen to conform with that of $g_{\perp}\ (\Gamma_6^{-}(^2T_2))$, that is the g-factor $g_{\|}\ (\Gamma_6^{-}(^2T_2))$ reduces to the spin only value (g_s = +2) when the simplification (K = K' = 0) and (k = k' = 1) has been carried out. Similarly as for the case treated previously, ($\mathcal{H} \perp$ c-axis), the excited state g-factor $g_{\|}\ (\Gamma_6^{+}(^2T_2))$ vanishes for the above approximations, thus the sign is left arbitrary.

TABLE 11

MATRIX ELEMENTS OF $H^m = \mu_o(\ell_z + g_s s_z)\mathcal{H}$ IN THE REPRESENTATION DIAGONALIZING THE FIELD INDEPENDENT TERMS

Γ_4, Γ_5

	ψ_3	ψ_4
ψ_3	$-\frac{2k'^2}{10Dq}\mu_o^2\mathcal{H}^2$	$[\frac{1}{2}g_s - k + \frac{2k'}{10Dq}(2K' + \zeta' + i\sqrt{2}\zeta')]\mu_o\mathcal{H}$
ψ_4		$-\frac{2k'^2}{10Dq}\mu_o^2\mathcal{H}^2$

Γ_6

	ψ_1^+	ψ_1^-
ψ_1^+	$\left(\frac{1}{2}(\alpha^2-\beta^2)g_s - \beta^2[k - \frac{2k'}{10Dq}(2K'-\zeta')] - 2\sqrt{2}\alpha\beta\frac{k'\zeta'}{10Dq}\right)\mu_o\mathcal{H} - \frac{2\beta^2k'^2}{10Dq}\mu_o^2\mathcal{H}^2$	$\left(\alpha\beta[g_s + k - \frac{2k'}{10Dq}(2K'-\zeta') + \sqrt{2}(\alpha^2-\beta^2)\frac{k'\zeta'}{10Dq}\right)\mu_o\mathcal{H}$
ψ_1^-		$\left(-\frac{1}{2}(\alpha^2-\beta^2)g_s - \alpha^2[k - \frac{2k'}{10Dq}(2K'-\zeta')] + 2\sqrt{2}\alpha\beta\frac{k'\zeta'}{10Dq}\right)\mu_o\mathcal{H} - 2\frac{\alpha^2k'^2}{10Dq}\mu_o^2\mathcal{H}^2$

TABLE 11 (continued)

Γ_6

	ψ_2^+	ψ_2^-
ψ_2^+	$\left(-\frac{1}{2}(\alpha^2-\beta^2)g_s+\beta^2[k-\frac{2k'}{10Dq}(2K'-\zeta')]\right.$ $\left.+2\sqrt{2}\alpha\beta\frac{k'\zeta'}{10Dq}\right)\mu_o\mathcal{H}-2\frac{\beta^2k'^2}{10Dq}\mu_o^2\mathcal{H}^2$	$\left(-\alpha\beta[g_s+k-\frac{2k'}{10Dq}(2K'-\zeta')]\right.$ $\left.-\sqrt{2}(\alpha^2-\beta^2)\frac{k'\zeta'}{10Dq}\right)\mu_o\mathcal{H}$
ψ_2^-		$\left(\frac{1}{2}(\alpha^2-\beta^2)g_s+\alpha^2[k-\frac{2k'}{10Dq}(2K'-\zeta')]\right.$ $\left.-2\sqrt{2}\alpha\beta\frac{k'\zeta'}{10Dq}\right)\mu_o\mathcal{H}-2\frac{\alpha^2k'^2}{10Dq}\mu_o^2\mathcal{H}^2$

CHAPTER IV

Cu^{2+} IN THE TETRAHEDRAL SITES OF CdS, ZnS AND ZnO

If the trigonal distortion is neglected $K = K' = 0$, the energy level splitting reduces to that shown in Figure 2. The symmetry species $E_{5/2}$ and G denote a twofold and a fourfold irreducible representation of the T_d double group respectively.[5] The spin-orbit energy splits the $^2T_2(T_d)$ manifold in the first order by the energy difference $(-\frac{3}{2}\zeta)$ while the $^2E(T_d)$ manifold remains degenerate. The second order spin-orbit energy then shifts the $G(^2E)$ and $G(^2T_2)$ levels by the factor $(-\frac{3}{2}\zeta^2/10Dq)$. The mixing coefficients may be obtained using the relations (III-18) for α and β respectively and it is found that $\alpha = \sqrt{\frac{2}{3}}$ and $\beta = \sqrt{\frac{1}{3}}$. The g-factor for the $E_{5/2}(^2T_2)$ ground state may then be found on reduction of either of the two relations (III-39) or (III-49) for $g_\perp$ or $g_{||}$ respectively, thus

$$g = 2\left[-\frac{1}{3} + \frac{2}{3}k\right].$$

If the orbital reduction parameter is approximately unity, the g-factor of the ground state is then near the spin only value $g_s = 2$.

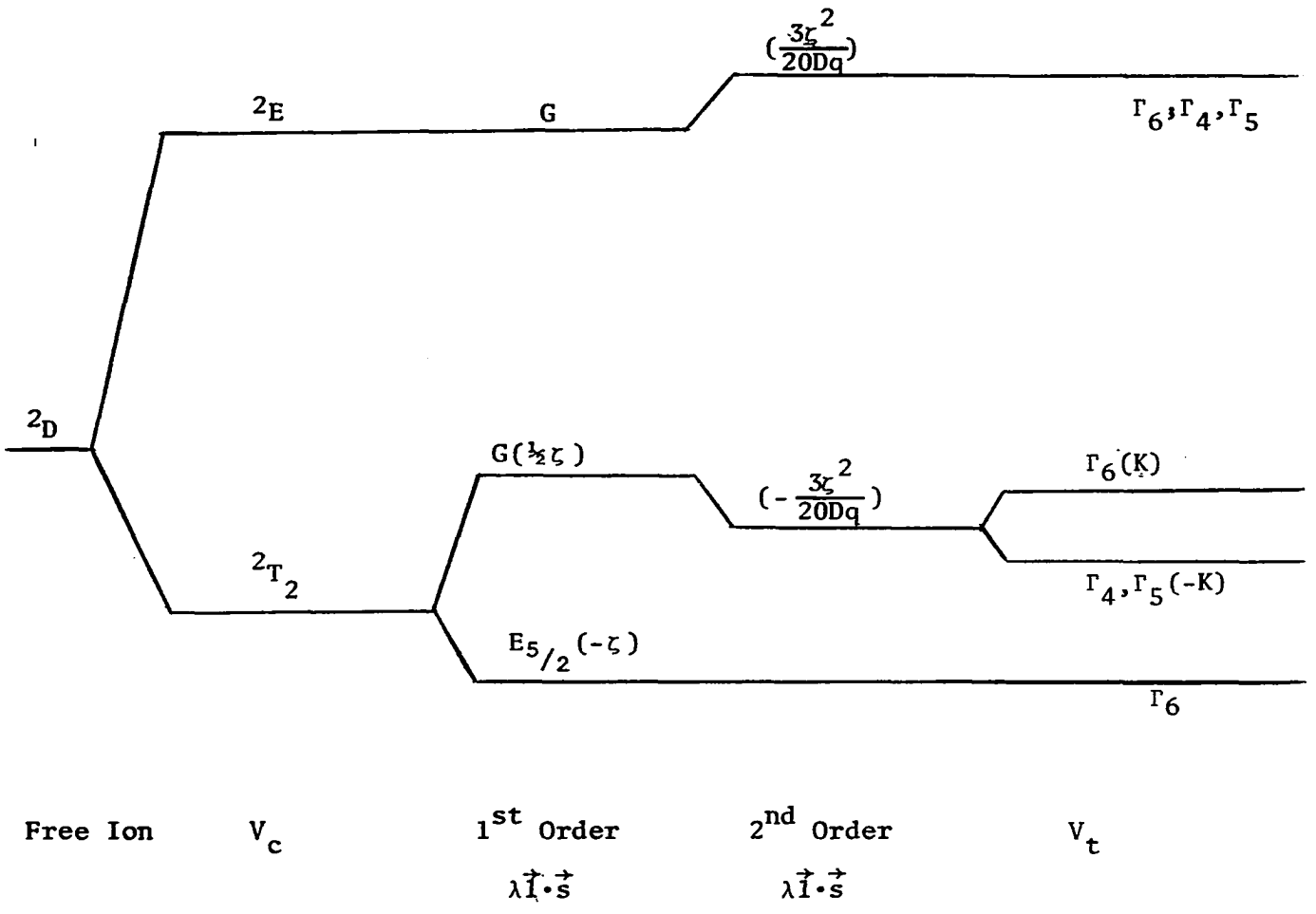

Figure 2. Energy level diagram of Cu^{2+} in a Tetrahedral field
(Weak axial field)

If now a small trigonal distortion exists along the hexagonal c-axis ($2K \sim \frac{3\zeta^2}{20Dq}$), the degeneracy of the $G(^2T_2)$ level is lifted as shown in Figure 2. The trigonal field splitting of the $G(^2T_2)$ level is determined from the relations (III-11) and (III-14) for $W(\Gamma_4,\Gamma_5(^2T_2))$ and $W^+(\Gamma_6(^2T_2))$; here the trigonal parameter K' and those terms less than K have been neglected as it is assumed that $K' \ll \zeta'$ and $K \sim \zeta^2/10Dq < \zeta$ respectively. The g-factors for the $\Gamma_6(^2T_2)$ ground state are given by the expressions (III-39) and (III-49) for $g_\perp(\Gamma_6^-(^2T_2))$ and $g_\parallel(\Gamma_6^-(^2T_2))$ respectively and on reduction it is found that

$$g_\parallel = 2\left[\frac{1}{3} + \frac{2}{3}k + \frac{8}{9}\frac{K}{\zeta}(2+k)\right] \qquad \text{(IV-1)}$$

and

$$g_\perp = 2\left[\frac{1}{3} + \frac{2}{3}k - \frac{4}{9}\frac{K}{\zeta}(2+k)\right], \qquad \text{(IV-2)}$$

where the approximate expressions for the mixing coefficients used in the reduction of the above expressions for $g_\parallel$ and $g_\perp$ are

$$\alpha = \left(\frac{2}{3} + \frac{8}{9}\frac{K}{\zeta}\right)^{\frac{1}{2}}$$

$$\beta = \left(\frac{1}{3} - \frac{8}{9}\frac{K}{\zeta}\right)^{\frac{1}{2}}$$

and only those terms of order of magnitude K/ζ have been retained.

As the free ion value for the spin-orbit parameter ζ of Cu^{2+} is about $\bar{8}30$ cm^{-1}, and if the trigonal distortion is small, one expects the spin-orbit splitting of the $^2T_2(T_d)$ level to be approximately

1000 cm^{-1}. The ground state g-factors should then be very near the spin-only value $g_s = 2$. The effect of a small trigonal distortion is to split the $G(^2T_2)$ level and to introduce anisotropy in the ground state g-factors.

Cu^{2+}:CdS

Broser et. al.[25] have measured the fine structure of the infraredabsorption and emission spectra of Cu^{2+} in ZnS and CdS crystals. From their interpretation of the optical spectra of Cu^{2+}:CdS, the energy level pattern shown in Figure 3 was obtained. The cubic field and spin-orbit parameters consistent with the energy level splittings shown in Figure 3 were given and it was found that Dq = 556 cm^{-1} and ζ = 565 cm^{-1}. The g-factors for the $\Gamma_6(^2T_2)$ ground state of Cu^{2+}:CdS have been measured by Morigaki[27] and the values obtained were

$$g_{\parallel} = 2.240 \pm 0.005$$

$$g_{\perp} = 1.75 \pm 0.05 .$$

The expressions (IV-1) and (IV-2) for the ground state g-factors may then be used to determine the orbital reduction parameter k and the ratio K/ζ. It was found that

$$k = 0.94$$

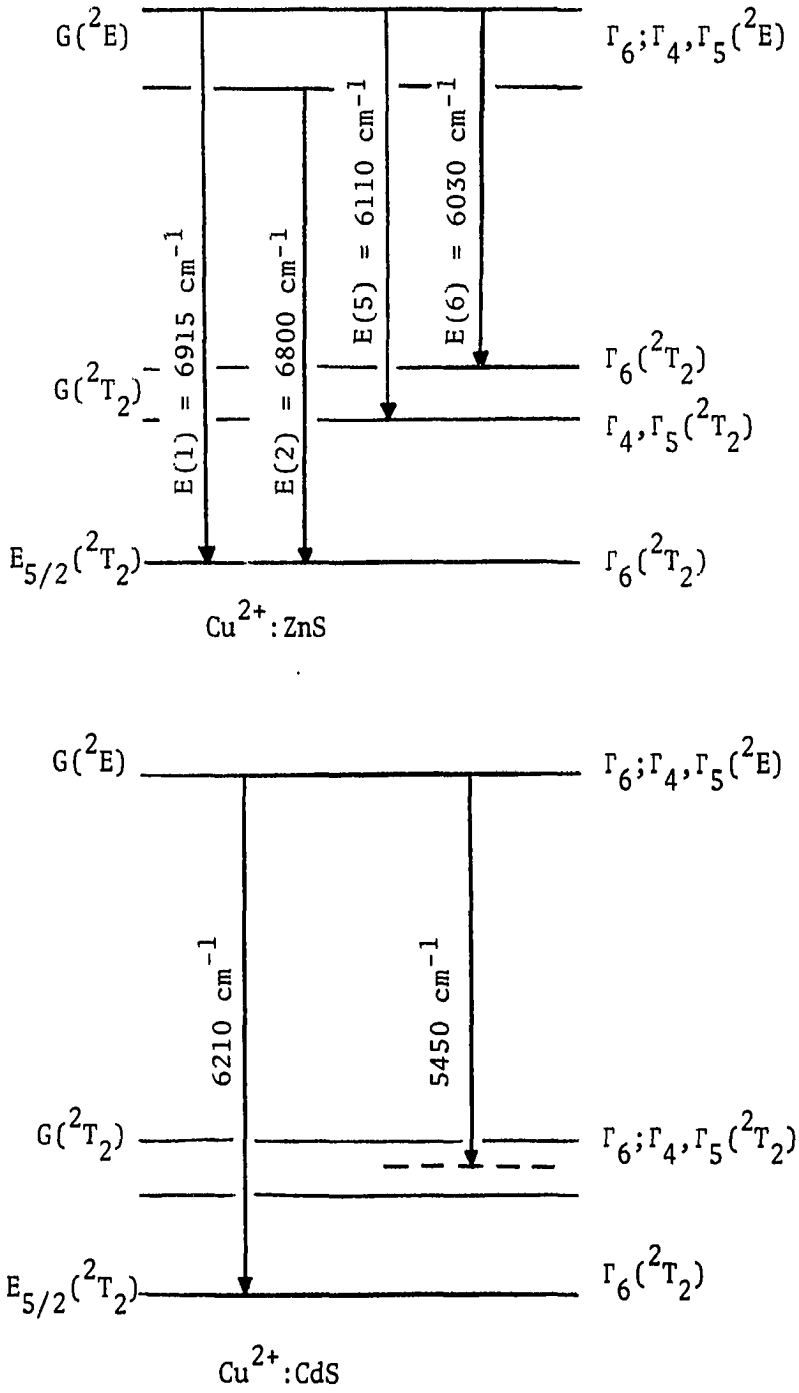

Figure 3. Optical emission spectra of Cu^{2+}:ZnS and Cu^{2+}:CdS[25]

and

$$K/\zeta = 0.0626 \quad .$$

The spin-orbit parameter given by Broser[25] may then be used to determine the value $K = 35\ cm^{-1}$ for the trigonal parameter. The trigonal splitting of the $G(^2T_2)$ level is then equal to $2K = 70\ cm^{-1}$.

Cu^{2+}:ZnS

Broser et. al.[25] made the following assignments from their observed infrared emission spectra of Cu^{2+}:ZnS, (see Figure 3). The symmetry assignments of the excited state levels in the $^2T_2(T_d)$ manifold were determined in this work from the observed anisotropy of the ground state g-factors ($g_{||} > g_{\perp}$), which indicates that the trigonal parameter is positive, thus placing the $\Gamma_6(^2T_2)$ level above the $\Gamma_4,\Gamma_5(^2T_2)$ level. As polarization studies of the observed spectra were not given, the relative positions of the $\Gamma_6(^2E)$ and $\Gamma_4,\Gamma_5(^2E)$ levels are not determined.

Broser determined the cubic field and spin-orbit parameters and found $Dq = 624\ cm^{-1}$ and $\zeta = 596\ cm^{-1}$. These values are consistent with the following relations

$$E(1) = 10Dq + \zeta + \frac{3\zeta^2}{20Dq}$$

and

$$E(1) - E(5) = \frac{3}{2}\left(\zeta - \frac{\zeta^2}{10Dq}\right) .$$

If instead of using the transitions E(1) and E(5) in the determination of Dq and ζ, one uses the energy splittings measured from the center of gravities of the $\Gamma_6(^2E);\Gamma_4,\Gamma_5(^2E)$ and $\Gamma_6^+(^2T_2);\Gamma_4,\Gamma_5(^2T_2)$ levels, the values for the spin-orbit parameter and Dq value are then found to be $\zeta = 627\ cm^{-1}$ and $Dq = 613\ cm^{-1}$ and are consistent with the relations

$$\frac{1}{2}[E(1) + E(2)] = 10Dq + \zeta + \frac{3\zeta^2}{20Dq}$$

$$\frac{1}{2}[E(1) + E(2)] = -\frac{1}{2}[E(6) + E(5)] = \frac{3}{2}\left(\zeta - \frac{\zeta^2}{10Dq}\right).$$

The trigonal parameter may be deduced from the observed splitting of the $G(^2T_2)$ spin-orbit level as this splitting is equal to 2K. Thus the trigonal parameter determined from the optical measurements is $K = 40\ cm^{-1}$.

Estle et. al.[29] have obtained the following values for the g-factors of the $\Gamma_6(^2T_2)$ ground state,

$$g_{\parallel} = 2.151$$

and

$$g_{\perp} = 1.990 .$$

Similarly as in the case for Cu^{2+}:CdS, equations (IV-1) and (IV-2)

may be used to determine the values for the orbital reduction parameter k and the ratio K/ζ . The values obtained were $k \simeq 1.0$ and $K/\zeta = 0.0283$. If the value $\zeta = 627\ cm^{-1}$ for the spin-orbit parameter is used, the trigonal parameter is then found to be $K = 18\ cm^{-1}$ and the trigonal splitting of the $G(^2T_2)$ level predicted from the anisotropy of the g-factors is $2K = 36\ cm^{-1}$. It is seen that the trigonal splitting of the $G(^2T_2)$ level predicted from the anisotropy of the g-factors is half that predicted from the infrared measurement $2K = 80\ cm^{-1}$. Possibly the discrepancy may be accounted for on noting that Estle et. al.[29] express doubt as to the possible model for the photosensitive copper center in ZnS. On the other hand if the following assignment

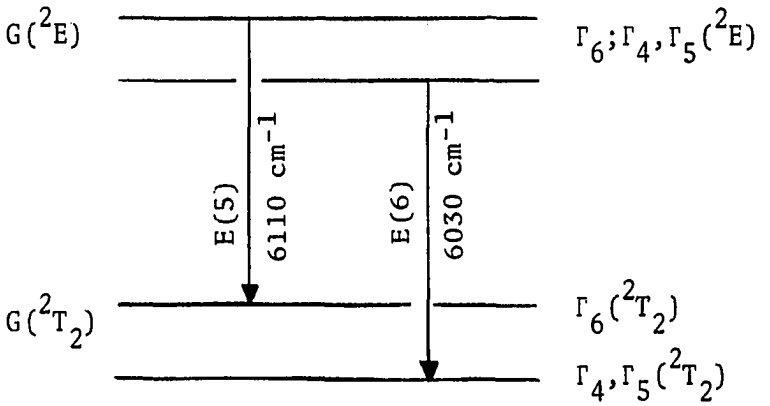

is made for the E(5) and E(6) transitions, one finds that the trigonal splitting 2K of the $G(^2T_2)$ level is then $35\ cm^{-1}$. This value agrees with that found from the anisotropy of the g-factors.

Cu^{2+}:ZnO

The optical absorption spectra of Cu^{2+}:ZnO has been measured by several investigators.[14, 26, 41] Dietz et. al.[14] measured the polarized absorption spectra and from interpretation of the fine structure made the following assignments, (see Figure 4). From interpretation of their optical spectra, Weakliem[26] and Dietz et. al.[14] have determined the Dq value to be 500 cm^{-1} and 569 cm^{-1} respectively. The discrepancy in the two values arise from the fact that Weakliem assumes the spin-orbit parameter to be near the free ion value ζ = 830 cm^{-1} while Dietz's value for ζ is approximately an order of magnitude smaller. The cubic field $^2T_2(T_d)$ level is split in the first order owing to the combined effect of the spin-orbit interaction energy and the trigonal field and Dietz et. al. assign a value of 123 cm^{-1} for the splitting of the two $\Gamma_6(^2T_2)$ levels. The cubic field $^2E(T_d)$ level is split in the second order owing to the interplay of the trigonal field and spin-orbit interaction energy and Dietz et. al. found this splitting to be 39 cm^{-1}. Previous optical measurements[26, 41] of Cu^{2+}:ZnO confirm the doublet structure of the spectra arising from transitions between the ground state and the excited $\Gamma_6(^2E)$ and $\Gamma_4,\Gamma_5(^2T_2)$ levels.

Estle et. al.[30] and Dietz et. al.[14] have measured the electron paramagnetic resonance spectra of Cu^{2+}:ZnO and obtained the g-factors for the $\Gamma_6(^2T_2)$ ground state, (see Table 12). The g-factors determined from the optical Zeeman effect for the $\Gamma_6(^2T_2)$ and $\Gamma_4,\Gamma_5(^2E)$ levels are also included in Table 12, (see reference 14).

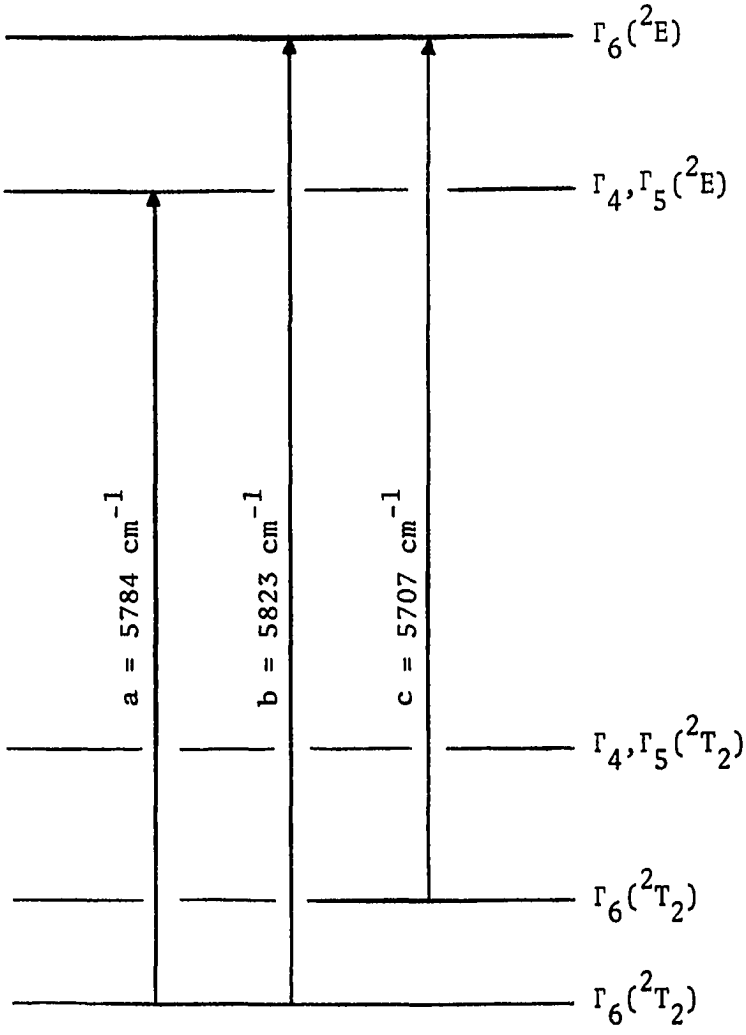

Figure 4. Optical obsorption spectrum of Cu^{2+}:ZnO[14]

TABLE 12

EXPERIMENTAL G-FACTORS OF Cu^{2+}:ZnO

Author	g-Factor	$\Gamma_4,\Gamma_5(^2E)$ Optical	$\Gamma_6(^2T_2)$ Optical	ESR
Dietz et. al.[14]	$g_{\parallel}$	1.63 $\pm$.03	0.76 $\pm$.06	0.74 $\pm$.02
	$g_{\perp}$	0.0 $\pm$.2	1.50 $\pm$.02	1.531 $\pm$.002
Estle et. al.[30]	$g_{\parallel}$			0.7383 $\pm$.0003
	$g_{\perp}$			1.5237 $\pm$.0003

Dietz et. al.[14] set up the secular equation for the $^2T_2(T_d)$ manifold and using the results from their optical and electron paramagnetic resonance measurements found the crystal field parameters for the $^2T_2(T_d)$ manifold to be $\zeta = 86\ cm^{-1}$, $K = -10\ cm^{-1}$ and $k = 0.46$. Here they neglected second order terms brought into the $^2T_2(T_d)$ manifold. From analysis of the second order splitting of the $^2E(T_d)$ level and the g-factors for the $\Gamma_4, \Gamma_5(^2E)$ level, Dietz et. al. found the following values for the crystal field parameters connecting the $^2T_2(T_d)$ and $^2E(T_d)$ manifolds, $K' = -77\ cm^{-1}$, $\zeta' = 720\ cm^{-1}$ and $k' = 0.87$.

The spin-orbit parameter ζ is seen to be reduced by an order of magnitude from that of the free ion value $\zeta = 830\ cm^{-1}$. This large reduction of the spin-orbit parameter may be attributed to the small value found for the splitting of the $\Gamma_6(^2T_2)$ levels as this splitting is about an order of magnitude smaller than would be expected. The orbital reduction parameter k is about 60% smaller than would be expected on the basis of the previous results for Cu^{2+}:CdS and Cu^{2+}:ZnS. This reduction arises from the small values found for the g-factors of the ground state compared to the spin-only value $g_s = 2$.

Due to the small value obtained for ζ, it is questionable whether a first order theory adequately describes the system and that the approximations used in analysing the previous crystals is valid, i.e., Cu^{2+}:CdS and Cu^{2+}:ZnS.

One may determine the orbital reduction parameter and the mixing coefficients for the $^2T_2(T_d)$ manifold using the second order

expressions for the g-factors given in equations (III-39) and (III-49). If one makes the parametric substitution

$$\alpha = \sin\theta$$

$$\beta = \cos\theta$$

for the mixing coefficients, the g-factors for the $\Gamma_6^-(^2T_2)$ level may then be written as

$$g_{\parallel}(\Gamma_6^-(^2T_2)) = -2\left(\frac{g_s}{2}\cos 2\theta - k\sin^2\theta - \frac{k'}{10Dq}\left[2(\zeta'-2K')\sin^2\theta - \sqrt{2}\,\zeta'\sin 2\theta\right]\right) \qquad \text{(IV-3)}$$

$$g_{\perp}(\Gamma_6^-(^2T_2)) = 2\left(\frac{g_s}{2}\cos^2\theta + \sqrt{\frac{1}{2}}\,k\sin 2\theta - \frac{k'}{10Dq}\left[\frac{1}{2}(\zeta'-2K')\sin 2\theta - 2\zeta'\cos^2\theta\right]\right)$$

The orbital reduction parameter k may be eliminated in the theoretical expressions for the g-factors given above on forming the following linear combination

$$\sqrt{\frac{1}{2}}\,g_{\perp}\tan\theta - g_{\parallel} = g_s\left[\frac{1}{2}\sqrt{\frac{1}{2}}\sin 2\theta + \cos 2\theta\right] - \frac{6k'}{10Dq}\sin\theta\left[(\zeta'-2K')\sin\theta - \sqrt{2}\,\zeta'\cos\theta\right]. \qquad \text{(IV-4)}$$

Equation (IV-4) shown above is then seen to depend only upon the parametric angle θ and the second order correction terms where the g-factors $g_{\parallel}$ and $g_{\perp}$ are determined from experiment. As the ratio K'/ζ' is not

determined, equation (IV-4) can be simplified on assuming that the trigonal parameter K' may be neglected relative to the spin-orbit parameter ζ', that is $2K' << \zeta'$, and hence equation (IV-4) reduces to that of a function of the parametric angle θ and the product $k'\zeta'$. The resulting expression may then be iterated to determine the angle θ for various values of the product $k'\zeta'$ and in Table 13 the mixing coefficients and the orbital reduction parameter consistent with the values obtained for the angle θ are shown.

On the other hand if the values for the interlevel elements $k' = 0.87$, $K' = -77\ cm^{-1}$ and $\zeta' = 720\ cm^{-1}$ given by Dietz are used in the determination of the parametric angle θ, the mixing coefficients and the orbital reduction parameter are found to be

$$\begin{aligned} \alpha &= 0.7478 \\ \beta &= 0.6639 \\ k &= 0.46 \end{aligned} \qquad \text{(IV-5)}$$

From inspection of Table 13 and equation (IV-5), it is seen that the values found for the mixing coefficients and orbital reduction parameter differ approximately by (± 0.005) in the third significant figure for a reasonable variation in the contribution from the second order correction terms. As this variation is not significant in the work to follow, those values given in equation (IV-5) will be used.

The spin-orbit parameter ζ may be determined using equation (III-21) for W_{12} and equation (III-23) relating the interaction energy W_{12} to the perturbed energy separation Δ_1 and on eliminating the

TABLE 13

SENSITIVITY OF THE MIXING COEFFICIENTS AND THE ORBITAL REDUCTION PARAMETER TO SECOND ORDER CORRECTIONS

$k'\zeta'(cm^{-1})$	α	β	k
800	0.757	0.653	0.454
600	0.755	0.656	0.454
400	0.752	0.659	0.456
200	0.749	0.662	0.458
000	0.746	0.665	0.461

trigonal parameter K' using the relation $K'\zeta'/10Dq = 4D$, it is found that

$$\zeta = \sqrt{2}\alpha\beta\Delta_1 + \frac{1}{2}D + \frac{\zeta'^2}{10Dq} \qquad \text{(IV-6)}$$

where D is the splitting of the $^2E(T_d)$ manifold and is approximately 40 cm^{-1}. The trigonal parameter K may be found using equation (III-22) and on eliminating the unperturbed energy splitting δ using equation (III-19) and the relation $K' = 4D \times 10Dq/\zeta'$, one obtains

$$K = \frac{1}{3}\left[\Delta_1(\alpha^2-\beta^2-\sqrt{\frac{1}{2}}\alpha\beta) + \frac{1}{4}D - \frac{D^2 10Dq}{8\zeta'^2}\right] \qquad \text{(IV-7)}$$

Thus relations for ζ and K have been found which depend only on quantities which may be inferred from experiment.

As the mixing coefficients are rather insensitive to second order corrections, the values given by equation (IV-5) are used in the determination of the spin-orbit and trigonal parameters. The parameters best fitting the reported perturbed energy separation $\Delta_1 = 123$ cm^{-1} and the interlevel spin-orbit parameter $\zeta' = 720$ cm^{-1} are

$$\zeta = 198 \text{ cm}^{-1}$$

$$K = -20 \text{ cm}^{-1}.$$

The spin-orbit parameter is still seen to be unusually low although its value has been increased to 25% of its free ion value. From the susceptibility fittings for Ni^{2+}:ZnO and Co^{2+}:ZnO, one would expect a reduction of about 55% as the free ion values of Ni^{2+} and

Co^{2+} are $\zeta = -340\ cm^{-1}$ and $\zeta = -178\ cm^{-1}$ respectively and it was found by Brumage that they were reduced to $\zeta = -175\ cm^{-1}$ and $\zeta = -104\ cm^{-1}$ for Ni^{2+}:ZnO[45] and Co^{2+}:ZnO[46] respectively. Although no values were reported for the orbital reduction parameter of Ni^{2+}:ZnO and Co^{2+}:ZnO, the orbital reduction parameter $k = 0.46$ for Cu^{2+}:ZnO is abnormally small as a reduction of 75% for k indicates strong covalency. The trigonal parameter determined for Cu^{2+}:ZnO, $K = -20\ cm^{-1}$, was found to be consistent with the value of K calculated from the trigonal parameters $D\sigma$ and $D\tau$ found by Brumage[46] for Ni^{2+}:ZnO, i.e., the calculated value was $K = -36\ cm^{-1}$.

As the second order elements folded into the $^2T_2(T_d)$ manifold were large ($\sim 100\ cm^{-1}$), the third order elements were evaluated to see if they made any significant correction to the energy. It was found that the third order correction was negligible, (see Appendix I). A fourth order transformation was carried out to determine whether the second order transformation effectively isolated the $^2T_2(T_d)$ manifold. In Appendix I it may be seen that this is the case as the fourth order elements were four orders of magnitude smaller than the second order correction.

CHAPTER V

MAGNETIC SUSCEPTIBILITY OF Cu^{2+} IN ZnO

Several investigators at the University of Oklahoma, W. H. Brumage, J. P. Mahoney, and C. R. Yarger, have measured the magnetic susceptibility of Cu^{2+}:ZnO in the temperature interval from 30°K to 300°K for both the hexagonal c-axis oriented parallel and perpendicular to the external magnetic field. The crystals on which the susceptibility measurements were carried out are those used by Weakliem[26] in his optical studies. The susceptibility measurements are given in Table 14 and in Figure 5 the susceptibility χ (per gram sample) has been plotted as a function of inverse temperature $°K^{-1}$. In Figure 5, it is seen that the susceptibility curves have not been adjusted so that the values of χ at the liquid nitrogen point 77°K for the nitrogen run ($77°K \leq T \leq 300°K$) corresponds to that of the helium run ($30°K \leq T \leq 77°K$).

The susceptibility curves are seen to exhibit large anisotropy over the temperature interval ($30°K \leq T \leq 300°K$); the curve obtained for $\chi_{\perp}$ lying above that obtained for $\chi_{\parallel}$. Measurements of $\chi_{\perp}$ exhibit Curie behavior up to the liquid nitrogen point while one must go to somewhat lower temperatures, ($\sim 50°K$), before the susceptibility curve obtained for $\chi_{\parallel}$ exhibits Curie behavior. The non-Curie behavior above 77°K is

TABLE 14

MAGNETIC SUSCEPTIBILITY (PER GRAM SAMPLE) OF Cu^{2+}-DOPED ZnO CRYSTAL.* CONCENTRATION: 1.1%

T (°K)	$\chi_{\parallel} \times 10^7$ (cgs-emu)	T (°K)	$\chi_{\perp} \times 10^7$ (cgs-emu)
77	6.63	77	7.96
93	5.81	91	6.89
104	5.57	110	6.39
124	4.97	135	5.74
148	4.62	164	5.17
213	3.12	213	3.94
292	1.98	247	2.78
		297	2.67
77	6.56	77	8.08
147	4.60	134	5.79
181	3.81	197	4.34
217	2.97	232	3.83
297	2.02	297	2.71

TABLE 14 (continued)

T (°K)	$\chi \times 10^7$ (cgs-emu)	T (°K)	$\chi \times 10^7$ (cgs-emu)
77	6.27	77	7.60
62	7.60	55	9.22
47	8.59	48	10.04
36	9.71	42	11.01
33	9.86	31	13.45
69	7.20		
67	7.44		
66	7.46		
77	6.67		

* Different groupings in the above measurements for the magnetic susceptibility corresponds to independent observations, for example the spread at the liquid nitrogen point gives a measure of the reproducibility.

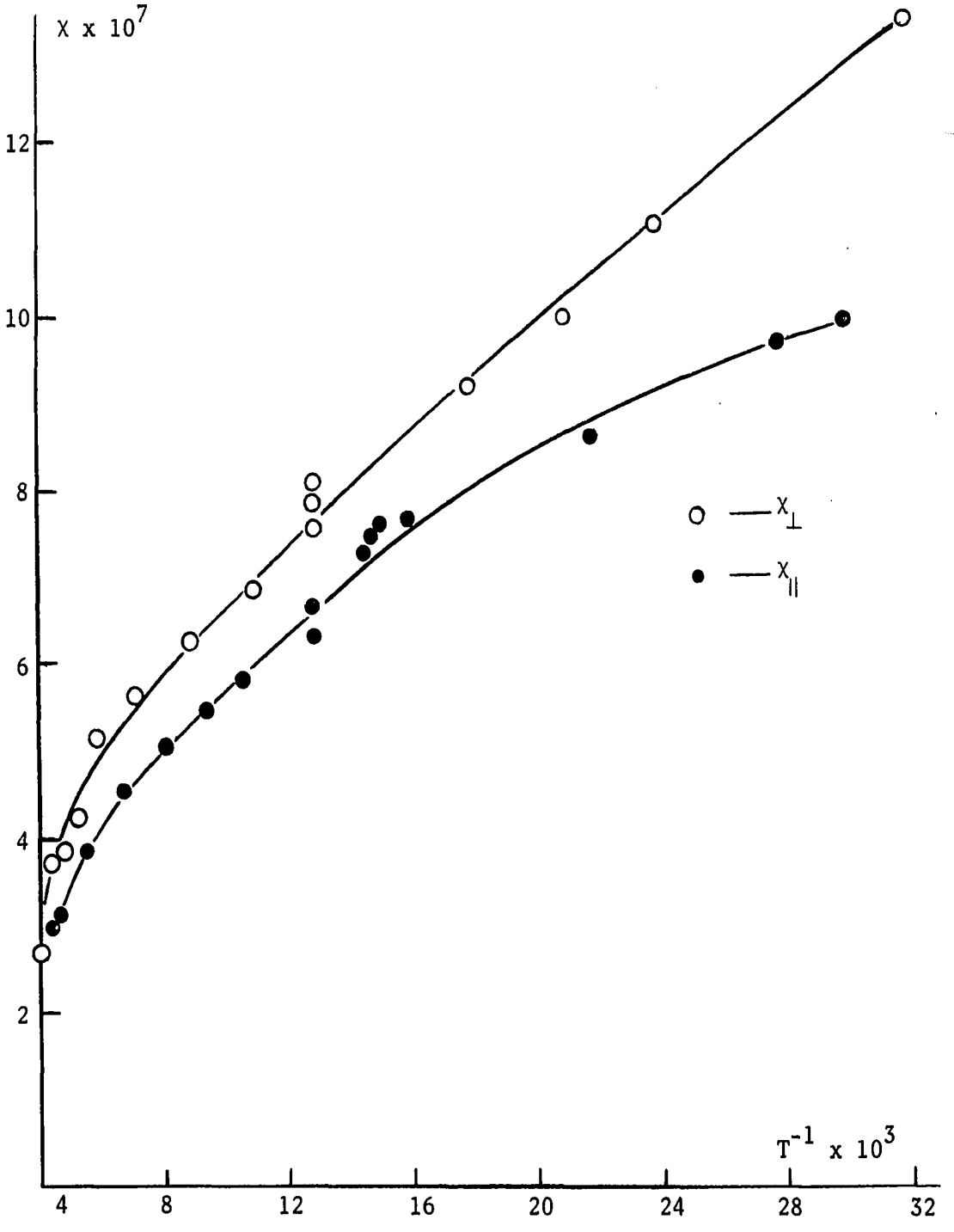

Figure 5. Magnetic susceptibility (per gram sample) of Cu^{2+}:ZnO

attributed to the presence of low lying magnetic levels of Cu^{2+} owing to the splitting of the cubic $^2T_2(T_d)$ manifold by the interplay of the spin-orbit interaction energy and the trigonal field. This gives independent confirmation of the optical results of Dietz as to the presence of an excited level lying near the $\Gamma_6(^2T_2)$ ground state, ($\sim$123 cm^{-1}).

The ratio of the Curie constants obtained from the slopes of the experimental susceptibility curves in the low temperature interval is approximately

$$C_{\parallel}/C_{\perp} = 0.23 - 0.25 \ .$$

This agrees well with the ratio of the square of the magnetic moments found from electron paramagnetic resonance measurement[14]

$$\left|g_{\parallel}/g_{\perp}\right|^2 = 0.234.$$

The molar concentration B, where

$$B = \frac{32}{3g^2} \text{ (mole wt. ZnO) } C$$

may be found using the spin only formalism[3] valid at low temperatures and it was found that for the Curie constants of both $\chi_{\parallel}$ and $\chi_{\perp}$ the concentration of the Copper ion in ZnO was approximately $\sim$1.1%.

Theoretical expressions for the molar susceptibility for both $\chi_{\parallel}$ and $\chi_{\perp}$ may be found using the general expression (I-10), therefore

$$\chi_{\parallel} = \frac{N\mu_o^2}{kZ}\left(\frac{|g_{\parallel}(\Gamma_6^-(^2T_2))|^2}{4T} - 2kW_{\parallel}^{(2)}\ (\Gamma_6^-(^2T_2))\right. \tag{V-1}$$

$$+ \left[\frac{|g_{\parallel}(\Gamma_6^+(^2T_2))|^2}{4T} - 2kW_{\parallel}^{(2)}\ (\Gamma_6^+(^2T_2))\right] e^{-\Delta_1/kT}$$

$$\left. + \left[\frac{|g_{\parallel}(\Gamma_4,\Gamma_5(^2T_2))|^2}{4T} - 2kW_{\parallel}^{(2)}\ (\Gamma_4,\Gamma_5(^2T_2))\right] e^{-\Delta_2/kT}\right)$$

and

$$\chi_{\perp} = \frac{N\mu_o^2}{kZ}\left(\frac{|g_{\perp}(\Gamma_6^-(^2T_2))|^2}{4T} - 2kW_{\perp}^{(2)}(\Gamma_6^-(^2T_2))\right. \tag{V-2}$$

$$+ \left[\frac{|g_{\perp}(\Gamma_6^+(^2T_2))|^2}{4T} - 2kW_{\perp}^{(2)}\ (\Gamma_6^+(^2T_2))\right] e^{-\Delta_1/kT}$$

$$\left. -2kW_{\perp}^{(2)}\ (\Gamma_4,\Gamma_5(^2T_2))\ e^{-\Delta_2/kT}\right),$$

where

$$Z = 1 + e^{-\Delta_1/kT} + e^{-\Delta_2/kT}$$

The expressions for the g-factors and the quadratic coefficients $W^{(2)}$ are given in Chapter III. The perturbed energy separations Δ_1 and Δ_2 are given by equations (III-20) and (III-34) respectively.

It is seen in the above relations (V-1) and (V-2) for $\chi_{\parallel}$ and $\chi_{\perp}$ respectively that the ^2E manifold does not contribute directly to the susceptibility as the Boltzmann factor nearly vanishes for the temperature interval under consideration.

Using the crystal field parameters best fitting the optical spectra, one finds that the calculated susceptibility curve shown in Figure 6 does not conform with that obtained from experiment. It is seen that the calculated curve for $\chi_{||}$ crossed that for $\chi_{\perp}$ at $T \simeq 60°K$ giving results contradicting the experimental curve. Below $T = 77°K$ the low temperature end of the susceptibility curves determined using the optical parameters did not conform well with the difference $\Delta\chi = (\chi_{\perp} - \chi_{||})$ found for the experimental curve. In Figure 7 the calculated curve using the parameters determined by Dietz et. al. is shown. Here the second order correction to the energies and to the linear and quadratic Zeeman effect is zero. Although the fit is somewhat better, the calculated curve does not show the correct curvature at high temperatures and in the low temperature interval the calculated curve for $\chi_{||}$ falls below that obtained from experiment.

On increasing the energy splitting of the two $\Gamma_6(^2T_2)$ levels to the value 150 cm^{-1}, one obtains the calculated curve shown in Figure 8. The values for the interlevel spin-orbit, trigonal field and orbital reduction parameters were those given by Dietz et. al.[14] It is seen that the curvature exhibited by the calculated curve has shifted to a slightly higher temperature, ($T \simeq 77°K$), while at low temperatures the curve for $\chi_{||}$ falls slightly below that obtained from experiment. This results from the fact that the quadratic Zeeman terms are directly proportional to the energy splittings of the $^2T_2$ manifold. Thus the difference between the temperature independent susceptibility for $\chi_{\perp}$

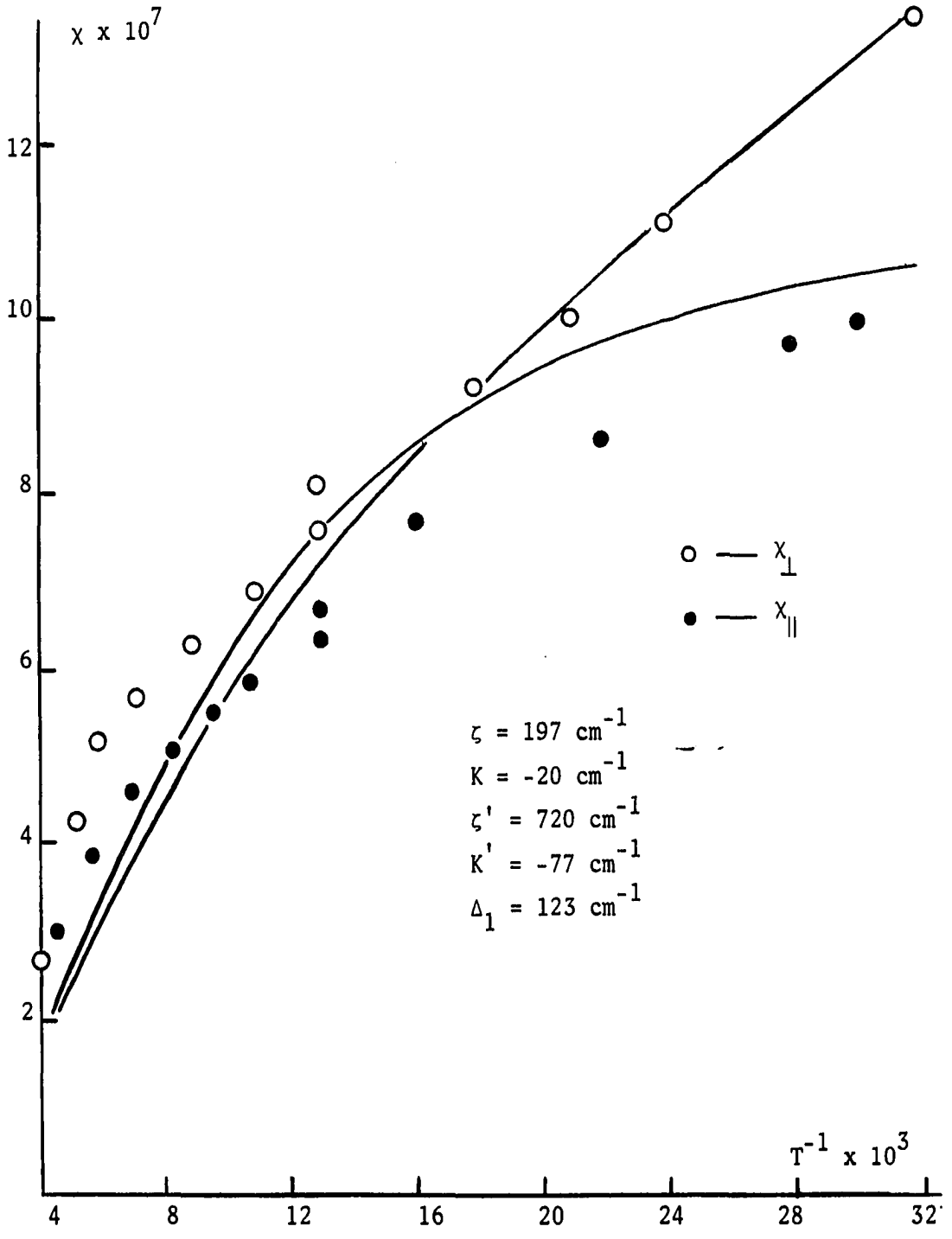

Figure 6. Calculated magnetic susceptibility of Cu^{2+}:ZnO (Optical Parameters)

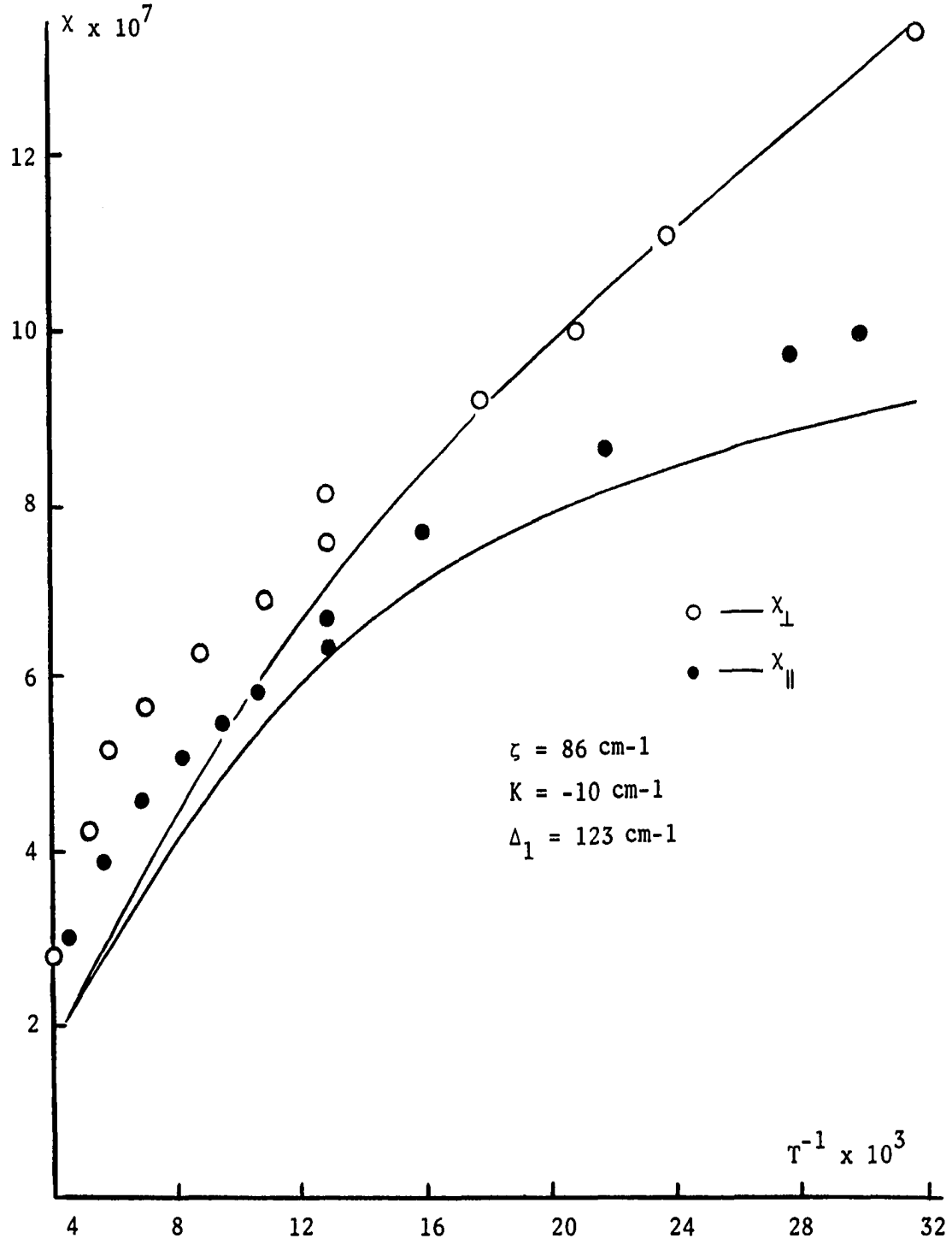

Figure 7. Calculated magnetic susceptibility of Cu^{2+}:ZnO (Dietz's parameters)

and $\chi_{||}$ becomes smaller for a larger energy separation. For temperatures above 77°K, the shape of the calculated susceptibility curves is largely dictated by the Boltzmann factor since the g-factors for the $^2T_2$ manifold remain nearly constant. The temperature at which $\chi_{||}$ crosses $\chi_{\perp}$ is seen to shift towards higher temperatures as the energy spacing Δ_1 is increased.

The effect of the second order corrections to the linear and quadratic Zeeman terms is shown in Figure 9. Here the energy splitting of the $\Gamma_6(^2T_2)$ levels remained at the value predicted experimentally, i.e., 123 cm^{-1}, and the product $k'\zeta'$ is 400 cm^{-1}. The interlevel trigonal parameter was assumed small relative to the larger spin-orbit parameter. It is seen in Figure 9 that the difference $\Delta\chi = (\chi_{\perp} - \chi_{||})$ for the low temperature interval has increased owing to the fact that the magnitude of the difference of the quadratic Zeeman coefficients

$$W_{||}^{(2)}(\Gamma_6^-(^2T_2)) - W_{\perp}^{(2)}(\Gamma_6^-(^2T_2))$$

becomes smaller as the second order corrections are decreased. Above 77°K the form of the calculated curve is largely dictated by the excited state g-factors as they are quite sensitive to second order corrections. The temperature at which $\chi_{||}$ crosses $\chi_{\perp}$ is seen to increase for smaller values of the interlevel spin-orbit parameter.

It is seen from inspection of Figures 8 and 9 that for the high temperature interval, (T>77°K), the curvature and placement of the calculated curves do not agree with that found from experiment. A satisfactory fit could not be found for reasonable variation of the crystal field parameters.

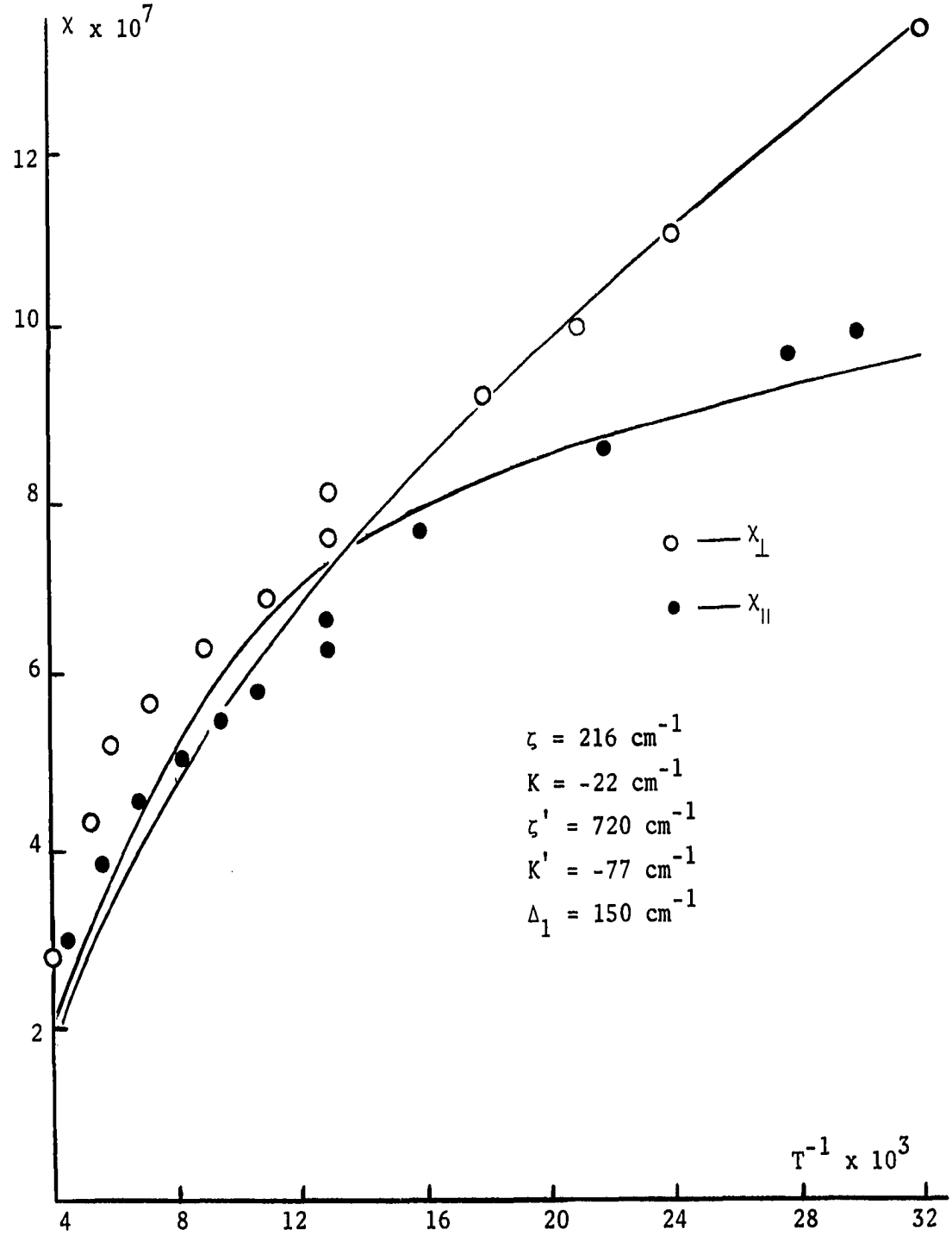

Figure 8. The calculated magnetic susceptibility (per gram sample) for a larger $\Gamma(^2T_2)$ ground state energy separation

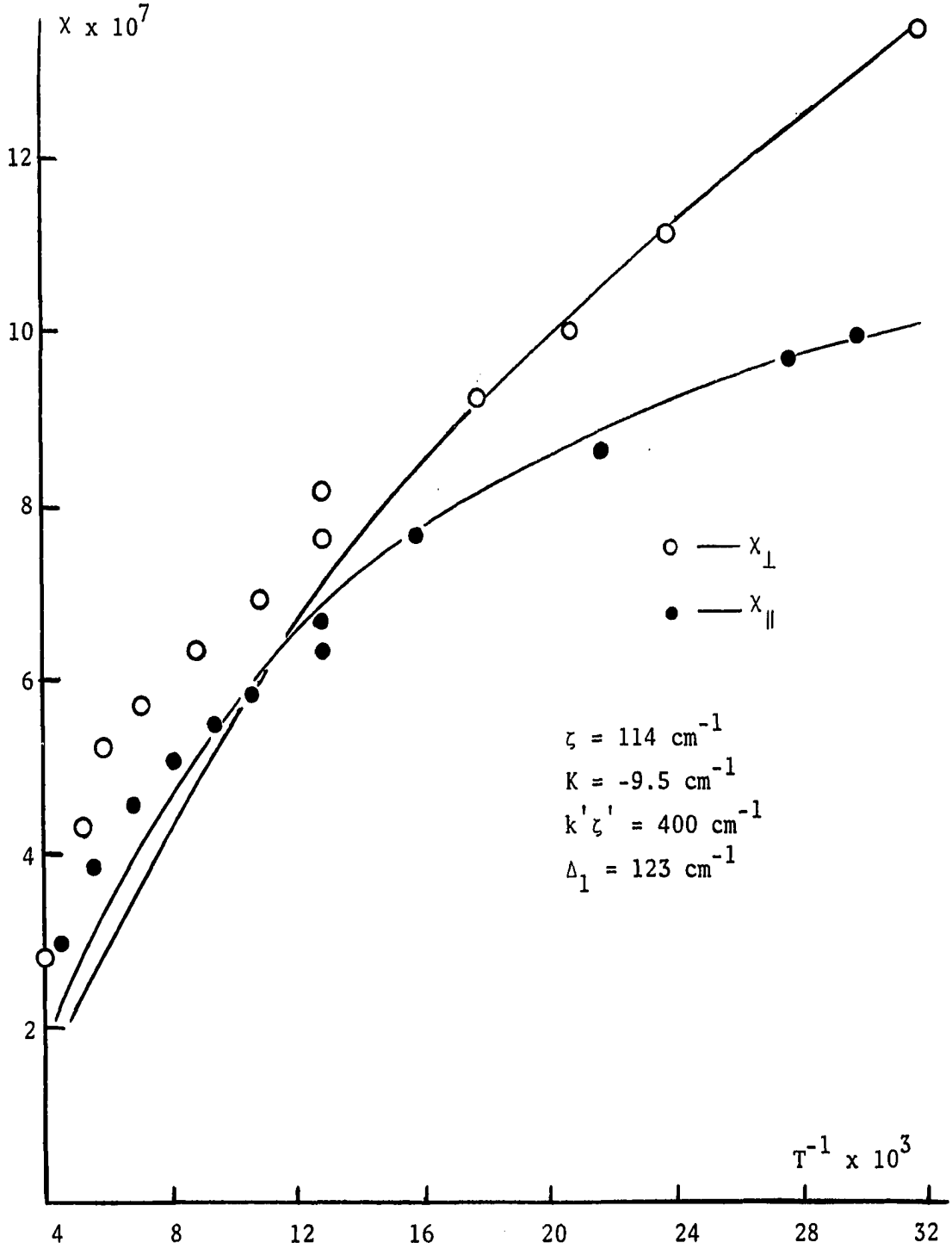

Figure 9. The calculated magnetic susceptibility (per gram sample) for a smaller value for the interlevel spin-orbit parameter

CHAPTER VI

DELOCALIZATION OF THE Cu^{2+} 3d ORBITAL

Orthogonalization to the Bloch Functions

As there is relatively little quantitative information concerning the character of the bonding of the compound ZnO, the bonding will be approximated by the ionic model. This model gives the simplification that the valence band functions are constructed from linear combinations of the doubly negatively ionized oxygen (2s) and (2p) atomic orbitals while the conduction band functions arise from the doubly ionized zinc (4s) and (4p) atomic orbitals.

The basis for the band functions will be taken as the normalized Bloch sum[31]

$$b_n(\vec{k},\vec{r}) = [N\Omega_n(\vec{k})]^{-\frac{1}{2}} \sum_i e^{i\vec{k}\cdot\vec{R}_i} \phi_n(\vec{r}-\vec{R}_i), \qquad \text{(VI-1)}$$

where the index i denotes a summation over the N equivalent lattice sites of the crystal and the term $\Omega_n(\vec{k})$ represents the integral

$$\Omega_n(\vec{k}) = \sum_i \int_{\substack{\text{entire}\\ \text{crystal}}} e^{-i\vec{k}\cdot\vec{R}_i} \phi_n^*(\vec{r})\phi_n(\vec{r}-\vec{R}_i)\, d\tau \qquad \text{(VI-2)}$$

The wave vector $\vec{k}$ labels the irreducible representation of the trans-

lation group under which the Bloch function $b_n(\vec{k},\vec{r})$ transforms and the quantum index n represents that collection of quantum numbers (n,ℓ,m) labeling the atomic orbitals from which the Bloch sum is constructed. The valence band functions may then be found using the method of tight binding and are given by

$$\chi_\nu(\vec{k},\vec{r}) = \sum_n C_\nu^n(\vec{k})\, b_n(\vec{k},\vec{r}), \qquad \text{(VI-3)}$$

where the band index ν labels the irreducible representation of "the group of the wave vector $\vec{k}$"[34] to which the valence band functions belongs. The summation over the quantum index n is then restricted to the Bloch functions constructed from the doubly ionized oxygen orbitals. In principle, the expansion coefficients $C_\nu^n(\vec{k})$ are found on setting up the energy matrix for the one electron Hamiltonian of ZnO using the Bloch functions as basis and solving the resulting secular equation.

Since the Cu^{2+} ion enters the ZnO lattice substitutionally forming a deep acceptor state, the unnormalized wave function for the localized Cu^{2+} hole is then

$$\psi_m(^2D) = \psi_m^\circ(^2D) + \sum_{\vec{k}} \sum_\nu \Lambda_\nu^m(\vec{k})\, \chi_\nu(\vec{k},\vec{r}) \qquad \text{(VI-4)}$$

where $\psi_m^\circ(^2D)$ is the unperturbed free ion wave function. The mixing coefficients $\Lambda_\nu^m(\vec{k})$ giving the amount of admixture of the delocalized valence band states into the localized state is to be determined from orthogonalization of the localized function with the valence band

functions. Unfortunately the expansion coefficients $C_{\nu}^{n}(\vec{k})$ defined in equation (VI-3) have not been evaluated for ZnO and hence the valence band functions are not known. Thus the mixing coefficients $\Lambda_{\nu}^{m}(\vec{k})$ defined by equation (VI-4) giving the amount of delocalization of the Cu^{2+} hole cannot be evaluated directly.

In this work, the localized function will be constructed by admixing the Bloch functions forming the basis for the valence band states with the Cu^{2+} free ion functions. The localized function is then given by

$$\psi_m(^2D) = \psi_m^{\circ}(^2D) + \sum_{\vec{k}} \sum_{n} \lambda_n^m(\vec{k})\, b_n(\vec{k},\vec{r}), \qquad \text{(VI-5)}$$

where the mixing coefficients $\lambda_n^m(\vec{k})$ are to be determined on orthogonalizing the localized functions to the Bloch sums. The condition of orthogonality is

$$\langle b_n'(\vec{k},\vec{r});\ \psi_m(^2D)\rangle = 0$$

or

$$\sum_{n} \lambda_n^m(\vec{k})\ \langle b_n'(\vec{k},\vec{r});\ b_n(\vec{k},\vec{r})\rangle = -\langle b_n'(\vec{k},\vec{r});\ \psi_m^{\circ}(^2D)\rangle\ , \qquad \text{(VI-6)}$$

where use has been made of the fact that the Bloch sums are orthogonal with respect to the wave vector $\vec{k}$. In general Bloch functions constructed from different atomic orbitals do not exhibit orthogonality for a general point in $\vec{k}$ space, thus a system of simultaneous linear equations

given by equation (VI-6) must be solved to determine the mixing coefficients.

Throughout the following discussion two simplifying approximations will be made. The first approximation to be made is that the overlap between atomic orbitals centered on neighboring ligand sites is small so that we can drop the overlap terms in equation (VI-6). The Bloch functions are then orthogonal in the quantum index n and equation (VI-6) reduces to

$$\lambda_n^m(\vec{k}) = - \langle b_n(\vec{k},\vec{r}); \psi_m^\circ(^2D) \rangle \ . \qquad \text{(VI-7)}$$

The second approximation to be made is that the mixing coefficient $\lambda_n^m(\vec{k})$ is determined primarily from the overlap between the localized copper 3d orbitals and its nearest neighbor ligands.

Crystal Structure of ZnO

The crystalline form of zinc oxide is wurtzite structure and belongs to the C_{6v}^4 space group.[47] The wurtzite lattice can be considered as two interpenetrating close-packed hexagonal lattices, one of zinc and one of oxygen, where the zinc lattice is displaced from that of oxygen by the translation $(uc\hat{t}_3)$ along the hexagonal c-axis. The lattice constant c is the distance between two adjacent equivalent sites along the hexagonal c-axis and for ideal wurtzite structure the parameter u is close to the value u = 3/8.

In Figure 10, the unit cell of wurtzite on the conventional hexagonal axis is shown; the origin is chosen to lie along the six fold screw axis $6_{1/2}$ while the glide plane $m_{1/2}$ contains the unit translation vector $\hat{t}_1$.

The coordinates of the ions in the unit cell given in terms of the conventional hexagonal axis are[47]

(I) (1/3, 2/3, 0)
(II) (2/3, 1/3, 1/2) (VI-8)

for the oxygen ligands represented by the open circles and

(III) (1/3, 2/3, u)
(IV) (2/3, 1/3, u+1/2) (VI-9)

for the zinc cations represented by the blackened circles where the first two coordinate points along the $\hat{t}_1$ and $\hat{t}_2$ axes respectively are given in units of the base lattice constant a, while the third coordinate point along $\hat{t}_3$ is given in units of the lattice constant c.

If it is assumed that the Cu^{2+} ion enters the zinc site at (1/3, 2/3, u), the nearest neighbor ligands to the copper ion are then situated at

(1) (1/3, 2/3, 0)
(2) (2/3, 1/3, 1/2)
(3) (2/3, 4/3, 1/2)
(4) (-1/3, 1/3, 1/2) (VI-10)

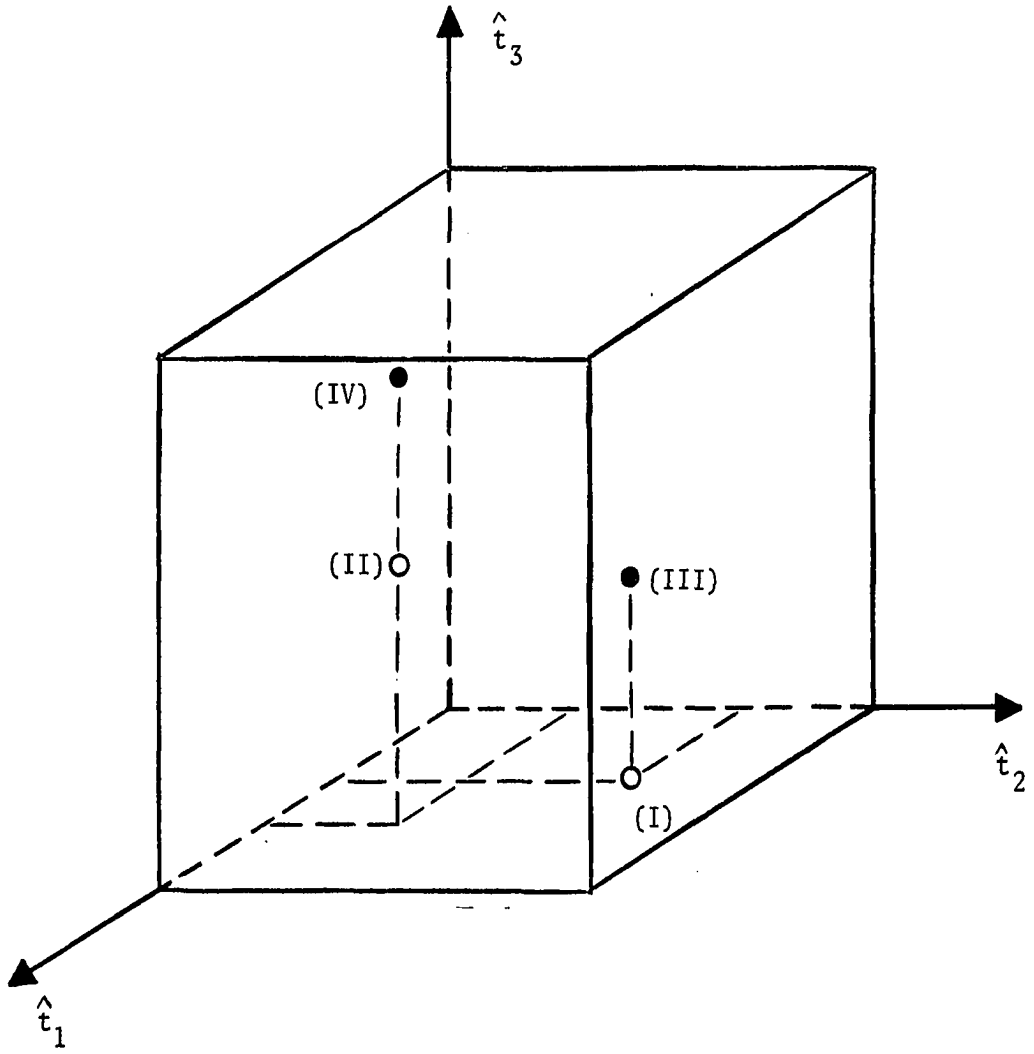

Figure 10. Unit cell of wurtzite on the conventional hexagonal axes

and in Figure 11, the base plane projection giving the relationship of the Cu^{2+} ion and its nearest neighbor ligands is shown. It is seen that the ligands situated at sites (3) and (4) are equivalent to that situated at the site (2), differing only by the fundamental translations ($a\,\hat{t}_2$) and ($-a\,\hat{t}_1$) respectively, while the ligand situated at site (1) is not equivalent to that at site (2) but does lie in the same unit cell.

The orientation of the Cartesian coordinate axes given in Figure 11 are chosen to conform with that of Bates;[35] the x axis is directed along the mirror plane σ_d while the y axis is contained in a glide plane $m_{1/2}$. Expressions relating the hexagonal system to the Cartesian system may be obtained from inspection of Figure 11 and it is found that

$$\hat{t}_1 = -\frac{1}{2}\sqrt{3}\,\hat{i} - \frac{1}{2}\,\hat{j}$$

$$\hat{t}_2 = \frac{1}{2}\sqrt{3}\,\hat{i} - \frac{1}{2}\,\hat{j}$$

$$\hat{t}_3 = \hat{k}$$

On expressing the ligand coordinates given in the hexagonal system into those of the Cartesian system, the nearest neighbor ligand sites are

$$O^{2-} \quad (1) \quad \left(\frac{1}{2}\sqrt{\frac{1}{3}},\ -\frac{1}{2},\ 0\right) \qquad \text{(VI-11)}$$

$$(2) \quad \left(-\frac{1}{2}\sqrt{\frac{1}{3}},\ -\frac{1}{2},\ \frac{1}{2}\right)$$

$$(3) \quad \left(\sqrt{\frac{1}{3}},\ -1,\ \frac{1}{2}\right)$$

$$(4) \quad \left(\sqrt{\frac{1}{3}},\ 0,\ \frac{1}{2}\right)$$

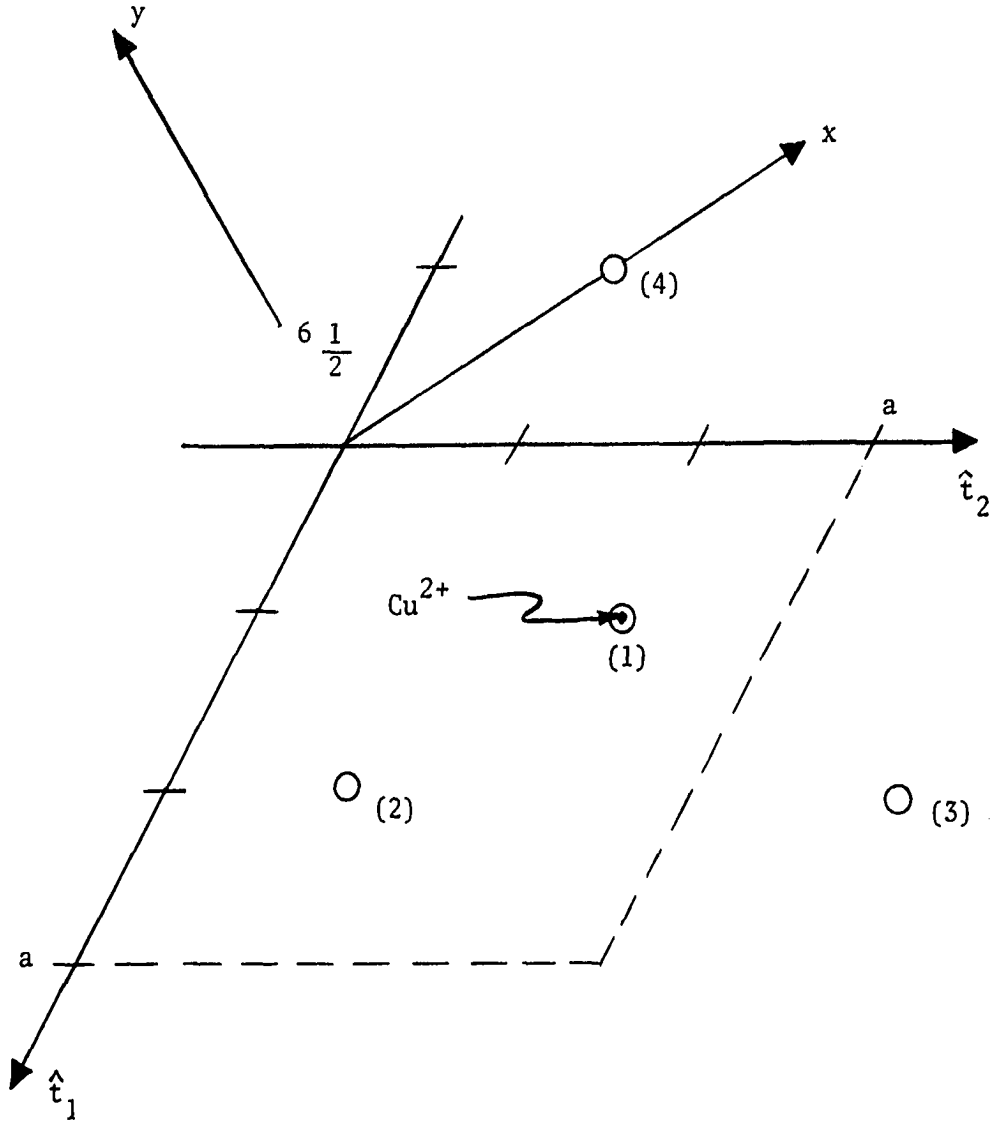

Figure 11. Base plane projection of the wurtzite structure

and the site for the Cu^{2+} ion is then given by

$$Cu^{2+} \qquad \left(\frac{1}{2}\sqrt{\frac{1}{3}}, -\frac{1}{2}, u \right) \tag{VI-12}$$

Similarly as for the coordinates in the hexagonal system, the Cartesian coordinates measured relative to the axes in the base plane are in units of the lattice constant a and those along the c-axis are given in units of c.

The direction cosines giving the relative orientation of the nearest neighbor ligand sites to that of the copper ion are found using the above coordinates expressed in the Cartesian system. Since the trigonal distortion is small, the ZnO lattice will be approximated by the ideal wurtzite structure and hence the parameter u = 3/8 and c/a = 8/3 are[33] used to determine the following direction cosines for the ligand sites

$$\begin{aligned} &(1) \quad (0,\ 0,\ -1) \\ &(2) \quad \left(-\frac{2}{3}\sqrt{2},\ 0,\ \frac{1}{3}\right) \\ &(3) \quad \left(\frac{1}{3}\sqrt{2},\ -\sqrt{\frac{2}{3}},\ \frac{1}{3}\right) \\ &(4) \quad \left(\frac{1}{3}\sqrt{2},\ \sqrt{\frac{2}{3}},\ \frac{1}{3}\right) . \end{aligned} \tag{VI-13}$$

Since the space group for wurtzite is nonsymmorphic, that is the two oxygen sites in the unit cell are not equivalent as they are not related by the fundamental translations but rather by operations involving a nonprimative translation, then in construction of the

Bloch functions the linear combination of the oxygen orbitals include only those orbitals centered on equivalent sites. The localized function given by equation (VI-5) then assumes the form

$$\psi(^2D) = \psi^\circ(^2D) + \sum_{\vec{k}} \sum_{n} [\lambda_n^{(I)}(\vec{k})\, b_n^{(I)}(\vec{k},\vec{r}) + \lambda_n^{(II)}(\vec{k})\, b_n^{(II)}(\vec{k},\vec{r})], \tag{VI-14}$$

where the superscripts (I) and (II) denote those Bloch functions constructed from the ligand orbitals situated on sites equivalent to the oxygen sites labeled (I) and (II) respectively. The mixing coefficients $\lambda_n^{(I)}$ and $\lambda_n^{(II)}$ are given by the relation (VI-7) and it is found that the localized function is given by

$$\psi_m(^2D) = \psi_m^\circ(^2D) - \sum_{\vec{k}} \sum_{n} [\langle b_n^{(I)}(\vec{k},\vec{r});\ \psi_m^\circ(^2D)\rangle\, b_n^{(I)}(\vec{k},\vec{r}) - \langle b_n^{(II)}(\vec{k},\vec{r});\ \psi_m^\circ(^2D)\rangle\, b_n^{(II)}(\vec{k},\vec{r})] \tag{VI-15}$$

Evaluation of the Two Center Overlap Integrals

The evaluation of the mixing coefficients given by the relation (VI-7) is simplified on expressing the ligand (2p) and the copper (3d) orbitals in terms of the real wave functions listed in Table 15, where the axis of quantization implied is the hexagonal c-axis and the phase chosen is that defined by Condon and Shortley. If now the vector $(\vec{R}_o - \vec{R}_{cu})$ defines the relative position of the O^{2-} ion to that of the Cu^{2+} ion, the directed orbitals given in Table 15 may then be

expressed in terms of functions quantized around the $(\vec{R}_o - \vec{R}_{cu})$ axis. That is if σ, π and δ refer to the component of angular momentum around the axis of quantization $(\vec{R}_o - \vec{R}_{cu})$, the real wave functions listed in Table 15 may then be expressed as linear combinations of the $p\sigma$ and $p\pi_{\pm}$ functions and the $d\sigma$, $d\pi_{\pm}$ and $d\delta_{\pm}$ functions for the p and d orbitals respectively. Thus the overlap integrals between the real wave functions may then be expressed as functions of the direction cosines (ℓ,m,n) giving the orientation of the vector $(\vec{R}_o - \vec{R}_{cu})$ stretching between the two sites relative to a space frame and the parameters $(sd\sigma)$, $(pd\sigma)$ and $(pd\pi)$. For example the parameter $(pd\pi)$ represents the overlap integrals between the oxygen $2p\pi_{\pm}$ functions with the copper $3d\pi_{\pm}$ functions.

Slater and Koster[36] have worked out expressions for the energy integrals of a crystal in terms of the parameters given above and from their results the expressions for the overlap integrals to be evaluated here are obtained and are listed in Table 16. Those overlap integrals not listed in Table 16 may be found on cyclically permuting the coordinates and direction cosines. The direction cosines found in equation (VI-13) may then be substituted into the relations listed in Table 16 to obtain explicit expressions for the overlap integrals between the real wave functions of the copper ion and the nearest neighbor oxygen ions. The results are given in Appendix III.

The radial dependence of the real wave functions given in

TABLE 15

THE REAL WAVE FUNCTIONS FOR THE 2p AND 3d ORBITALS

2p

$$p_x = \sqrt{\frac{3}{4\pi}}\, R_p(r)\, \left(\frac{x}{r}\right) = \sqrt{\frac{1}{2}}\, (p_{-1} - p_1)$$

$$p_y = \sqrt{\frac{3}{4\pi}}\, R_p(r)\, \left(\frac{y}{r}\right) = i\sqrt{\frac{1}{2}}\, (p_1 + p_{-1})$$

$$p_z = \sqrt{\frac{3}{4\pi}}\, R_p(r)\, \left(\frac{z}{r}\right) = p_o$$

3d

$$d_{xy} = \sqrt{\frac{15}{4\pi}}\, R_d(r)\, \left(\frac{xy}{r^2}\right) = -i\sqrt{\frac{1}{2}}\, (d_2 - d_{-2})$$

$$d_{xz} = \sqrt{\frac{15}{4\pi}}\, R_d(r)\, \left(\frac{xz}{r^2}\right) = -\sqrt{\frac{1}{2}}\, (d_1 - d_{-1})$$

$$d_{yz} = \sqrt{\frac{15}{4\pi}}\, R_d(r)\, \left(\frac{yz}{r^2}\right) = i\sqrt{\frac{1}{2}}\, (d_1 + d_{-1})$$

$$d_{x^2-y^2} = \frac{1}{2}\sqrt{\frac{15}{4\pi}}\, R_d(r)\, \left(\frac{x^2-y^2}{r^2}\right) = \sqrt{\frac{1}{2}}\, (d_2 + d_{-2})$$

$$d_{z^2} = \frac{1}{2}\sqrt{\frac{15}{4\pi}}\, R_d(r)\, \left(\frac{3z^2-r^2}{r^2}\right) = d_o$$

TABLE 16

THE TWO CENTER OVERLAP INTEGRALS EXPRESSED

IN TERMS OF THE SLATER-KOSTER PARAMETERS*

$$\langle s;xy\rangle = \sqrt{3}\ \ell m\ (sd\sigma)$$

$$\langle s;x^2-y^2\rangle = \frac{1}{2}\sqrt{3}\ (\ell^2-m^2)(sd\sigma)$$

$$\langle s;z^2\rangle = [n^2 - \frac{1}{2}\ (\ell^2+m^2)]\ (sd\sigma)$$

$$\langle x;xy\rangle = \sqrt{3}\ \ell^2 m(pd\sigma) + m(1-2\ell^2)(pd\pi)$$

$$\langle x;yz\rangle = \sqrt{2}\ \ell mn(pd\sigma) - 2\ell mn(pd\pi)$$

$$\langle x;xz\rangle = \sqrt{3}\ \ell^2 n(pd\sigma) + n(1-2\ell^2)(pd\pi)$$

$$\langle x;x^2-y^2\rangle = \frac{1}{2}\sqrt{3}\ \ell(\ell^2-m^2)(pd\sigma) + \ell(1-\ell^2+m^2)(pd\pi)$$

$$\langle y;x^2-y^2\rangle = \frac{1}{2}\sqrt{3}\ m(\ell^2-m^2)(pd\sigma) - m(1+\ell^2-m^2)(pd\pi)$$

$$\langle z;x^2-y^2\rangle = \frac{1}{2}\sqrt{3}\ n(\ell^2-m^2)(pd\sigma) - n(\ell^2-m^2)(pd\pi)$$

$$\langle x;z^2\rangle = \ell[n^2 - \frac{1}{2}\ (\ell^2+m^2)](pd\sigma) - \sqrt{3}\ell n^2(pd\pi)$$

$$\langle y;z^2\rangle = m\ [n^2 - \frac{1}{2}\ (\ell^2+m^2)](pd\sigma) - \sqrt{3}mn^2(pd\pi)$$

$$\langle z;z^2\rangle = n\ [n^2 - \frac{1}{2}\ (\ell^2+m^2)](pd\sigma) + \sqrt{3}n(\ell^2+m^2)(pd\pi)$$

*The real wave function $d_{3z^2-r^2}$ has been abbreviated as d_{z^2}.

Table 15 was obtained from the Hartree-Fock functions found for the Cu^{2+} and O^{2-} ions as the atomic orbitals of these ions serve as basis for the localized ^2D state and the unperturbed valence band states respectively. The normalized Hartree-Fock radial functions given by Clementi[39,40] are

$$R_{2s}(r) = 8.473\, e^{-7.617r} + 1.055\, e^{-12.22r} + r[-10.385\, e^{-2.762r} + 12.733\, e^{-7.09r} - 1.251\, e^{-1.486r}] \quad \text{(VI-16)}$$

$$R_{2p}(r) = r[2.077\, e^{-1.557r} + 7.336\, e^{-3.43r} + 7.223\, e^{-0.43r} - 3.478\, e^{-0.55r} + 2.274\, e^{-8.127r}]$$

$$R_{3d}(r) = (r)^2\, [33.43\, e^{-4.532r} + 97.73\, e^{-13r} + 113.14\, e^{-7.287r} + 5.03\, e^{-2.702r} + 0.36\, e^{-1.829r}]$$

The free ion 2p and 3d radial functions are seen to be constructed from the Slater type nodeless 2p and 3d orbitals respectively while the free ion 2s function is constructed from the 1s and 2s Slater type orbitals. The angular dependence for the 2s, 2p and 3d functions may be found in Table 15.

The Slater-Koster parameters may be determined on evaluation of the following overlap integrals

$$\langle e^{-\alpha_1 r_A} ; x_B z_B e^{-\alpha_2 r_B} \rangle$$

$$\langle r_A e^{-\alpha_1 r_A} ; x_B z_B e^{-\alpha_2 r_B} \rangle$$

$$\langle y_a e^{-\alpha_1 r_A} ; y_B z_B e^{-\alpha_2 r_B} \rangle$$

between unnormalized Slater type nodeless functions appearing in the expansion of the following overlap integrals

$$\langle 2s; 3d_{xz} \rangle = \sqrt{3}\, \ell n(sd\sigma)$$

$$\langle 2p_y; 3d_{yz} \rangle = \sqrt{3}\, m^2 n(pd\sigma) + n(1-2m^2)(pd\pi).$$

The vector $\vec{r}_A$ and $\vec{r}_B$ are to be measured relative to the O^{2-} and Cu^{2+} sites respectively. Once the overlap integrals given above have been evaluated for several orientations of the oxygen anion, the Slater-Koster parameters are easily obtained.

The requisite two center integrals involving two unnormalized Slater type nodeless functions can be reduced to a single center one dimensional integral on using the technique of Gaussian transformation,[37] (for discussion and relevant formulas see references 38 and 48). After carrying out the transformation indicated above, the expressions for the overlap integrals were found to be

$$\langle e^{-\alpha_1 r_A}; x_B z_B e^{-\alpha_2 r_B} \rangle = -\ell n \alpha_1 \alpha_2 a_o \xi_1$$

$$\langle r_A e^{-\alpha_1 r_A}; x_B z_B e^{-\alpha_2 r_B} \rangle = \ell n [\alpha_2 a_o \xi_1 - \alpha_1^2 \alpha_2 a_o^3 \xi_2] \qquad \text{(VI-17)}$$

$$\langle y_A e^{-\alpha_1 r_A}; y_B z_B e^{-\alpha_2 r_B} \rangle = n \alpha_1 \alpha_2 a_o^2 [\xi_2 - m^2 \xi_3]$$

The one dimensional integrals ξ_1, ξ_2 and ξ_3 appearing above are given by

$$\xi_1 = 2\pi \int_o^1 \frac{f^3}{(1-u)^2} [3(fg)^{-\frac{5}{2}} + 3(fg)^{-2} + (fg)^{-\frac{3}{2}}] e^{-\sqrt{fg}} du \qquad \text{(VI-18)}$$

$$\xi_2 = 2\pi \int_o^1 \frac{f^3}{(1-u)} [15(fg)^{-\frac{7}{2}} + 15(fg)^{-3} + 6(fg)^{-\frac{5}{2}} + (fg)^{-2}] e^{-\sqrt{fg}} du$$

$$\xi_3 = 2\pi \int_o^1 \frac{f^3}{(1-u)} [3(fg)^{-\frac{5}{2}} + 3(fg)^{-2} + (fg)^{-\frac{3}{2}}] e^{-\sqrt{fg}} du ,$$

where the parameters f(u) and g(u) are defined as follows

$$f(u) = u(1-u)\, a_o^2$$

and

$$g(u) = \alpha_1^2/u + \alpha_2^2/(1-u)$$

The one dimensional integrals ξ_1, ξ_2 and ξ_3 may then be evaluated by numerical quadrature once the orbital exponents α_1 and α_2 appearing in the expansion for the radial functions given in (VI-16) for O^{2-} and Cu^{2+} orbitals respectively and the ionic distance a_o are known. For ZnO the ionic distance was taken to be 1.96 $\mathring{A}$ [32] and the Slater-Koster parameters obtained were

$$(sd\sigma) = 0.03088$$

$$(pd\sigma) = 0.05434 \qquad \text{(VI-19)}$$

$$(pd\pi) = 0.0393$$

Since we are interested in the orthogonalization of the cubic wave functions given in Table 1 with the valence band functions, the cubic wave functions must be expressed in terms of the real wave functions given in Table 15 and its found that

$$t_2^+ = \sqrt{1/3}[d_{x^2-y^2} - \sqrt{\tfrac{1}{2}}\, d_{xy} + i\, d_{xy} + i\sqrt{\tfrac{1}{2}}\, d_{yz}] \qquad \text{(VI-20)}$$

$$t_2^o = d_{3z^2-r^2}$$

$$t_2^- = \sqrt{1/3}[-d_{x^2-y^2} + \sqrt{1/2}\, d_{xz} + i\, d_{xy} + i\sqrt{1/2}\, d_{yz}]$$

$$e = \sqrt{1/3}\,[\sqrt{1/2}\, d_{x^2-y^2} + d_{xz} + i\sqrt{1/2}\, d_{xy} - i\, d_{yz}]$$

$$e' = \sqrt{1/3}\,[-\sqrt{1/2}\,d_{x^2-y^2} - d_{xz} + i\sqrt{1/2}\,d_{xy} - i\,d_{yz}]$$

The overlap integrals between the cubic wave functions and the nearest neighbor ligands may be expressed in terms of the two center parameters on using the results given in Appendix III for the expressions of the two-center integrals between the real wave functions and the cubic wave functions. These results are given in Appendix IV. Those integrals not listed in Appendix IV may be found using the relations

$$\langle i;\, t_2^- \rangle = - \langle i;\, t_2^+ \rangle^* \qquad \text{(VI-21)}$$

and

$$\langle i;\, e' \rangle = - \langle i; e \rangle^* \qquad \text{(VI-22)}$$

where i takes on the values x,y,z.

Normalization of the Delocalized Functions

The normalization integral for the delocalized functions given by (VI-15) assumes the form

$$\langle \psi_\Gamma; \psi_\Gamma \rangle = 1 - \sum_{\vec{k}} \sum_{n} \left(|\langle b_n^{(I)}(\vec{k},\vec{r});\, \psi_\Gamma^o \rangle|^2 + |\langle b_n^{(II)}(\vec{k};\vec{r});\, \psi_\Gamma^o \rangle|^2 \right), \qquad \text{(VI-23)}$$

where in the reduction of the expression for the normalization integral use has been made of the following: the overlap integrals in the expression for the normalization integral are Hermitian, the cubic field

functions denoted by ψ_Γ° are normalized and the approximation that the Bloch functions are orthogonal. The indices n and n' in the above expression (VI-23) denotes a summation over the real wave functions x, y, and z of the oxygen ligands. On expanding the Bloch sums, one finds that the above expression becomes

$$\langle\psi_\Gamma\ \psi_\Gamma\rangle\ 1 - \frac{1}{N} \sum_{\vec{k}} \sum_{n} \sum_{\vec{\tau}} \left|\sum_{\alpha} e^{i\vec{k}\cdot\vec{R}_\alpha} \langle\phi_n(\vec{r}-\vec{\tau}-\vec{R}_\alpha);\psi_\Gamma^\circ\rangle\right|^2 \qquad \text{(VI-24)}$$

where the summation over the vector $\vec{\tau}$, i.e.,

$$\vec{\tau}_1 = -\frac{1}{2}\sqrt{\frac{3}{2}}\,\hat{k}\,a,$$

$$\vec{\tau}_2 = \left(-\sqrt{\frac{1}{3}}\,\hat{i} + \frac{1}{6}\sqrt{\frac{3}{2}}\,\hat{k}\right) a,$$

denotes the summation over the two inequivalent lattice sites designated by (I) and (II), (see equation (VI-8)). If the expression enclosed in the brackets of equation (VI-24) is now expanded, the normalization integral is given by

$$\langle\psi_\Gamma\ \psi_\Gamma\rangle = 1-\frac{1}{N}\sum_{\vec{k}}\sum_{n}\sum_{\vec{\tau}}\Bigg(\sum_{\alpha}\left[\left|\langle\phi_n(\vec{r}-\vec{\tau}-\vec{R}_\alpha);\psi_\Gamma^\circ\right|^2\right. \qquad \text{(VI-25)}$$

$$\left.+\sum_{\alpha}\sum_{\substack{\beta\\ \neq\alpha}}\left[e^{-i\vec{k}\cdot(\vec{R}_\alpha-\vec{R}_\beta)}\left(\langle\phi_n(\vec{r}-\vec{\tau}-\vec{R}_\alpha);\psi_\Gamma^\circ\rangle\langle\phi_n(\vec{r}-\vec{\tau}-\vec{R}_\beta);\psi_\Gamma^\circ\rangle^*\right)\right]\Bigg).$$

The last term in equation (VI-25) containing the $\vec{k}$ dependence vanishes as the vector $(\vec{R}_\alpha-\vec{R}_\beta)_{\alpha\neq\beta}$ is a translation vector of the lattice and

hence

$$\sum_{\vec{k}} e^{-i\vec{k}\cdot(\vec{R}_\alpha - \vec{R}_\beta)} = N\,\delta_{\alpha\beta}\,, \qquad \text{(VI-26)}$$

where the summation is over the first Brillouin zone. Thus the normalization integral reduces to

$$\langle\psi_\Gamma;\psi_\Gamma\rangle = 1 - \sum_n \sum_\alpha \sum_{\vec{\tau}} |\langle\phi_n(\vec{r} - \vec{\tau} - \vec{R}_\alpha),\ \psi_\Gamma^\circ\rangle|^2 \qquad \text{(VI-27)}$$

Approximate expressions for the normalization integrals of the cubic field functions are obtained on substituting the expressions for the overlap integrals between the cubic field functions with the directed orbitals of the nearest neighbor ligands listed in Appendix IV into the above relation (VI-27) and on reduction its found that

$$\mathcal{N}^2 = \langle\psi_{t_2}^{+};\psi_{t_2}^{+}\rangle = \langle\psi_{t_2}^{\circ};\psi_{t_2}^{\circ}\rangle = \langle\psi_{t_2}^{-};\ \psi_{t_2}^{->} = 1 - \frac{4}{3}\,[(sd\sigma)^2 \qquad \text{(VI-28)}$$

$$+ (pd\sigma)^2 + \frac{2}{3}(pd\pi)^2]$$

and

$$\langle\psi_e;\psi_e\rangle = \langle\psi_{e'};\psi_{e'}\rangle = 1 - \frac{8}{3}\,(pd\pi)^2 \qquad \text{(VI-29)}$$

Orbital Reduction Parameter

The orbital reduction parameter within the $^2T_2(T_d)$ manifold was previously defined as

$$k = \langle t_2^+ | \ell_z | t_2^+ \rangle ,$$

(See equation (II-8)). It is now of interest to evaluate the orbital reduction parameter using the delocalized functions given by equation (VI-15), that is

$$k = \langle \psi_{(t_2^+)} | \ell_z | \psi_{(t_2^+)} \rangle .$$

On substituting the expression for the delocalized function $\psi_{(t_2^+)}$ into the above relation for k, one finds that

$$k = \mathcal{N}^2 (H_1 + H_2 + H_3), \qquad \text{(VI-30)}$$

where

$$H_1 = \langle t_2^+ | \ell_z | t_2^+ \rangle \qquad \text{(VI-31)}$$

$$H_2 = - \sum_{\vec{\tau}} \sum_{\vec{k}} \sum_{n} [\langle b_n^{\vec{\tau}}(\vec{k},\vec{r}); t_2^+ \rangle^* \langle b_n^{\vec{\tau}}(\vec{k},\vec{r}) | \ell_z | t_2^+ \rangle \qquad \text{(VI-32)}$$

$$+ \langle b_n^{\vec{\tau}}(\vec{k},\vec{r}); t_2^+ \rangle \langle b_n^{\vec{\tau}}(\vec{k},\vec{r}) | \ell_z | t_2^+ \rangle^*]$$

and

$$H_3 = \sum_{\vec{\tau}} \sum_{\vec{k}',\vec{k}} \sum_{n',n} \langle b_n^{\vec{\tau}}(\vec{k}',\vec{r});t_2^+\rangle^* \qquad \text{(VI-33)}$$

$$\cdot \langle b_n^{\vec{\tau}}(\vec{k},\vec{r});t_2^+\rangle \langle b_n^{\vec{\tau}}(\vec{k}',\vec{r}) \mid \ell_z \mid b_n^{\vec{\tau}}(\vec{k},\vec{r})\rangle .$$

In the above relations for H_2 and H_3, the summation over the vector $\vec{\tau}$ represents the summation over the two inequivalent lattice sites designated by (I) and (II). The Hermitian property of ℓ_z along with the approximation that the Bloch functions are orthogonal has been used in the reduction of the above expressions for H_2 and H_3.

The value of the term H_1 may be found from Table 5 on setting the parameter k appearing there to its ionic value, thus

$$H_1 = \langle t_2^+ \mid \ell_z \mid t_2^+ \rangle = 1$$

If now ℓ_z operates on the cubic field orbital t_2^+ in the expression (VI-32) for H_2, then

$$(\ell_z)_{op} \mid t_2^+\rangle = \mid t_2^+ \rangle + \sqrt{2} \mid e\rangle$$

and the expression for H_2 becomes

$$H_2 = -\sum_{\vec{\tau}} \sum_{\vec{k}} \sum_{n} [2 \langle b_n^{\vec{\tau}}(\vec{k},\vec{r});t_2^+\rangle^* \langle b_n^{\vec{\tau}}(\vec{k},\vec{r});t_2^+\rangle$$

$$+ \sqrt{2}(\langle b_n^{\vec{\tau}}(\vec{k},\vec{r});t_2^+\rangle^* \langle b_n^{\vec{\tau}}(\vec{k},\vec{r});e\rangle + \langle b_n^{\vec{\tau}}(\vec{k},\vec{r});t_2^+\rangle \langle b_n^{\vec{\tau}}(\vec{k},\vec{r});e\rangle^*)]$$

The Bloch function $b_n^{\vec{\tau}}(\vec{k},\vec{r})$ appearing in the above expression for H_2 may be expanded using the relation (VI-1) and on reduction its found that

$$H_2 = -\frac{1}{N}\sum_{\vec{\tau}}\sum_{n}\sum_{\vec{k}}\sum_{\alpha}\sum_{\beta} e^{i\vec{k}\cdot(\vec{R}_\alpha-\vec{R}_\beta)}$$

$$[2\langle\phi_n(\vec{r}-\vec{R}_\alpha-\vec{\tau});t_2^+\rangle^*\langle\phi_n(\vec{r}-\vec{R}_\beta-\vec{\tau});t_2^+\rangle + \sqrt{2}(\langle\phi_n(\vec{r}-\vec{R}_\alpha-\vec{\tau});t_2^+\rangle^*$$

$$\cdot\langle\phi_n(\vec{r}-\vec{R}_\beta-\vec{\tau});e\rangle + \langle\phi_n(\vec{r}-\vec{R}_\beta-\vec{\tau});t_2^+\rangle\langle\phi_n(\vec{r}-\vec{R}_\alpha-\vec{\tau});e\rangle^*)]$$

or on noting that

$$\sum_{\vec{k}} e^{i\vec{k}\cdot(\vec{R}_\alpha-\vec{R}_\beta)} = N\,\delta_{\alpha\beta}\ ,$$

the expression for H_2 reduces to

$$H_2 = -\sum_{\vec{\tau}}\sum_{\alpha}\sum_{n}[2|\langle\phi_n(\vec{r}-\vec{R}_\alpha-\vec{\tau});t_2^+\rangle|^2 \qquad \text{(VI-34)}$$

$$+\sqrt{2}(\langle\phi_n(\vec{r}-\vec{R}_\alpha-\vec{\tau});t_2^+\rangle^*\langle\phi_n(\vec{r}-\vec{R}_\alpha-\vec{\tau}),\ e\rangle$$

$$+\langle\phi_n(\vec{r}-\vec{R}_\alpha-\vec{\tau}),t_2^+\rangle\langle\phi_n(\vec{r}-\vec{R}_\beta-\vec{\tau});e\rangle^*)].$$

On expressing the overlap integrals appearing in the above expression for H_2 in terms of the Slater-Koster parameters given in Appendix IV, one finds that after reduction H_2 becomes

$$H_2 = -\frac{8}{3}\left[(sd\sigma)^2 + (pd\sigma)^2 + \frac{2}{3}(pd\pi)^2\right] \qquad \text{(VI-35)}$$

The band term H_3, (equation (VI-33)) may be expressed in terms of the ligand orbitals on expansion of the Bloch sums and after reduction H_3 is given by

$$H_3 = \left(\frac{1}{N}\right)^2 \sum_{\vec{\tau}} \sum_{\vec{k},\vec{k}'} \sum_{n,n'} \sum^{\alpha,\gamma} \sum_{\beta\ \delta} e^{i\vec{k}'\cdot(\vec{R}_\alpha - \vec{R}_\gamma)} e^{i\vec{k}\cdot(\vec{R}_\delta - \vec{R}_\beta)}$$

$$\cdot \langle \phi_{n'}(\vec{r}-\vec{R}_\alpha-\vec{\tau}); t_2^+ \rangle^* \langle \phi_n(\vec{r}-\vec{R}_\beta-\vec{\tau}); t_2^+ \rangle \langle \phi_n \langle (\vec{r}-\vec{R}_\gamma-\vec{\tau}) | \ell_z | \phi_n(\vec{r}-\vec{R}_\delta-\vec{\tau}) \rangle .$$

The above expression may be simplified on summing over the wave vectors k and k' using the relation (VI-26), and then summing over the lattice vectors $\vec{R}_\alpha$ and $\vec{R}_\beta$. After performing the summations indicated above, the expression for H_3 becomes

$$H_3 = \sum_{\vec{\tau}} \sum_{n,n'} \sum_{\alpha,\beta} \langle \phi_{n'}(\vec{r}-\vec{R}_\alpha-\vec{\tau}); t_2^+ \rangle^*$$

$$\cdot \langle \phi_n(\vec{r}-\vec{R}_\beta-\vec{\tau}); t_2^+ \rangle \langle \phi_{n'}(\vec{r}-\vec{R}_\alpha-\vec{\tau}) | \ell_z | \phi_n(\vec{r}-\vec{R}_\beta-\vec{\tau}) \rangle$$

Since the approximation that the Bloch functions constructed from the ligand orbitals centered on inequivalent lattice sites are orthogonal, the above expression for H_3 reduces to

$$H_3 = \sum_{\vec{\tau}} \sum_{n,n'} \sum_{\alpha} \langle \phi_{n'}(\vec{r}-\vec{R}_\alpha-\vec{\tau}); t_2^+ \rangle^* \qquad \text{(VI-36)}$$

$$\cdot \langle \phi_n(\vec{r}-\vec{R}_\alpha-\vec{\tau}); t_2^+ \rangle \langle \phi_{n'}(\vec{r}-\vec{R}_\alpha-\vec{\tau}) | \ell_z | \phi_n(\vec{r}-\vec{R}_\alpha-\vec{\tau}) \rangle \ .$$

For the impurity problem under consideration, the angular momentum operator ℓ_z is to be centered at the impurity site, thus on noting that

$$\ell_z = \frac{\hbar}{i}(x\partial/\partial y - y\partial/\partial x) = \frac{\hbar}{i}[(x-X_\alpha-\tau_x)\ \partial/\partial y$$

$$-(y-Y_\alpha-\tau_y)\partial/\partial x + (X_\alpha+\tau_x)\partial/\partial y-(Y_\alpha+\tau_y)\partial/\partial x]$$

or

$$\ell_z = (\ell_z)^{\alpha+\tau} + \frac{\hbar}{i}\ [(X_\alpha+\tau_x)\partial/\partial y - (Y_\alpha+\tau_y)\partial/\partial x] \ ,$$

where $(\ell_z)^{\alpha+\tau}$ is the angular momentum operator ℓ_z centered at the $(\vec{R}_\alpha+\vec{\tau})$ ligand site, one finds that the expression (VI-36) for H_3 is then given by

$$H_3 = \sum_{\vec{\tau}} \sum_{n,n'} \sum_{\alpha} \langle \phi_{n'}(\vec{r}-\vec{R}_\alpha-\vec{\tau}); t_2^+ \rangle^* \langle \phi_n(\vec{r}-\vec{R}_\alpha-\vec{\tau}); t_2^+ \rangle$$

$$\cdot [\langle \phi_{n'}(\vec{r}-\vec{R}_\alpha-\vec{\tau}) | (\ell_z)^{\alpha+\tau} | \phi_n(\vec{r}-\vec{R}_\alpha-\vec{\tau}) \rangle$$

$$+ \frac{\hbar}{i} \langle \phi_{n'}(\vec{r}-\vec{R}_\alpha-\vec{\tau}) | (X_\alpha+\tau_x)\partial/\partial y- (Y_\alpha+\tau_y)\partial/\partial x | \phi_n(\vec{r}-\vec{R}_\alpha-\vec{\tau}) \rangle]$$

and since the integrals involving the operators $(\ell_z)^{\alpha+\tau}$, $\partial/\partial x$ and $\partial/\partial y$ are independent of a particular ligand site, then

$$H_3 = \sum_{\vec{\tau}} \sum_{n,n'} \Big(\langle \phi_{n'}(\vec{r}) | \ \ell_z | \ \phi_n(\vec{r}) \rangle \qquad \text{(VI-37)}$$

$$\cdot \sum_{\alpha} \langle \phi_{n'}(\vec{r}-\vec{R}_\alpha-\vec{\tau}); t_2^+ \rangle^* \langle \phi_n(\vec{r}-\vec{R}_\alpha-\vec{\tau}); t_2^+ \rangle$$

$$+ \frac{\hbar}{i} \langle \phi_{n'}(\vec{r}) | \partial/\partial y | \phi_n(\vec{r}) \rangle \Big[\sum_{\alpha} (X_\alpha+\tau_x) \langle \phi_{n'}(\vec{r}-\vec{R}_\alpha-\vec{\tau}); t_2^+ \rangle^* \langle \phi_n(\vec{r}-\vec{R}_\alpha-\vec{\tau}); t_2^+ \rangle \Big]$$

$$- \frac{\hbar}{i} \langle \phi_{n'}(\vec{r}) | \partial/\partial x | \phi_n(\vec{r}) \rangle \Big[\sum_{\alpha} (Y_\alpha+\tau_y) \langle \phi_{n'}(\vec{r}-\vec{R}_\alpha-\vec{\tau}); t_2^+ \rangle^* \langle \phi_n(\vec{r}-\vec{R}_\alpha-\vec{\tau}); t_2^+ \rangle \Big] \Big).$$

If the summation over the ligand orbitals is carried out, the first term in the above expression for H_3 becomes

$$\sum_{\vec{\tau}} \sum_{n,n'} \langle \phi_{n'}(\vec{r}) | \ell_z | \phi_n(\vec{r}) \rangle \sum_{\alpha} \langle \phi_{n'}(\vec{r}-\vec{R}_\alpha-\vec{\tau}); t_2^+ \rangle^* \langle \phi_n(\vec{r}-\vec{R}_\alpha-\vec{\tau}); t_2^+ \rangle$$

$$= i \sum_{\vec{\tau}} \sum_{\alpha} \Big(\langle 2p_y(\vec{r}-\vec{R}_\alpha-\vec{\tau}); t_2^+ \rangle^* \langle 2p_x(\vec{r}-\vec{R}_\alpha-\vec{\tau}); t_2^+ \rangle \qquad \text{(VI-38)}$$

$$- \langle 2p_x(\vec{r}-\vec{R}_\alpha-\vec{\tau}); t_2^+ \rangle^* \langle 2p_y(\vec{r}-\vec{R}_\alpha-\vec{\tau}); t_2^+ \rangle \Big),$$

where use has been made of the following relations

$$(\ell_z)_{op} \ |2s\rangle = 0$$

$$(\ell_z)_{op} \ |2p_z\rangle = 0$$

$$(\ell_z)_{op} \ |2p_x\rangle = i|2p_y\rangle$$

and

$$(\ell_z)_{op} \, |2p_y\rangle = - i \, |2p_x\rangle \, .$$

On summing over the ligand sites, (over the indices α and $\vec{\tau}$), and expressing the overlap integrals in terms of the Slater-Koster parameters given in Appendix IV, equation (VI-38) reduces to

$$4/9 \, [2\sqrt{3} \, (pd\sigma) - (pd\pi)] \, (pd\pi) \qquad \text{(VI-39)}$$

The second and third terms appearing in the expression (VI-37) may be evaluated as follows

$$\frac{\hbar}{i} \sum_{n,n'} \langle \phi_{n'}(\vec{r}) | \, \partial/\partial y \, | \phi_n(\vec{r}) \rangle \, [\sum_{\vec{\tau}} \sum_{\alpha} (X_\alpha + \tau_x)$$

$$\cdot \langle \phi_{n'}(\vec{r}-\vec{R}_\alpha-\vec{\tau}); t_2^+ \rangle^* \langle \phi_n(\vec{r}-\vec{R}_\alpha-\vec{\tau}); t_2^+ \rangle]$$

becomes

$$\frac{\hbar}{i} \langle 2s(r) | \partial/\partial y | \, 2p_y(r) \rangle \, [\sum_{\vec{\tau}} \sum_{\alpha} (X_\alpha + \tau_x) \qquad \text{(VI-40)}$$

$$\cdot (\langle 2s(\vec{r}-\vec{R}_\alpha-\vec{\tau}); t_2^+ \rangle^* \langle 2p_y(\vec{r}-\vec{R}_\alpha-\vec{\tau}); t_2^+ \rangle$$

$$- (\langle 2s(\vec{r}-\vec{R}_\alpha-\vec{\tau}); t_2^+ \rangle \langle 2p_y(\vec{r}-\vec{R}_\alpha-\vec{\tau}); t_2^+ \rangle^*)]$$

on noting that due to parity considerations, the only nonvanishing elements of

$$\langle \phi_{n'}(\vec{r}) | \partial/\partial y | \phi_n(\vec{r}) \rangle$$

are of the form

$$\langle 2s | \partial/\partial y | 2p_y \rangle$$

$$\langle 2p_y | \partial/\partial y | 2s \rangle ,$$

and as directed ligand orbitals may be chosen to be real, the Hermitian property of the operator $\frac{1}{i}\frac{\partial}{\partial y}$ may then be used to obtain the result that

$$\langle 2s | \partial/\partial y | 2p_y \rangle = - \langle 2p_y | \partial/\partial y | 2s \rangle .$$

The indices α and $\vec{\tau}$ may now be summed over the nearest neighbor ligand sites and on expressing the overlap integrals in terms of the Slater-Koster parameters, it is found that equation (VI-40) becomes

$$\frac{1}{i} \langle 2s(r) | \partial/\partial y | 2p_y(r) \rangle \sum_{\vec{\tau}} \sum_{\alpha} (X_\alpha + \tau_x) \qquad \text{(VI-41)}$$

$$(\langle 2s(\vec{r}-\vec{R}_\alpha-\vec{\tau}); t_2^+ \rangle^* \langle 2p_y(\vec{r}-\vec{R}_\alpha-\vec{\tau}); t_2^+ \rangle$$

$$- \langle 2s(\vec{r}-\vec{R}_\alpha-\vec{\tau}); t_2^+ \rangle \langle 2p_y(\vec{r}-\vec{R}_\alpha-\vec{\tau}); t_2^+ \rangle^*)$$

$$= \frac{4}{3}\sqrt{\frac{1}{3}}\,(sd\sigma)(pd\pi)\langle 2s | \partial/\partial y | 2p_y \rangle .$$

Similarly as shown above, the last term in equation (VI-37) for H_3 reduces to

$$- \frac{1}{i} \sum_{n,n'} \langle \phi_{n'}(\vec{r}) | \partial/\partial x | \phi_n(\vec{r}) \rangle \sum_{\vec{\tau}} \sum_{\alpha} (Y_\alpha + \tau_y) \qquad \text{(VI-42)}$$

$$\langle \phi_{n'}(\vec{r}-\vec{R}_\alpha-\vec{\tau}); t_2^+ \rangle^* \langle \phi_n(\vec{r}-\vec{R}_\alpha-\vec{\tau}); t_2^+ \rangle$$

$$= \frac{4}{3}\sqrt{\frac{1}{3}}\,(sd\sigma)(pd\pi)\,\langle 2s|\partial/\partial x|2p_x\rangle \,.$$

Thus on compiling the results given in equations (VI-39), (VI-41) and (VI-42), one finds that H_3 is given by

$$H_3 = \frac{4}{9}\,[2\sqrt{3}\,(pd\sigma) - (pd\pi)]\,(pd\pi) \qquad \text{(VI-43)}$$

$$+ \frac{4}{3}\sqrt{\frac{1}{3}}\,(sd\sigma)(pd\pi)\,(\langle 2s|\partial/\partial y|2p_y\rangle + \langle 2s|\partial/\partial x|2p_x\rangle)\,.$$

The orbital reduction parameter k may be expressed in terms of the Slater-Koster parameters on compiling the results given by equations (VI-28), (VI-35), (VI-43) for $\mathcal{N}^2$, H_2 and H_3 respectively and after reduction it is found that

$$k = \left(1 - \frac{4}{3}\,(sd\sigma)^2 + (pd\sigma)^2 + \frac{2}{3}\,(pd\pi)^2\right)^{-1} \qquad \text{(VI-44)}$$

$$\cdot\left(1 + \frac{8}{3}\,[(sd\sigma)^2 + (pd\sigma)^2] + \frac{8}{3}\sqrt{\frac{1}{3}}\,(pd\sigma)(pd\pi)\right.$$

$$- \frac{20}{9}\,(pd\pi)^2 + \frac{4}{3}\sqrt{\frac{1}{3}}\,(sd\sigma)(pd\pi)(\langle 2s|\partial/\partial y|2p_y\rangle$$

$$\left. + \langle 2s|\partial/\partial x|2p_x\rangle\right)\,.$$

On substituting the values given in equation (VI-19) for the Slater-Koster parameters, one finds that for the terms independent of the matrix elements of the operators $\partial/\partial x$ and $\partial/\partial y$ the contribution to the orbital reduction parameter k is 0.989. The contribution to k from the last term in equation (VI-44) may be estimated using the radial functions given by equations (VI-16) and is found to be less than 1%.

Spin Orbit Parameter

The spin-orbit interaction energy is given by

$$H_{so} = (\hbar^2/4m^2c^2)(\vec{\nabla}V_c \times \vec{p}) \cdot \vec{\sigma} \ ,$$

where V_c is the crystalline potential and $\vec{\sigma}$ the Pauli spin matrix. The spin-orbit parameter will be evaluated assuming the following. Since most of the spin-orbit interaction arises when the electron is close to the nucleus[49], the interaction energy will then be approximated by

$$\frac{\hbar^2}{4m^2c^2} \left(\frac{1}{r} \ \frac{\partial V}{\partial r} \right) \ \vec{\ell} \cdot \vec{s} \ ,$$

where V is the atomic potential of the nucleus. Matrix elements of the operator $\left(\frac{1}{r} \ \frac{\partial V}{\partial r} \right)$ between orbitals centered at different lattice sites will then be neglected as the magnitude of the operator $\left(\frac{1}{r} \ \frac{\partial V}{\partial r} \right)$

is appreciable only near the nucleus where overlap is small. The value of the radial integral

$$\frac{h^2}{4m^2c^2} < R(r) | \frac{1}{r} \frac{\partial V}{\partial r} | R(r) >$$

will be treated as a parameter to be determined from the free ion intervals.

The spin-orbit parameter within the $^2T_2(T_d)$ manifold was previously defined as (see Chapter II)

$$\zeta = -2 < \frac{1}{2} t_2^+ | H_{so} | \frac{1}{2} t_2^+ >$$

and for the delocalized picture will be given by

$$\zeta = -2 < \frac{1}{2} \psi_{t_2}^+ | H_{so} | \frac{1}{2} \psi_{t_2}^+ > ,$$

where the wave function $\frac{1}{2} \psi_{t_2}^+$ is the product of the spin function $\frac{1}{2}$ and the delocalized orbital given by equation (VI-14). On neglecting the cross terms as they are small, one then obtains

$$\zeta = -2 \mathcal{N}^2 [< \frac{1}{2} t_2^+ | H_{so} | \frac{1}{2} t_2^+ > + \sum_{\vec{\tau}} \sum_{\vec{k},\vec{k}'} \sum_{n,n'} <b_n^{\vec{\tau}}(\vec{k}',\vec{r}); t_2^+ >^*$$

$$\cdot <b_n^{\vec{\tau}}(\vec{k},\vec{r}); t_2^+> <\frac{1}{2} b_{n'}^{\vec{\tau}}(\vec{k}',\vec{r}) | H_{so} | \frac{1}{2} b_n^{\vec{\tau}}(\vec{k},\vec{r})>$$

or

$$\zeta = -2\,\frac{\mathcal{N}^2}{N^2}\,[\langle \tfrac{1}{2}t_2^+|\,H_{so}\,|\,\tfrac{1}{2}t_2^+\rangle + \sum_{\vec{\tau}}\sum_{\vec{k},\vec{k}'}\sum_{n,n'} \tag{VI-45}$$

$$\cdot \sum_{\alpha,\beta}\sum_{\gamma,\delta} e^{i\vec{k}'\cdot(\vec{R}_\alpha-\vec{R}_\gamma)}\, e^{i\vec{k}\cdot(\vec{R}_\delta-\vec{R}_\beta)} \langle \phi_{n'}(\vec{r}-\vec{R}_\alpha-\vec{\tau});t_2^+\rangle^*$$

$$\cdot \langle \phi_n(\vec{r}-\vec{R}_\beta-\vec{\tau});t_2^+\rangle \langle \tfrac{1}{2}\,\phi_{n'}(\vec{r}-\vec{R}_\gamma-\vec{\tau})\,|H_{so}|\,\tfrac{1}{2}\,\phi_n(\vec{r}-\vec{R}_\delta-\vec{\tau})\rangle\ ] .$$

The above expression (VI-45) may be simplified on summing the wave vector k and k' over the first Billouin zone and then summing over the lattice vectors $\vec{R}_\alpha$ and $\vec{R}_\delta$. After carrying out the above simplifications, one finds that

$$\zeta = -2\mathcal{N}^2\,[\langle -\tfrac{1}{2}\,t_2^+\,|H_{so}|\,\tfrac{1}{2}t_2^+\rangle + \sum_{\vec{\tau}}\sum_{\alpha,\beta}\sum_{n,n'}$$

$$\langle \phi_{n'}(\vec{r}-\vec{R}_\alpha-\vec{\tau});t_2^+\rangle^* \langle \phi_n(\vec{r}-\vec{R}_\beta-\vec{\tau});t_2^+\rangle \langle \tfrac{1}{2}\,\phi_{n'}(\vec{r}-\vec{R}_\alpha-\vec{\tau})\,|H_{so}|\,\tfrac{1}{2}\,\phi_n(\vec{r}-\vec{R}_\beta-\vec{\tau})\rangle].$$

Since two center integrals involving the spin-orbit interaction energy are small the above expression for the spin-orbit parameter then becomes

$$\zeta = -2\,\mathcal{N}^2\,[\lambda_{cu}\,\langle \tfrac{1}{2}\,t_2^+|\,\vec{\ell}\cdot\vec{s}\,|\,\tfrac{1}{2}\,t_2^+\rangle \tag{VI-46}$$

$$+ \lambda_o \sum_{n,n'} \langle \tfrac{1}{2}\,\phi_{n'}(\vec{r})\,|\ell\cdot s|\,\tfrac{1}{2}\,\phi_n(\vec{r})\rangle \sum_{\vec{\tau}}\sum_{\alpha} \langle \phi_{n'}(\vec{r}-\vec{R}_\alpha-\vec{\tau});t_2^+\rangle^* \langle \phi_n(\vec{r}-\vec{R}_\alpha-\vec{\tau});t_2^+\rangle],$$

where the radial integrals involving the operator $\left(\frac{\hbar}{4m^2c^2}\frac{1}{r}\frac{\partial}{\partial r}\right)$ are to be replaced by the value of the free ion spin-orbit parameter λ to be determined from experiment.

The matrix elements of the operator $(\vec{\ell}\cdot\vec{s})$ appearing in the above relation may be evaluated using the following relations

$$(\vec{\ell}\cdot\vec{s})_{op} \mid \tfrac{1}{2} t_2^+ > = \tfrac{1}{2} \mid \tfrac{1}{2} t_2^+ > - \sqrt{\tfrac{1}{2}} \mid - \tfrac{1}{2} t_2^\circ > + \sqrt{\tfrac{1}{2}} \mid \tfrac{1}{2} e >$$

$$(\vec{\ell}\cdot\vec{s})_{op} \mid \tfrac{1}{2} s > = 0$$

$$(\vec{\ell}\cdot\vec{s})_{op} \mid \tfrac{1}{2} p_x > = \tfrac{1}{2} \mid - \tfrac{1}{2} p_z > + \tfrac{i}{2} \mid \tfrac{1}{2} p_y >$$

$$(\vec{\ell}\cdot\vec{s})_{op} \mid \tfrac{1}{2} p_y > = - \tfrac{i}{2} \mid \tfrac{1}{2} p_x > + \tfrac{i}{2} \mid - \tfrac{1}{2} p_z >$$

$$(\vec{\ell}\cdot\vec{s})_{op} \mid \tfrac{1}{2} p_z > = - \tfrac{1}{2} \mid - \tfrac{1}{2} p_x > - \tfrac{i}{2} \mid - \tfrac{1}{2} p_y > \ ,$$

where the phase of the ligand 2p orbitals is that given by Condon and Shortley. On summing over the quantum indices n' and n denoting a sum over the ligand orbitals, one then finds that the expression (VI-46) for the spin-orbit parameter reduces to

$$\zeta = - 2\mathcal{N}^2 \left[\tfrac{1}{2}\lambda_{cu} + \tfrac{i}{2}\lambda_o \sum_{\vec{\tau}} \sum_{\alpha} \left(\langle p_y(\vec{r}-\vec{R}_\alpha-\vec{\tau}); t_2^+ \rangle^* \right.\right.$$

$$\left.\left. \cdot \langle p_x(\vec{r}-\vec{R}_\alpha-\vec{\tau}); t_2^+ \rangle - \langle p_x(\vec{r}-\vec{R}_\alpha-\vec{\tau}) t_2^+ \rangle^* \langle p_y(\vec{r}-\vec{R}_\alpha-\vec{\tau}); t_2^+ \rangle \right) \right].$$

The overlap integrals in the above relation may be expressed in terms of the Slater-Koster parameters given in Appendix IV on summing over

the nearest neighbor ligand sites to the impurity center. On reduction one then obtains

$$\zeta = -\left(1 - \frac{4}{3}\left[(sd\sigma)^2 + (pd\sigma)^2 + \frac{2}{3}(pd\pi)^2\right]\right)^{-1} \cdot \left(\lambda_{cu} + \frac{8}{3}\sqrt{\frac{1}{3}}\,\lambda_o\left[(pd\sigma) - \frac{1}{2}\sqrt{\frac{1}{3}}(pd\pi)\right](pd\pi)\right) \tag{VI-47}$$

where the normalization term $\mathcal{N}^2$ is given by (VI-28). If the values for the Slater-Koster parameters given by equation (VI-19) are substituted in the above expression for ζ, there results

$$\zeta = -\frac{1}{0.9934}\left[\lambda_{cu} - 0.00397\,\lambda_o\right]$$

Thus for a value of $\lambda_o = 150\ cm^{-1}$ for the spin-orbit parameter of the oxygen 2p orbital it is seen that there is no reduction.

CONCLUSION

Recently the spin-orbit coupling in the valence bands of ionic crystals with zincblend and wurtzite structure was investigated in the tight binding approximation.[50] For these compounds the spin-orbit splitting of the valence band at $\Gamma(\vec{k}=0)$ deviates from the one electron average of the splittings for the two atoms in the unit cell in contrast to that for the predominately covalent semiconductors. It was shown that for ZnO a small admixture of the 3d orbital of the cation with the 2p orbital of the anion could account for the inverted nature of the spin-orbit splitting of the valence band at $\vec{k} = 0$. This results from the fact that the 3d orbital of the cation contributes a negative term to the spin-orbit coupling in the valence band at $\vec{k} = 0$. An emperical estimate of the amount of admixing was made by Shindo et.al.[50] and from their results the admixture of the 2p band with the copper 3d orbital is expected to be approximately one order of magnitude greater than that obtained here ($\simeq 0.3$ vs $\simeq 0.06$). For a value of 0.3 for the mixing coefficient, it is found that the spin-orbit parameter of the copper 3d orbital is only reduced to approximately 88% of its free ion value. Thus from these considerations, admixture of the valence band with the localized 3d orbital may not fully account for the large reduction.

An alternative approach to account for the large reduction in the spin-orbit parameter is to consider the problem in the strong field limit. That is the crystal field overcomes the electrostatic interactions between equivalent electrons and the ground state electronic configuration belongs to the crystal field $3d^9(t_2^5e^4)$ configuration rather than the free ion $3d^9(^2D)$ term. As the absence of the center of inversion symmetry element in the T_d group introduces an odd parity term in the crystal field potential, the crystal field $4p(t_2)$ orbital of copper may then mix with the $3d(t_2)$ orbital. Thus owing to the fact that matrix elements of the angular momentum vector ℓ within the $^2T_2(T_d)$ manifold are the same as those of the angular momentum vector for an atomic p state except for a multiplicative constant of (-1), the mixing of the $4p(t_2)$ orbital with the $3d(t_2)$ orbital will then introduce a term in the expression for the spin-orbit parameter

$$\zeta_{3d} = \frac{1}{1+k^2}\left[\lambda_{3d} - k^2\lambda_{4p}\right] \quad ,$$

which then leads to reduction.

C. A. Bates has made a theoretical study of Cu^{2+}:ZnO in order to account for the large hyperfine constants found from experiment.[35] Here the $(Ar)3d^84p$ configuration was mixed with the ground state $(Ar)3d^9$ configuration through the odd parity term appearing in the crystal potential. Bates estimated that the mixing coefficient to be approximately (k = 1/3). In this work the free ion energy splitting of 125,000 cm^{-1} was used. On the other hand as the promotion energy

between a 3d and 4p orbital is expected to decrease due to the effect of the crystal potential of the lattice, the amount of admixture may be quite large. For example if the promotion energy is approximately 70,000 cm^{-1}, the spin-orbit parameter is seen to reduce to $\sim$25% of its free ion value. It is then seen that a quantitative formulation of the qualitative argument presented above may account for reduction.

APPENDIX I

HIGHER ORDER PERTURBATION THEORY

As the second order elements brought into the $^2T_2(T_d)$ manifold are of the same order of magnitude as the first order intrablock elements, e.g., $G_2(kj;kj') \simeq 100\ cm^{-1}$ for $\zeta' = 720\ cm^{-1}$, the corrections to the energy for the $^2T_2(T_d)$ manifold given by the third and fourth order terms will now be investigated and will be shown to be negligible.

The expression for the third order correction to the energy may be found on retaining terms up through the third order in λ in the expansion of the transformed Hamiltonian G, (see Equation (III-3)),

$$G = G_o + \lambda G_1 + \lambda^2 G_2 + \lambda^3 G_3.$$

The third order correction G_3 is then found to be

$$G_3 = i(H_2S-SG_2) + \frac{1}{2}(S^2G_1-H_1S^2) + \frac{i}{6}(S^3G_o-H_oS^3) , \qquad \text{(AI-1)}$$

where

$$G_2 = H_2 + i(H_1S-SG_1) - \frac{1}{2}(H_oS^2-S^2G_o) \qquad \text{(AI-2)}$$

or on substituting for G_2 given by equation (AI-2) into the expression (AI-1) for G_3, the third order correction becomes

$$G_3 = i(H_2S-SH_2) + SH_1S - \frac{1}{2}(S^2G_1 + H_1S^2) \qquad \text{(AI-3)}$$

$$+ \frac{i}{6}[3SH_oS^2 - 2S^3G_o - H_oS^3].$$

Since here there are only two manifolds labeled by the high frequency index k, e.i., $^2E(T_d)$ and $^2T_2(T_d)$, the last term in equation (AI-3) is seen to vanish for the intrablock elements $G_3(kj;kj')$ as $S(kj;kj') = 0$ and G_o and H_o are diagonal in the high frequency index k. The term SH_1S in equation (AI-3) is also seen to vanish as matrix elements of the perturbation $H_1 = -\zeta\vec{\ell}\cdot\vec{s} + V_t$ within the $^2E(T_d)$ manifold are zero, (see Table 7). Since $H_2 = 0$ for the problem under consideration, the third order energy correction for the intralevel elements of the $^2T_2(T_d)$ manifold may then be written here as

$$G_3 = -\frac{1}{2}(S^2G_1 + H_1S^2),$$

or on expanding it is found that

$$G_3(T_2j;T_2j') = -\frac{1}{2}\sum_{j''}\sum_{j'''}[S(T_2j;Ej'')S(Ej'',T_2j''')G_1(T_2j''';T_2j')$$

$$+ H_1(T_2j;T_2j'')S(T_2j'';Ej''')S(Ej''';T_2j')], \qquad \text{(AI-4)}$$

where the term $-iSH_2$ has been neglected as $H_2 = 0$. In the above relation for G_3 it is seen that the summation over the high frequency index k has been carried out as there are only two manifolds labeled by k and only those terms have been retained which do not vanish owing to the fact that $S(kj;kj') = 0$. If the relation (III-5) for S is substituted into the above expression for G_3 and one notes that $G_1(kj;kj') = H_1(kj;kj')$, the third order correction term may then be written as

$$G_3(T_2j;T_2j') = -\frac{1}{2(10Dq)^2}\sum_{j''}\sum_{j'''}[H_1(T_2j;T_2j'')H_1(T_2j'';Ej''') \qquad \text{(AI-5)}$$

$$\cdot H_1(Ej''';T_2j') + H_1(T_2j;Ej'')H_1(Ej'';T_2j''')H_1(T_2j''';T_2j')],$$

where the energy denominator has been replaced by $(10Dq)^2$.

Explicit expressions for the third order terms are found on substituting the expressions for H_1 listed in Table 7 into the above equation for G_3 and on reduction the third order corrections to the ground state manifold are given by

$$G_3(\psi_3;\psi_3) = G_3(\psi_4;\psi_4) = \frac{1}{2(10Dq)^2}(K-\tfrac{1}{2}\zeta)[(2K'+\zeta')^2+2\zeta'^2] \qquad \text{(AI-6)}$$

$$G_3(\tfrac{1}{2}t_2^\circ;\tfrac{1}{2}t_2^\circ) = G_3(-\tfrac{1}{2}t_2^\circ;-\tfrac{1}{2}t_2^\circ)$$

$$= \frac{1}{2(10Dq)^2}[-4K\zeta'^2+\zeta\zeta'(2K'-\zeta')]$$

$$G_3(-\tfrac{1}{2}t_2^-;-\tfrac{1}{2}t_2^-) = G_3(\tfrac{1}{2}t_2^+;\tfrac{1}{2}t_2^+)$$

$$= \frac{1}{2(10Dq)^2}[(K+\tfrac{1}{2}\zeta)(2K'-\zeta')^2+\zeta\zeta'(2K'-\zeta')]$$

$$G_3(\tfrac{1}{2}t_2^\circ;-\tfrac{1}{2}t_2^-) = G_3(-\tfrac{1}{2}t_2^\circ;\tfrac{1}{2}t_2^+)$$

$$= \frac{1}{2}\sqrt{\frac{1}{2}}\ \frac{1}{(10Dq)^2}[(K-\tfrac{1}{2}\zeta)\zeta'(2K'-\zeta')$$

$$-\tfrac{1}{2}\zeta(2K'-\zeta')^2 - \zeta\zeta'^2]$$

The third order correction to the energy may now be estimated using the values obtained for the crystal field parameters determined from the fit of the optical data, i.e., $\zeta = 200\ cm^{-1}$, $K = -20\ cm^{-1}$, $\zeta' = 720\ cm^{-1}$ and $K' = -77\ cm^{-1}$, and it was found that $G_3(kj;kj')$ was two orders of magnitude smaller than that obtained for the second order correction $G_2(kj;kj')$ given by equations (III-9) and (III-12).

It is now of interest to investigate the order of magnitude of the fourth order terms folded into the $^2T_2(T_d)$ manifold on performing a second Van Vleck transformation. The order of magnitude of these terms determine how effective the first transformation isolated the $^2T_2(T_d)$ manifold from the $^2E(T_d)$ manifold.

The fourth order correction to the energy obtained on folding the second order interlevel elements $G_2(kj;k'j')$ into the $^2T_2(T_d)$ manifold is found from a simple extension of the second order theory

described in Chapter III and it can be shown that

$$G_4(kj;kj') = \sum_{k' \neq k} \sum_{j''} \frac{G_2(kj;k'j'')G_2(k'j'';kj')}{E_k^\circ - E_{k'}^\circ} \qquad \text{(AI-7)}$$

The second order interblock elements may be found using equation (III-4) for G_2 and on reduction it is found that

$$G_2(T_2j,Ej') = \frac{1}{10Dq} \sum_{j''} [H_1(T_2j;T_2j'')H_1(T_2j'';Ej') - H_1(T_2j,Ej'')H_1(Ej'',Ej')],$$

where the summation over the high frequency index k has been carried out and the energy denominator $(E_k^\circ - E_{k'}^\circ)$ has been replaced by (-10Dq). The results of Table 7 for H_1 may then be used to obtain explicit expressions for the second order interlevel elements and on reduction it is found that

$$G_2(\psi_4;\psi_6) = G_2^* (\psi_3;\psi_5) = \frac{1}{10Dq}(-K+\frac{1}{2}\zeta)[\sqrt{\frac{1}{2}}(2K'+\zeta') - i\,\zeta'] \qquad \text{(AI-8)}$$

$$G_2(-\frac{1}{2}t_2^\circ;\frac{1}{2}e) = G_2(\frac{1}{2}t_2^\circ;-\frac{1}{2}e')$$

$$= \frac{1}{(10Dq)}[-2K\zeta' + \zeta(K' - \frac{1}{2}\zeta')]$$

$$G_2(\tfrac{1}{2}t_2^+;\ \tfrac{1}{2}e) = G_2(-\tfrac{1}{2}t_2^-;-\tfrac{1}{2}e')$$

$$= -\sqrt{\frac{1}{2}}\ \frac{1}{(10Dq)}\ [(K+\tfrac{1}{2}\zeta)(2K'-\zeta')+\zeta\zeta']$$

On substituting the above results for $G_2(kj;k'j')$ into the expression (AI-7) for $G_4(kj;kj')$, one then finds that

$$G_4(\psi_3;\psi_3) = G_4(\psi_4;\psi_4) = -\frac{1}{2(10Dq)^3}(-K+\tfrac{1}{2}\zeta)^2[(2K'+\zeta')^2+2\zeta'^2]$$

$$G_4(\tfrac{1}{2}t_2^\circ;\ \tfrac{1}{2}t_2^\circ) = G_4(-\tfrac{1}{2}t_2^\circ;-\tfrac{1}{2}t_2^\circ)$$

$$= -\frac{1}{(10Dq)^3}\ [-2K\zeta' + \zeta(K'-\tfrac{1}{2}\zeta')]^2 \qquad \text{(AI-9)}$$

$$G_4(\tfrac{1}{2}t_2^+;\ \tfrac{1}{2}t_2^+) = G_4(-\tfrac{1}{2}t_2^-;-\tfrac{1}{2}t_2^-)$$

$$= -\frac{1}{2(10Dq)^3}[(K+\tfrac{1}{2}\zeta)(2K'-\zeta')+\zeta\zeta']^2$$

$$G_4(-\tfrac{1}{2}t_2^\circ;\ \tfrac{1}{2}t_2^+) = G_4(\tfrac{1}{2}t_2^\circ;-\tfrac{1}{2}t_2^-)$$

$$= \sqrt{\frac{1}{2}}\ \frac{1}{(10Dq)^3}\ [-2K\zeta'+\zeta(K'-\tfrac{1}{2}\zeta')]$$

$$\times\ [(K+\tfrac{1}{2}\zeta)(2K'-\zeta')+\zeta\zeta']$$

If the values of the crystal field parameters determined from the fit of the optical spectra are used in the evaluation of the fourth order elements folded into the $^2T_2(T_d)$ manifold, then it is found that the fourth order elements are four orders of magnitude smaller than the second order elements folded into the $^2T_2(T_d)$ manifold, (see Chapter III). Thus it is seen that the second order transformation effectively isolates the $^2T_2(T_d)$ manifold.

APPENDIX II

CHARACTER TABLES FOR THE T_d AND C_{3v} POINT GROUPS AND THEIR DOUBLE GROUPS

The notation labeling the irreducible representations is that of both Mulliken's, (see Wilson, Decius and Cross[43,44] for character tables for the T_d and C_{3v} point groups respectively and D. S. McClure[5] for the T_d double group) and Bethe's (see G. F. Koster[42] for character tables).

T_d

			E	$8C_3$	$3C_2$	$6S_4$	$6\sigma_d$
Γ_1	Γ_1	A_1	1	1	1	1	1
Γ_2	Γ_2	A_2	1	1	1	-1	-1
Γ_{12}	Γ_3	E	2	-1	2	0	0
Γ_{25}	Γ_5	T_1	3	0	-1	1	-1
Γ_{15}	Γ_4	T_2	3	0	-1	-1	1

		C_{3v}		
		E	$2C_3$	$3\sigma_v$
Γ_1	A_1	1	1	1
Γ_2	A_2	1	1	-1
Γ_3	E	2	-1	0

Additional Characters of the Double Group $\overline{T}_d$

						$3\overline{C}_2$			$6\overline{\sigma}_d$
		E	$\overline{E}$	$8C_3$	$8\overline{C}_3$	$3C_2$	$6S_4$	$6\overline{S}_4$	$6\sigma_d$
Γ_6	$E_{1/2}$	2	-2	1	-1	0	$\sqrt{2}$	$-\sqrt{2}$	0
Γ_7	$E_{5/2}$	2	-2	1	-1	0	$-\sqrt{2}$	$\sqrt{2}$	0
Γ_8	G	4	-4	-1	1	0	0	0	0

Additional Characters of the Double Group $\overline{C}_{3v}$

	E	$\overline{E}$	$2C_3$	$2\overline{C_3}$	$3\sigma_v$	$3\overline{\sigma}_v$
Γ_6	2	-2	1	-1	0	0
Γ_4	1	-1	-1	1	i	-i
Γ_5	1	-1	-1	1	-i	i

APPENDIX III

EXPRESSIONS FOR THE TWO-CENTER OVERLAP INTEGRALS BETWEEN THE REAL WAVE FUNCTIONS IN TERMS OF THE SLATER-KOSTER PARAMETERS

The direction cosines (ℓ,m,n) gives the orientation of the oxygen ligand relative to the Cartesian system defined in Figure 11. All overlap integrals not listed are zero.

$\underline{(0,0,-1)}$

$$\langle s;z^2\rangle = (sd\sigma)$$

$$\langle x;xz\rangle = -(pd\pi)$$

$$\langle y;yz\rangle = -(pd\pi)$$

$$\langle z;z^2\rangle = -(pd\sigma)$$

$\underline{(-2\sqrt{2}/3,0,1/3)}$

$$\langle s;xz\rangle = -\frac{2}{3}\sqrt{\frac{2}{3}}\,(sd\sigma)$$

$$\langle s;x^2-y^2\rangle = \frac{4}{3}\sqrt{\frac{1}{3}}\,(sd\sigma)$$

$$\langle s;z^2\rangle = -\frac{1}{3}\,(sd\sigma)$$

$$\langle x;xz\rangle = -\frac{1}{9}\left[-8\sqrt{\frac{1}{3}}\,(pd\sigma) + \frac{7}{3}\,(pd\pi)\right]$$

$$\underline{(-2\sqrt{2}/3,0,1/3)}$$

$$\langle x;x^2-y^2\rangle = -\frac{2}{9}\sqrt{2}\left[4\sqrt{\frac{1}{3}}\ (pd\sigma) + \frac{1}{3}\ (pd\pi)\right]$$

$$\langle x;z^2\rangle = \frac{2}{9}\sqrt{2}\left[(pd\sigma) + \sqrt{\frac{1}{3}}\ (pd\pi)\right]$$

$$\langle y;xy\rangle = -\frac{2}{3}\sqrt{2}\ (pd\pi)$$

$$\langle y;yz\rangle = \frac{1}{3}\ (pd\pi)$$

$$\langle z;xz\rangle = -\frac{2}{9}\sqrt{2}\left[\sqrt{\frac{1}{3}}\ (pd\sigma) + \frac{7}{3}\ (pd\pi)\right]$$

$$\langle z;x^2-y^2\rangle = -\frac{4}{9}\left[-\sqrt{\frac{1}{3}}\ (pd\sigma) + \frac{2}{3}\ (pd\pi)\right]$$

$$\langle z;z^2\rangle = -\frac{1}{9}\left[(pd\sigma) - 8\sqrt{\frac{1}{3}}\ (pd\pi)\right]$$

$$\underline{(\sqrt{2}/3,\ -\sqrt{2/3},1/3)}$$

$$\langle s;xy\rangle = -\frac{2}{3}\ (sd\sigma)$$

$$\langle s;xz\rangle = \frac{1}{3}\sqrt{\frac{2}{3}}\ (sd\sigma)$$

$$\langle s;yz\rangle = -\frac{1}{3}\sqrt{2}\ (sd\sigma)$$

$$\langle s;x^2-y^2\rangle = -\frac{2}{3}\sqrt{\frac{1}{3}}\ (sd\sigma)$$

$$\langle s;z^2\rangle = -\frac{1}{3}\ (sd\sigma)$$

$$\langle x;xy\rangle = -\frac{1}{9}\sqrt{2}\left[2(pd\sigma) + 5\sqrt{\frac{1}{3}}\ (pd\pi)\right]$$

$(\sqrt{2}/3, -\sqrt{2/3}, 1/3)$

$$\langle x;xz\rangle = \frac{1}{9}\left[2\sqrt{1/3}\,(pd\sigma) + \frac{5}{3}\,(pd\pi)\right]$$

$$\langle x;yz\rangle = -\frac{2}{9}\left[(pd\sigma) - 2\sqrt{1/3}\,(pd\pi)\right]$$

$$\langle x;x^2-y^2\rangle = -\frac{1}{9}\sqrt{2}\left[2\sqrt{\frac{1}{3}}\,(pd\sigma) - \frac{13}{3}\,(pd\pi)\right]$$

$$\langle x;z^2\rangle = -\frac{1}{9}\sqrt{2}\left[(pd\sigma) + \sqrt{\frac{1}{3}}\,(pd\pi)\right]$$

$$\langle y;xy\rangle = -\frac{1}{3}\sqrt{2}\left[-2\sqrt{\frac{1}{3}}\,(pd\sigma) + \frac{1}{3}\,(pd\pi)\right]$$

$$\langle y;xz\rangle = -\frac{2}{9}\left[(pd\sigma) - 2\sqrt{\frac{1}{3}}\,(pd\pi)\right]$$

$$\langle y;yz\rangle = -\frac{1}{3}\left[-2\sqrt{\frac{1}{3}}\,(pd\sigma) + \frac{1}{3}\,(pd\pi)\right]$$

$$\langle y;x^2-y^2\rangle = \frac{1}{9}\sqrt{2}\left[2(pd\sigma) + 5\sqrt{\frac{1}{3}}\,(pd\pi)\right]$$

$$\langle y;z^2\rangle = \frac{1}{3}\sqrt{2}\left[\sqrt{\frac{1}{3}}\,(pd\sigma) + \frac{1}{3}\,(pd\pi)\right]$$

$$\langle z;xy\rangle = -\frac{2}{9}\left[(pd\sigma) - 2\sqrt{\frac{1}{3}}\,(pd\pi)\right]$$

$$\langle z;xz\rangle = \frac{1}{9}\sqrt{2}\left[\sqrt{\frac{1}{3}}\,(pd\sigma) + \frac{7}{3}\,(pd\pi)\right]$$

$$\langle z;yz\rangle = -\frac{1}{9}\sqrt{2}\left[(pd\sigma) + 7\sqrt{\frac{1}{3}}\,(pd\pi)\right]$$

$$\langle z;x^2-y^2\rangle = -\frac{2}{9}\left[\sqrt{\frac{1}{3}}\,(pd\sigma) - \frac{2}{3}\,(pd\pi)\right]$$

$$\langle z;z^2\rangle = -\frac{1}{9}\left[(pd\sigma) - 8\sqrt{\frac{1}{3}}\,(pd\pi)\right]$$

$\underline{(\sqrt{2}/3, \sqrt{2/3}, 1/3)}$

$$\langle s;xy\rangle = \frac{2}{3}(sd\sigma)$$

$$\langle s;xz\rangle = \frac{1}{3}\sqrt{\frac{2}{3}}\,(sd\sigma)$$

$$\langle s;yz\rangle = \frac{1}{3}\sqrt{2}\,(sd\sigma)$$

$$\langle s;x^2-y^2\rangle = -\frac{2}{3}\sqrt{\frac{1}{3}}\,(sd\sigma)$$

$$\langle s;z^2\rangle = -\frac{1}{3}\,(sd\sigma)$$

$$\langle x;xy\rangle = \frac{1}{9}\sqrt{2}\,[2(pd\sigma) + 5\sqrt{\frac{1}{3}}\,(pd\pi)]$$

$$\langle x;xz\rangle = \frac{1}{9}\,[2\sqrt{\frac{1}{3}}\,(pd\sigma) + \frac{5}{3}\,(pd\pi)]$$

$$\langle x;yz\rangle = -\frac{2}{9}\,[-(pd\sigma) + 2\sqrt{\frac{1}{3}}\,(pd\pi)]$$

$$\langle x;x^2-y^2\rangle = -\frac{\sqrt{2}}{9}[\;2\sqrt{\frac{1}{3}}(pd\sigma) - \frac{13}{3}\,(pd\pi)]$$

$$\langle x;z^2\rangle = -\frac{1}{9}\sqrt{2}\,[\;(pd\sigma) + \sqrt{\frac{1}{3}}\,(pd\pi)]$$

$$\langle y;xy\rangle = -\frac{1}{3}\sqrt{2}\,[-2\sqrt{\frac{1}{3}}\,(pd\sigma) + \frac{1}{3}\,(pd\pi)]$$

$$\langle y;xz\rangle = -\frac{2}{9}\,[-(pd\sigma) + 2\sqrt{\frac{1}{3}}\,(pd\pi)]$$

$$\langle y;yz\rangle = -\frac{1}{3}\,[-2\sqrt{\frac{1}{3}}\,(pd\sigma) + \frac{1}{3}\,(pd\pi)]$$

$$\langle y;x^2-y^2\rangle = -\frac{1}{9}\,\sqrt{2}\,[2(pd\sigma) + 5\sqrt{\frac{1}{3}}\,(pd\pi)]$$

$\underline{(\sqrt{2}/3, \sqrt{2/3}, 1/3)}$

$$\langle y; z^2 \rangle = -\frac{1}{3}\sqrt{2}\left[\sqrt{\frac{1}{3}}\,(pd\sigma) + \frac{1}{3}\,(pd\pi)\right]$$

$$\langle z; xy \rangle = -\frac{2}{9}\left[(pd\sigma) + 2\sqrt{\frac{1}{3}}\,(pd\pi)\right]$$

$$\langle z; xz \rangle = \frac{1}{9}\sqrt{2}\left[\sqrt{\frac{1}{3}}\,(pd\sigma) + \frac{7}{3}\,(pd\pi)\right]$$

$$\langle z; yz \rangle = \frac{1}{9}\sqrt{2}\left[(pd\sigma) + 7\sqrt{\frac{1}{3}}\,(pd\pi)\right]$$

$$\langle z; x^2-y^2 \rangle = -\frac{2}{9}\left[\sqrt{\frac{1}{3}}\,(pd\sigma) - \frac{2}{3}\,(pd\pi)\right]$$

$$\langle z; z^2 \rangle = -\frac{1}{9}\left[(pd\sigma) - 8\sqrt{\frac{1}{3}}\,(pd\pi)\right]$$

APPENDIX IV

THE TWO CENTER OVERLAP INTEGRALS FOR THE CUBIC WAVE FUNCTIONS IN TERMS OF THE SLATER-KOSTER PARAMETERS

The direction cosines (ℓ,m,n) gives the orientation of the oxygen ligand relative to the Cartesian system defined in Figure 11. All overlap integrals not listed are zero.

$\underline{(0,0,-1)}$

$$\langle s;t_2^o\rangle = (sd\sigma)$$

$$\langle x;t_2^+\rangle = \sqrt{\frac{1}{6}}\ (pd\pi)$$

$$\langle x;e\rangle = -\sqrt{\frac{1}{3}}\ (pd\pi)$$

$$\langle y;t_2^+\rangle = -i\sqrt{\frac{1}{6}}\ (pd\pi)$$

$$\langle y;e\rangle = i\sqrt{\frac{1}{3}}\ (pd\pi)$$

$$\langle z;t_2^o\rangle = -(pd\sigma)$$

$\underline{(-2\sqrt{2}/3,0,1/3)}$

$$\langle s;t_2^+\rangle = \frac{2}{3}\ (sd\sigma)$$

$$\langle s;t_2^o\rangle = -\frac{1}{3}\ (sd\sigma)$$

$(-2\sqrt{2}/3, 0, 1/3)$

$$\langle x; t_2^+ \rangle = -\sqrt{2}/18\ [8(pd\sigma) - \sqrt{1/3}(pd\pi)]$$

$$\langle x; t_2^\circ \rangle = 2\sqrt{2}/9\ [(pd\sigma) + \sqrt{1/3}\ (pd\pi)]$$

$$\langle x; e \rangle = -\frac{1}{3}\sqrt{\frac{1}{3}}\ (pd\pi)$$

$$\langle y; t_2^+ \rangle = -i\sqrt{1/6}\ (pd\pi)$$

$$\langle y; e \rangle = -i\sqrt{1/3}\ (pd\pi)$$

$$\langle z; t_2^+ \rangle = 2/9\ [(pd\sigma) + \sqrt{1/3}\ (pd\pi)]$$

$$\langle z; t_2^\circ \rangle = -\frac{1}{9}\ [(pd\sigma) - 8\sqrt{1/3}\ (pd\pi)]$$

$$\langle z; e \rangle = -\frac{2}{3}\sqrt{2/3}\ (pd\pi)$$

$(\sqrt{2}/3, -\sqrt{2/3}, 1/3)$

$$\langle s; t_2^+ \rangle = -1/3\ (1+i\sqrt{3})\ (sd\sigma)$$

$$\langle s; t_2^\circ \rangle = -1/3\ (sd\sigma)$$

$$\langle x; t_2^+ \rangle = -\sqrt{2}/18\ [2(1+\sqrt{3}i)\ (pd\sigma) + \sqrt{\frac{1}{3}}\ (-7+2\sqrt{3}i)\ (pd\pi)]$$

$$\langle x; t_2^\circ \rangle = -\sqrt{2}/9\ [(pd\sigma) + \sqrt{1/3}\ (pd\pi)]$$

$$\langle x; e \rangle = -\frac{1}{3}\sqrt{1/3}\ (-2+i\sqrt{3})\ (pd\pi)$$

$$\langle y; t_2^+ \rangle = -\sqrt{2}/3[-\sqrt{1/3}(1+\sqrt{3}i)\ (pd\sigma) + \frac{1}{6}\ (-2+\sqrt{3}i)(pd\pi)]$$

$\underline{(\sqrt{2}/3, -\sqrt{2/3}, 1/3)}$

$$\langle y;t_2^{\circ}\rangle = \sqrt{2}/3\ [\sqrt{1/3}\ (pd\sigma) + \frac{1}{3}\ (pd\pi)]$$

$$\langle y;e\rangle = 1/3\ (pd\pi)$$

$$\langle z;t_2^{+}\rangle = -\ 1/9\ (1+i\sqrt{3})\ [(pd\sigma) + \sqrt{1/3}\ (pd\pi)]$$

$$\langle z;t_2^{\circ}\rangle = -\ 1/9\ [(pd\sigma) - 8\sqrt{1/3}\ (pd\pi)]$$

$$\langle z;e\rangle = \frac{1}{3}\sqrt{\frac{2}{3}}\ (1 + i\sqrt{3})\ (pd\pi)$$

$\underline{(\sqrt{2}/3, \sqrt{2/3}, 1/3)}$

$$\langle s;t_2^{+}\rangle = -\ \frac{1}{3}\ (1-i\sqrt{3})\ (sd\sigma)$$

$$\langle s;t_2^{\circ}\rangle = -\ 1/3\ (sd\sigma)$$

$$\langle x;t_2^{+}\rangle = -\sqrt{2}/18\ [2(1-i\sqrt{3})\ (pd\sigma) - \sqrt{1/3}\ (7+2\sqrt{3}i)\ (pd\pi)]$$

$$\langle x;t_2^{\circ}\rangle = -\sqrt{2}/9\ [(pd\sigma) + \sqrt{1/3}\ (pd\pi)]$$

$$\langle x;e\rangle = \frac{1}{3}\sqrt{1/3}\ (2+i\sqrt{3})\ (pd\pi)$$

$$\langle y;t_2^{+}\rangle = -\sqrt{2}/3\ [\sqrt{1/3}\ (1-i\sqrt{3})\ (pd\sigma) + \frac{1}{6}\ (2+i\sqrt{3})\ (pd\pi)]$$

$$\langle y;t_2^{\circ}\rangle = -\sqrt{2}/3\ [\sqrt{1/3}\ (pd\sigma) + 1/3\ (pd\pi)]$$

$$\langle y;e\rangle = -\ 1/3\ (pd\pi)$$

$\underline{(\sqrt{2}/3, \sqrt{2/3}, 1/3)}$

$$\langle z; t_2^+ \rangle = -\ 1/9\ (1-i\sqrt{3})\ [(pd\sigma) + \sqrt{1/3}\ (pd\pi)]$$

$$\langle z; t_2^o \rangle = -\ 1/9\ [(pd\sigma) - 8\sqrt{1/3}\ (pd\pi)]$$

$$\langle z; e \rangle = -\ \frac{1}{3}\sqrt{2/3}\ (-1+i\sqrt{3})\ (pd\pi)$$

LIST OF REFERENCES

1. J. H. Van Vleck, The Theory of Electric and Magnetic Susceptibility (Oxford University Press, London, 1932 chap. XI.

2. Ibid., 182.

3. Ibid., 233.

4. D. S. McClure, Solid State Physics 9, 399 (1959).

5. D. S. McClure, loc. cit., 4.

6. J. C. Slater, Phys. Rev. 76, No. 11, 1592 (1949).

7. E. U. Condon and G. H. Shortley, The Theory of Atomic Spectra (Cambridge University Press, Cambridge, 1959), p. 300.

8. Ibid., 178.

9. J. S. Griffith, The Theory of Tansition Metal Ions (Cambridge University Press, Cambridge, 1961), p. 245.

10. C. J. Ballhausen, Introduction To Ligand Field Theory (McGraw-Hill Book Co., Inc., New York, 1962), p. 62.

11. Ibid., 103.

12. Ibid., 68.

13. Wyckoff, R. W. G., Crystal Structures (Interscience Publishers, Inc., New York, 1948), Vol. 1.

14. R. E. Dietz, H. Kamimura, M. D. Sturge and A.Yariv , Phys. Rev. 132, No. 4, 1559 (1963).

15. A. Abragam and M. Pryce, Proc. Roy. Soc. A205, 135 (1951).

16. J. H. Van Vleck, Physica 26, 544 (1960).

17. M. Tinkham, Group Theory and Quantum Mechanics (McGraw-Hill Book Co., Inc., New York, 1964), p. 181.

18. Ibid., 76.

19. M. Hammermesh, Group Theory and Its Application to Physical Problems (Addison-Wesley Publishing Co., Inc., 1962), p. 118.

20. J. C. Slater, Quantum Theory of Atomic Structure (McGraw-Hill Book Co., Inc., New York, 1960), p. 72.

21. C. E. Moore, Atomic Energy Levels, National Bureau of Standards, Circular 467 Vol. II 1952.

22. J. H. Van Vleck, Phys. Rev. 33, 467 (1929).

23. O. M. Jordahl, Phys. Rev. 45, 87 (1934).

24. E. C. Kemble, The Fundamental Principles of Quantum Mechanics With Elementary Application (Dover Publications, Inc., New York, 1958), p. 394.

25. I. Broser, H. Maier and H.-J. Shultz, Phys. Rev. 140, No. 6A, 2136 (1965).

26. H. A. Weakliem, J. Chem. Phys. 36, 2117 (1962).

27. K. Morigaki, J. Phys. Soc. Japan 19, 1240 (1964).

28. W. H. Brumage and C. C. Lin, Phys. Rev. 134, No. 4A, 950 (1964).

29. W. C. Holton, T. L. Estle and M. DeWitt, Bul. Am. Phys. Soc. II, 9, 249 (1964).

30. M. DeWitt and T. L. Estle, Bul. Am. Phys. Soc. II, 8,24 (1963).

31. J. C. Slater, Quantum Theory of Molecules and Solids (McGraw-Hill Book Co., Inc., 1965), p. 218.

32. Ibid., 339.

33. Ibid., 60.

34. L. P. Bouckaert, R. Smoluchowski and W. Wigner, Phys. Rev. 50, 58 (1936).

35. C. A. Bates, Proc. Phys. Soc. 83, 465 (1964).

36. J. C. Slater and G. F. Koster, Phys. Rev. 94, 1498 (1954).

37. I. Shavitt, in Method In Computational Physics, edited by B. Adder, S. Fernback and M. Rotenberg (Academic Press Inc., New York, 1963), Vol. 2, p. 1.

38. E. E. Lafon and C. C. Lin, Phys. Rev. 152, No. 2, 579 (1966).

39. E. Clementi, Supple. to "Ab Initio Calculations in Atoms and Molecules", I.B.M. Journal 9, 2 (1965).

40. E. Clementi and A. D. McLean, Phys. Rev. 133, No. 2A, 419 (1964).

41. R. Pappalardo, J. Mole. Spectry 6, 554 (1961).

42. G. F. Koster, Solid State Physics 9, 399 (1959).

43. E. B. Wilson, J. C. Decius and P. C. Cross, Molecular Vibrations (McGraw-Hill Book Co., Inc., New York, 1955), p. 331.

44. Ibid., 330.

45. Ibid., 325.

46. W. H. Brumage, Magnetic Susceptibilities of Paramagnetic Ions In Host Crystals, (Unpublished Ph.D. Dissertation, Dept. of Physics, University of Oklahoma).

47. J. L. Birman, Phys. Rev. 115, No. 6, 1493 (1959).

48. E. E. Lafon, Energy Band Structure of Lithium by the Tight-Binding Method, (Unpublished Ph.D. Dissertation, Dept. of Physics, University of Oklahoma).

49. R. J. Elliott, Phys. Rev. 96, No. 2, 280 (1954).

50. K. Shindo, A. Morita and H. Kamimura, J. Phys. Soc. Japan 20, No11, 2054 (1965).